Aus dem Institut der Experimentellen Neurologie
der Medizinischen Fakultät Charité – Universitätsmedizin Berlin

DISSERTATION

Histone Methylation and Neuroprotection in Experimental Cerebral Ischemia

zur Erlangung des akademischen Grades
Doctor of Philosophy (PhD)

vorgelegt der Medizinischen Fakultät
Charité – Universitätsmedizin Berlin

von

Sophie Schweizer

aus Heidelberg

Datum der Promotion: 04.09.2015

Table of Contents

Index of figures

Abbreviations

Ac	Acetylated
BDNF	Brain derived neurotrophic factor
ChIP	Chromatin immunoprecipitation
CTRL	Control (condition/experiment)
DIV	Day in vitro
DNA	Deoxyribonucleic acid
DNMT	DNA methyltransferase
H3	Histone 3
H3K4	Histone 3 Lysine 4
H3K9	Histone 3 Lysine 9
HDAC	Histone deacetylases
HIF	Hypoxia inducible factor
KDM	Histone lysine demethylase
KMT	Histone lysine methyltransferase
LDH	Lactate dehydrogenase
Me	Methylated
Me1/2/3	Mono-/di-/trimethylated
Mi-	miR-shRNA (microRNA short hairpin construct)
mRNA	Messenger ribonucleic acid

N	Sample size
OGD	Oxygen glucose deprivation
PCR	Polymerase chain reaction
PBS	Phosphate buffered saline
PTM	Post-translational histone modification
REST	Repressor element-1 silencing transcription factor
RFP	Red fluorescent protein
RT	Room temperature
SD	Standard deviation

1. Summary

Cerebral ischemia leads to great transcriptional changes, primarily gene silencing. According to studies conducted in rodent models, stroke outcome can be improved by manipulating epigenetic players. Inhibition of transcriptional repressors on the level of DNA methylation and histone acetylation in ischemia leads to the maintenance of activating epigenetic marks, the restoration of the transcriptional balance and the attenuation of damage. At present, the role of histone methylation in this context is unexplored.

As epigenetic players act in concert, we hypothesized that

- histone methylation is involved in ischemic damage development;
- the manipulation of enzymes on the level of histone methylation influences neuronal survival following ischemia;
- neuroprotection can be induced by inhibiting transcriptional repressors on the level of histone methylation, based on the transcriptional activation of protective genes.

An in vitro model of stroke using rat primary cortical neurons subjected to oxygen glucose deprivation was employed, followed by cell survival analysis.

First, the state of global histone methylation at selected methylation sites (histone 3 lysine 9 H3K9 and histone 3 lysine 4 H3K4) was examined post oxygen glucose deprivation. However, no recurring pattern was observed that clearly indicated gene repression, or highlighted a single methylation state (un-/mono-/di- or tri-methylated).

Next, the expression of selected histone de-/methylating enzymes was analysed and manipulated. A marked upregulation of both mRNA and protein levels of the histone demethylase KDM3A was detected in hypoxic cortical neuron cultures. This effect was not observed for further candidate enzymes (SUV39H1, G9a, ESET and LSD1) and suggests an important role for KDM3A in hypoxia. Nevertheless, exogenous overexpression of the transcriptional activator KDM3A did not influence neuronal survival following experimental ischemia. Neither did the overexpression of transcriptional repressors (SUV39H1, LSD1), where an exacerbation of neuronal damage was expected upon hypoxic metabolic stress.

In contrast, neuroprotection was successfully induced by inhibiting the transcriptional repressors LSD1, ESET, SUV39H1 and G9a with various pharmacological agents. SUV39H1 and G9a inhibitor Chaetocin was used in a neurological context for the first time and identified as novel neuroprotective agent. The histone demethylases SUV39H1 and G9a were chosen for closer analysis. Knockdown of both enzymes conferred protection to neurons in experimental stroke and confirmed the result achieved upon pharmacological inhibition. Chromatin immunoprecipitation followed by sequencing revealed altered histone 3 (H3K9) modification states in promoter regions of certain genes upon SUV39H1 and G9a inhibition via Chaetocin. Activating promoter marks occurred together with elevated mRNA levels of the genes vascular endothelial growth factor (VEGF) and brain derived neurotrophic factor (BDNF). Further, BDNF blockade attenuated the protective effect of Chaetocin treatment, which distinguishes BDNF as a mediator of Chaetocin-induced neuroprotection.

The findings of this thesis demonstrate that manipulating aberrant histone methylation upon experimental ischemia can alter cellular gene expression patterns and improve neuronal viability. As current treatment options in ischemia remain limited, the broadened understanding of epigenetic signalling and the identification of novel epigenetic neuroprotective agents and targets in histone methylation are promising and might potentially impact neuroprotective drug development.

1.1. Abstrakt

Zerebrale Ischämie führt zu veränderter Genexpression, wobei es verstärkt zu einer Verminderung der Transkription kommt. Schlaganfallstudien an Nagetieren zeigen, dass eine ischämische Schädigung durch gezielte Manipulation epigenetischer Faktoren eingegrenzt werden kann. Die Inhibition transkriptioneller Repressoren, sowohl auf DNA-Methylierungs-Ebene als auch auf der Ebene der Histon-Acetylierung, kann zur Erhaltung aktivierender epigenetischer Faktoren führen und durch die Wiederherstellung der transkriptionellen Balance schadenseindämmend wirken. Bislang wurde die Rolle von Histon-Methylierung in diesem Zusammenhang wenig erforscht.

Da epigenetische Faktoren interagieren, ergibt sich die Hypothese, dass

- Histon-Methylierung bei ischämischer Schadensentwicklung eine Rolle spielt;
- Neuroprotektion erreicht werden kann, indem transkriptionelle Repressoren auf Histon-Methylierungsebene inhibiert werden, was eine Aktivierung protektiver Gene erlaubt.

Eingesetzt wurde ein *in vitro* Schlaganfallmodell, in dem primäre postmitotische Ratten-Neuronen einer Sauerstoff-Glukose-Deprivation unterzogen wurden. Anschließend folgten Untersuchungen zum zellulären Überleben.

Untersucht wurden globale Histon-Methylierungsmuster an ausgewählten Positionen (Histon H3 Lysin 9 und Histon H3 Lysin 4) nach Sauerstoff-Glukose-Deprivation. Ausgeprägte Muster wurden hierbei allerdings nicht beobachtet.

Des Weiteren wurde die Expression von Histon-Methyltransferasen und -Demethylasen analysiert und manipuliert. In hypoxischen Neuronen wurde die Demethylase KDM3A, im Unterschied zu anderen Enzym-Kandidaten (SUV39H1, G9a, ESET und LSD1), auf mRNA- und Protein-Ebene induziert. Die exogene Überexpression von KDM3A beeinflusste den neuronalen Schaden nach Sauerstoff-Glukose-Deprivation allerdings nicht. Die Überexpression zweier transkriptioneller Repressoren (SUV39H1, LSD1) blieb ebenfalls folgenlos.

Im Gegensatz dazu führte die pharmakologische Inhibition der transkriptionellen Repressoren LSD1, ESET, SUV39H1 und G9a erfolgreich zu Neuroprotektion. Chaetocin, ein Suv39H1 und G9a Inhibitor, wurde zum ersten Mal in einem neurologischen Kontext eingesetzt und als neue neuroprotektive Substanz identifiziert. Auch der Knockdown der Histon-Methyltransferasen SUV39H1 und G9a führte bei experimentellem Schlaganfall zum Schutz von Neuronen. Nach Blockade von

SUV39H1 und G9a mit Chaetocin konnten mittels Chromatin-Immunpräzipitation und Sequenzierung veränderte Histon H3 Lysin 9 Modifikationen in Promotorbereichen protektiver Gene nachgewiesen werden. Dabei wurde in den Genen des *Vascular endothelial growth factor* (VEGF) und des *Brain-derived neurotrophic factor* (BDNF) neben epigenetischen Markern aktiver Genexpression ebenfalls erhöhte mRNA-Werte festgestellt. Außerdem schwächte die Blockade von BDNF den protektiven Effekt von Chaetocin auf Neuronen unter Sauerstoff-Glukose-Deprivation ab. BDNF wurde somit als wichtiger Vermittler von Chaetocin-induzierter Neuroprotektion in experimenteller Ischämie erkannt.

Insgesamt bestätigen die Ergebnisse die Hypothese, dass die Inhibition transkriptioneller Repressoren auf der epigenetischen Ebene der Histon-Methylierung erfolgreich zu Neuroprotektion führen kann. Durch die Inhibition repressiver Histon-Methyltransferasen wird die aktive Transkription wichtiger Mediatoren der Neuroprotektion, wie zum Beispiel BDNF, induziert. Die Wirkung epigenetischer Inhibitoren wie Chaetocin ist vielversprechend und könnte für eine erfolgreiche medikamentöse Schlaganfall-Therapie von Nutzen sein.

2. Introduction

2.1. Cerebral ischemia

Stroke is the second leading cause of death and long-term disability in developed countries according to World Health Organisation statistics (http://www.who.int/mediacentre/factsheets/fs310/en/index.html). Ischemic stroke occurs as a result of a transient or permanent reduction in cerebral blood flow originating from a cerebral artery being occluded by either an embolus or thrombosis [*Dirnagl et al.*, 1999]. As a consequence brain tissue remains unsupplied with oxygen and glucose. This shortage generates a highly complex series of spatial and temporal events and affects different ischemic areas in diverse manners.

2.1.1. Ischemic pathophysiology

Neuronal tissue is characterized by high energy consumption, which renders it particularly vulnerable to a lack of oxygen and glucose. In the ischemic core, the zone most affected by restricted energy supply, cells die within minutes as energy failure prevents the maintenance of the fine-balanced membrane potential, which is crucial for proper functioning and cell survival [*Dirnagl et al.*, 1999; *Kostandy*, 2012]. In the penumbra, the area surrounding the ischemic core, energy metabolism is partially preserved [*Hossmann*, 1994]. In this region cells are predominantly confronted with propagating excitotoxicity [*Auer*, 1991] oxidative [*Weisbrot-Lefkowitz et al.*, 1998] and nitric stress [*Kader et al.*, 1993] as well as secondary phenomena like inflammation [*Giulian and Vaca*, 1993; *Rothwell and Strijbos*, 1995], spreading depolarization [*Dreier*, 2011] and delayed cell death [*Mehta et al.*, 2007]. These events occur during an extended period of time over hours and even days [*Dereski et al.*, 1993; *Dirnagl et al.*, 1999] **(Fig. 1**).

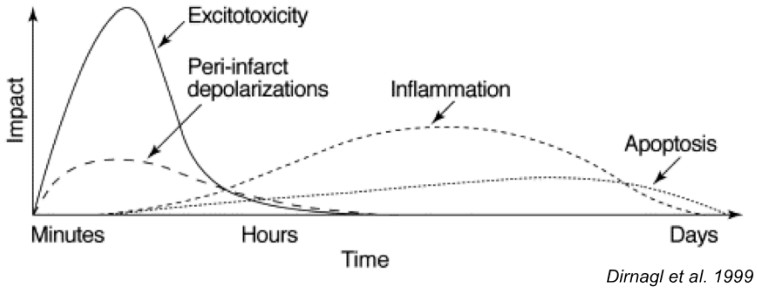

Figure 1 Cascade of damaging events in focal cerebral ischemia

Intricate disease mechanisms evolve over time affecting the survival of cells. The *x*-axis reflects the evolution of the cascade over time, while the *y*-axis illustrates the impact of each element of the cascade on final outcome.

2.1.1.1. Excitotoxicity, calcium overload and ionic imbalance

Below a certain blood flow threshold (20 ml/100 g/min) the energy-dependent maintenance of the membrane potential is impaired, neurons depolarize and release the neurotransmitter glutamate excessively into the extracellular space [*Shimada et al.*, 1989]. Lack of energy impedes the function of the ATP-dependent sodium/potassium pump and physiological repolarization processes. As a consequence, glutamate accumulates and induces excitotoxic cell death [*Beal*, 1992; *Novelli et al.*, 1988]. It further induces overstimulation of glutamate receptors in neighbouring cells, followed by depolarization-stimulated calcium influx and a second fatal wave of calcium that sets irreversible cell death processes in motion, killing the cells in the hours following the ischemic onset [*Szydlowska and Tymianski*, 2010]. Owing to intracellular ion accumulations, water passively enters the cell, causing cellular swelling and brain oedema [*Rosenberg*, 1999] (**Fig. 2**).

2.1.1.2. The penumbra: oxidative stress and inflammation

Partial energy preservation in the penumbra leads to more delayed mechanisms of damage. The series of signalling events following increased calcium influx induces the generation of reactive oxygen species (ROS) in the cells, mainly released by dysfunctional mitochondria. Mitochondrial electron transport is hampered. Free electrons accumulate and form ROS in reaction with oxygen following reperfusion. Mitochondrial damage not only marks the end of cellular energy metabolism it additionally triggers secondary inflammatory pathways and cell death signalling cascades [*Kostandy*, 2012; *Weisbrot-Lefkowitz et al.*, 1998]. The ensuing tissue damage

activates astrocytes and microglia, producing pro-inflammatory cytokines and chemokines. These attract further players of the immune response, invading the injured brain in a complex temporal pattern. They contribute to both, tissue repair and peri-infarct injury [*Gelderblom et al.*, 2009]. Peripheral leukocytes, recruited by chemokine signalling, start infiltrating the ischemic zone only several days post ischemic onset and exacerbate tissue damage at this late stage [*Shichita et al.*, 2009].

A model of the pathophysiological interplay following ischemia is shown in **Figure 2**.

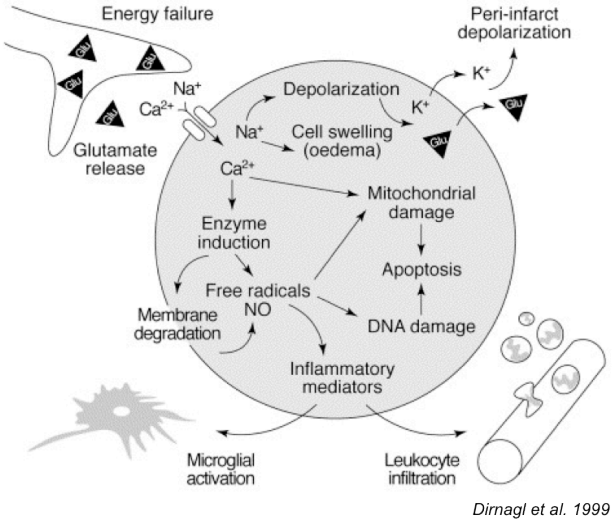

Figure 2 Overview of pathophysiological mechanisms in the ischaemic brain

Energy failure leads to glutamate excitotoxicity, oxidative and nitric stress, inflammation, spreading depolarization and delayed cell death, all processes contributing to ischemic damage.

2.1.2. Endogenous pathways of protection and regeneration

All cells possess stress sensors and can react to danger by activating endogenous protective pathways [*Dirnagl and Meisel*, 2008]. Alongside the detrimental cascades set in motion by an ischemic insult the injured brain responds by activating defence and repair mechanisms. Some inflammatory processes in the ischemic brain promote cerebral tissue survival and repair, such as certain cytokines and growth factors released by activated immune cells [*Feuerstein and Wang*, 2001]. To limit oxidative stress ROS scavenger production is turned on in neurons [*Danielisova et al.*, 2005]; to promote survival, levels of anti-apopotic signalling molecules are increased, such as members of the B-cell lymphoma 2 (BCL-2) family [*Ouyang and Giffard*, 2004] and heat shock

proteins (HSP) [*Yenari et al.*, 2005]; to promote tissue regeneration and repair, factors such as brain derived neurotrophic factor (BDNF) are released [*Marini et al.*, 2008]. One crucial modulator of the ischemic response is the transcription factor hypoxia-inducible factor (HIF), activated upon hypoxia [*Ruscher et al.*, 1998; *Semenza*, 1996]. Upon hypoxic stress, HIF induces the expression of typical representatives of innate protective response pathways, promoting oxygen and energy transport and antagonizing cellular damage, such as erythropoietin (EPO) and vascular endothelial growth factor (VEGF) [*Prass et al.*, 2003; *Sun et al.*, 2003].

Endogenous protection and repair pathways can be induced upon sub-threshold stimulation, known as preconditioning. Ischemic preconditioning leads to a certain period of tolerance to subsequent injury [*Dirnagl et al.*, 2009]. The investigation of endogenous protective pathways is of major interest as targeted manipulation of protective and regenerative players might represent a treatment option for stroke patients. Especially interesting in this context are disease mechanisms observed in the penumbra as their slow progression provides a window for pharmacological intervention [*Dirnagl et al.*, 1999].

2.1.3. Treatment options

A growing understanding of the intricate disease etiology of stroke has led to a whole list of neuroprotective agents identified in bench side findings. They target the whole range of involved pathways: some inhibit excitotoxic cell death [*Cook et al.*, 2012; *Cui et al.*, 2007], others interfere with oxidative stress [*Ha et al.*, 2013; *Yabuki and Fukunaga*, 2013] or promote cell survival signalling [*Han et al.*, 2000; *Ma et al.*, 2001], still others enhance blood flow [*Winkler et al.*, 2013], stimulate neurogenesis and plasticity or display anti-inflammatory properties [*DeGraba*, 1998; *Dirnagl et al.*, 2009; *Liesz et al.*, 2011]. In spite of these advances, clinical treatment options remain few and limited and the translation to clinical practice has been a challenging endeavour [*Ducruet et al.*, 2009]. Until today, tissue plasminogen activator, applicable within the narrow time range of 4.5 hours, remains the main treatment option [*Thurman et al.*, 2012]. Translational difficulties originate in part from inappropriate preclinical modelling of the disorder and actual stroke care as well as insufficient preclinical testing [*Mergenthaler and Meisel*, 2012].

2.1.4. Gene expression in ischemia

During all the ischemic cascades described above substantial changes in gene expression occur. They affect hundreds of genes [*Kogure and Kato*, 1993;

Trendelenburg et al., 2002]. This genomic response is regulated by diverse players, which concurrently induce both, beneficial and harmful pathways [*Papadopoulos et al.*, 2000], [*Stenzel-Poore et al.*, 2007]. Compared to other neurological diseases, the changes in gene expression in stroke during the different phases of damage evolvement are capital (Fig. 3). As such, epigenetic players - being the key regulators of gene transcription - newly emerge as candidates of major interest in the struggle of limiting ischemic damage.

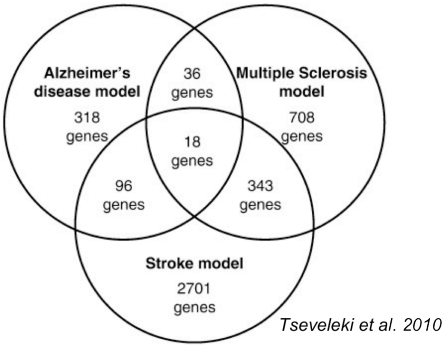

Figure 3 Venn diagram of differentially regulated genes from three pathologies

Stroke shows the largest number of changes in gene expression compared to wild type brains. The analysis is based on global gene expression profiling from mouse brains for the various disease models.

2.2. Epigenetics

Conrad Waddington coined the term *epigenetics* in the 1950s focusing on heritability and the development of phenotypes from genotypes independent of alterations in DNA sequence [*Sananbenesi and Fischer*, 2009]. Together with the evolvement of a whole field of study united under the name of *epigenetics*, the term underwent an expansion of meaning. *Goldberg et al*. suggested considering "cellular differentiation" in general an epigenetic phenomenon [*Goldberg et al.*, 2007]. In an attempt to unify the prevailing usage of the term *Adrian Bird* stated its subject matter to be concerned with the structural adaptation of regions of the chromosome to register, signal or perpetuate altered activity states [*Bird*, 2007].

Epigenetic players show highly conserved structures across species. They orchestrate the dynamic regulation of gene expression and are crucial for a stable cell fate definition as well as for a flexible adaptive response to environmental changes. Classically considered as parts of the epigenetic machinery are DNA methylation and histone modifications. As of late, noncoding RNAs are sometimes included [*Kaikkonen et al.*, 2011].

2.2.1. The nucleosome

In the eukaryotic cell, the nucleosome represents the basic unit of DNA packaging. It consists of a segment of approximately 147 base pairs of DNA, wrapped around an octamer of histone proteins forming two superhelical turns [*Luger et al.*, 1997]. The octamer is composed of two copies of each of the core histones H2A, H2B, H3 and H4 (**Fig. 4a**). Chains of nucleosomes are successively folded to higher order structures and ultimately form the chromosome [*Wolffe and Pruss*, 1996]. The nucleosome plays a fundamental role in the regulation of gene expression as the transcriptional control is largely dependent on chromatin structure [*Zhang and Dean*, 2001]. Whether the chromatin is organized in a structure that allows access to the transcriptional machinery or not, is mainly regulated by post-translational histone modifications (PTMs), referred to as epigenetic modifications [*Jenuwein and Allis*, 2001].

2.2.2. Post-translational histone modifications

Histone proteins have a mainly globular structure with an n-terminal histone tail protruding from the surface of the nucleosome. This histone tail is subject to multiple post-translational modifications, that govern chromatin compaction and function [*Schones and Zhao*, 2008]. Modifications include histone acetylation, methylation, phosphorylation, sumoylation and ubiquitinilation, and more recently discovered phenomena such as ADP-ribosylation, proline isomerization, citrullination, butyrylation, propionylation, and glycosylation [*Gardner et al.*, 2011]. All these PTMs occur at certain residues of the histone protein and exist in elaborate combinations (**Fig. 4b**). Over 60 residues available for modifications have been detected [*Kouzarides*, 2007]. Recent findings suggest that modifications are not confined to histone tails but occur at the globular parts of histone proteins as well [*Tropberger and Schneider*, 2010; 2013]. Together they influence transcription as well as replication and chromosome structure.

2.2.3. Chromatin structure and epigenetic crosstalk

In 2000, the concept of the "histone code" was proposed, postulating that "multiple histone modifications, acting in a combinatorial or sequential fashion on one or multiple histone tails, specify unique downstream functions" [*Strahl and Allis*, 2000]. Most PTMs do not alter chromatin compaction directly but act as signals to recruit effector proteins, or so-called "readers", that can specifically bind to individual or multiple modifications. Some PTMs on the other hand, such as histone acetylation and phosphorylation directly influence the structure of the chromatin.

Acetylation at histone lysine residues, one of the most extensively studied epigenetic marks, neutralizes the positive charge of the histone molecule and thus reduces the association to the negatively charged DNA. Consequently, this open form of chromatin (euchromatin) allows transcription factors and transcriptional co-activators to access specific gene promoters and induce active transcription [*Narlikar et al.*, 2002]. The lack of acetyl-groups on the other hand generates condensed hetero-chromatin, usually associated with gene repression [*Hebbes et al.*, 1988; *Marks*, 2010]**.** All PTMs are dynamically regulated and hence allow a quick transcriptional response according to needs. The writing and eradication of epigenetic marks is carried out by specified enzymes and protein complexes. Acetylation of lysine residues (of histones as well as non-histone proteins) is effected by histone acetyltransferases (HATs) [*Kuo and Allis*, 1998], while the removal of acetyl groups is performed by different families of histone deacetylases (HDACs) [*de Ruijter et al.*, 2003]. Crosstalk with other epigenetic marks – also comprising other levels of modification, such as DNA methylation - exists. DNA methylation occurs directly at CpG islands of the DNA and usually confers repression to the gene localized in the surrounding [*Bergman and Mostoslavsky*, 1998]. The methylation step is carried out by DNA methyltransferases (DNMT) and the subsequent repressive effect is mediated by the recruitment of chromatin modifiers that bind to the methylated site, for example members of the family of methyl-CpG-binding proteins

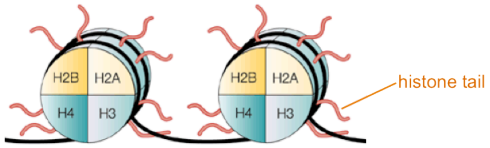

Modified from Marks et al. 2001

Figure 4a The nucleosome
The nucleosome consists of 147 base pairs of DNA wrapped around the histone octamer.

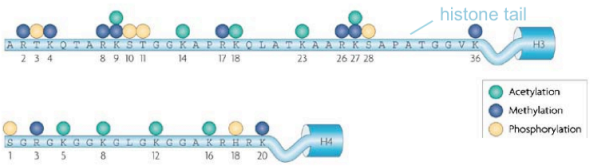

Modified from Spivakov et al. 2007

Figure 4b Histone tails H3 and H4
Histone tails are post-translationally modified. Among many modifications, certain residues can for example be acetylated, methylated or phosphorylated.

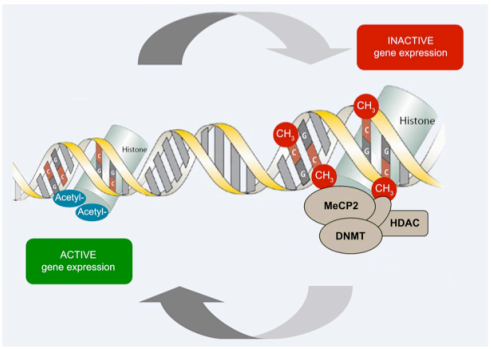

Modified from http://www.esf.org/coordinating-research/eurocores/running-programmes/euroepinomics/projects-crps/epigenet.html

Figure 4c Chromatin structure and epigenetic crosstalk
Multiple epigenetic mechanisms work in concert to orchestrate the regulation of gene expression. DNA methyltransferases and Histone deacetylases interact in repressive complexes to promote gene silencing .

(MBD). These proteins form transcriptional repressor complexes together with histone deacetylases [*Gregory et al.*, 2001; *Nan et al.*, 1998]. Direct interactions between DNA methyltransferase 1 (DNMT1) and a histone deacetylase (HDAC1) have been suggested [*Fuks et al.*, 2000; *Robertson et al.*, 2000] (**Fig. 4c**). Further, a close interplay exists between histone acetylation and another PTM, which has recently emerged as major player in the regulation of genes - namely histone methylation.

2.2.4. Histone methylation

In a dynamic process lysine (K) and arginine (R) residues of histone molecules can be methylated by histone methyltransferases and demethylated by histone demethylases. Methylation marks at lysine residues can act as both, activating or repressive marks depending on site specificity in the histone as well as the distinct methylation state [*Schones and Zhao*, 2008]. Three different methylation states can be distinguished according to the amount of methyl groups added to the residue: mono-, di- and trimethylation. All states display high biochemical stability [*Fischle*, 2012].

Typical methylation marks of transcriptional repression are H3K9 tri- and dimethylation (me3/me2), as well as H3K27me3, H3K27me2 and H4K20me3. Clustered appearance of these marks can be monitored in the genome [*Wang et al.*, 2008].

Common marks on histone 3 that correlate with active transcription and accessible chromatin sites are H3K4me3/me2/me1, H3K9me1, H3K36me3 and H3K79me1/2/3. Unlike histone acetylation, histone methylation has no direct influence on the accessibility of chromatin structure. Methyl-marks act as platforms for effector proteins regulating gene transcription. The marks coexist in combination with other modifications and jointly affect gene expression. In open chromatin the methylation marks mentioned above correlate with PTMs at other histone molecules of the octamer (H2BK12ac, H2AZ, H4K8ac, etc.) as well as at the same H3 molecule (H3K9ac, H3K27ac, H3K36ac).

In this study the focus lies on the residues H3K9 and H3K4 (**Fig. 5**).

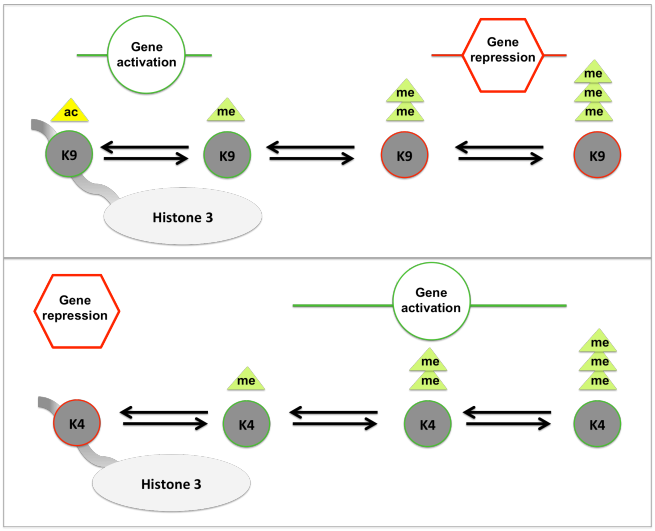

Figure 5 Histone methylation at histone 3 lysine 9 (H3K4) and lysine 4 (H3K4)
H3K9 me2 and me3 are repressive epigenetic marks, while H3K9 me1, as well was the unmethylated state, which can be acetylated (H3K9ac) are found in actively transcribed genes.
H3K4 me3/me2/me1 are marks, located in actively transcribed genes, while the unmethylated state H3K4me0 is associated with gene repression.

2.2.5. Histone lysine methyltransferases and demethylases

The first histone lysine methyltransferase (KMT) SUV39H1, methylating histone lysine residues in all eucaryotes from yeast to human, was discovered in 2000 [*Rea et al.*, 2000]. At the time, the dynamic nature of histone methylation was a matter of debate, up to the discovery of the first histone demethylase (KDM), LSD1 in 2004 [*Shi et al.*, 2004]. A number of enzymes catalysing histone de-/methylation have since been discovered on the basis of sequence homology of the catalytic domains.

Regarding histone methyltransferases two classes are currently distinguished. The first group are enzymes containing the catalytic SET domain (around 33 enzymes in humans). The second class without SET domain has for the moment one single representative, KMT4. Both classes rely on S-adenosyl-L-methionine as methyl group donor [*Black et al.*, 2012]. KMTs display very high specificity regarding the recognition of site and degree of methylation just like their demethylating counterparts, the KDMs. Up to now, 21 demethylating enzymes have been described. They are grouped according to two different demethylase domains, the LSD1 domain and the JmjC domain [*Black et al.*, 2012]. Members of the LSD1 domain act in the presence of molecular oxygen and flavin while KDMs equipped with a catalytic JmjC domain need the cofactor iron, alpha-ketoglutarate and molecular oxygen for proper functioning. This class of enzymes was discovered in 2006 only [*Cloos et al.*, 2006; *Tsukada et al.*, 2006; *Yamane et al.*, 2006].

Literature on histone de-/methylating enzymes is still scarce. However, some candidates have been analysed in functional assays, mainly in cancer research.

2.3. Epigenetic mechanisms and the brain

The ability to dynamicly modulate gene transcription is prerequisite for cellular processes such as cell differentiation, homeostasis or adaptation to stress. This dynamic regulation occurs on the epigenetic level. As post-mitotic neurons are not subject to constant renewal, well-orchestrated response mechanisms ensuring proper functioning can become vital even for the whole organism that depends on brain function. In the brain, mutations and maladaptations of the epigenetic machinery are now known to be implied in neuro-developmental, neuro-degenerative as well as neuro-psychiatric disease contexts [*Graff et al.*, 2011; *Sananbenesi and Fischer*, 2009]. Involved are all levels of epigenetic regulation - including DNA methylation and histone modification. Currently, the fundamental role of HDACs as regulators of transcription has been recognized. Perturbation of acetylation homeostasis is now acknowledged to be a central event in neurological pathologies. Pharmacological inhibition of HDACs shows significant neuroprotective and neuroregenerative properties in most diverse neuropathological conditions [*Abel and Zukin*, 2008; *Shein and Shohami*, 2011], such as Huntington's disease [*Ferrante et al.*, 2003], status epilepticus [*Huang et al.*, 2002], spinal muscular atrophy [*Minamiyama et al.*, 2004], and experimental autoimmune encephalitis [*Camelo et al.*, 2005]. Targeted manipulation of aberrant histone acetylation also shows promising results in the treatment of ischemic damage.

2.3.1. Epigenetic mechanisms and neuroprotection in ischemia

The epigenetic levels reflect the great alterations in gene expression evoked by ischemic injury. Typical epigenetic marks of gene silencing are increased in the ischemic brain. Global amounts of DNA methylation are elevated post ischemia, which correlates with augmented brain injury [*Endres et al.*, 2000; *Endres et al.*, 2001]. Further, numerous studies from our and other groups show a general decrease of histone H3 acetylation [*Faraco et al.*, 2006; *Kim et al.*, 2007; *Lanzillotta et al.*, 2012; *Ren et al.*, 2004; *Wang et al.*, 2011] and H4 acetylation levels [*Langley et al.*, 2008; *Xuan et al.*, 2012; *Yildirim et al.*, 2008] in and around the ischemic core.

Due to the dynamic nature of epigenetic modifications the possibility of reversing the state of gene repression arises as interesting option to modulate outcome. Pharmacological inhibition of DNA methylation as well as a reduction of DNMT1 levels in neurons ameliorate neurological deficits in a rodent model of ischemia [*Endres et al.*, 2000; *Endres et al.*, 2001]. Further, the diverse group of HDAC inhibitors has been subject to extensive analysis and emerges as promising therapeutic option in ischemia. In stroke, treatment with HDAC inhibitors (such as Trichostatin A, Valproic

acid, Sodium butyrate, Suberoylanilide hydroxamic acid, or MS-275) leads to maintenance of histone 3 and 4 acetylation levels during ischemia, or their re-establishment after late administration. In spite of a selectivity for only about 2-5% of all genes [*Marks*, 2004; *Van Lint et al.*, 1996], beneficial transcriptional changes induced by HDAC inhibition can be monitored in all known pathways involved in the complex course of ischemic injury development ranging from attenuation of cell death, suppression of inflammatory processes, to enhanced blood flow and the stimulation of repair mechanisms as well as increased plasticity [*Schweizer et al.*, 2013].

Interestingly, HDAC inhibitors exert their influence not only by inducing gene activation, but also global transcriptional changes including the down-regulation of certain genes.

HDAC inhibition both as pre- and post-treatment up to seven hours after the insult, significantly reduces infarct volume, attenuates brain damage and promotes functional recovery in rodent models of stroke [*Faraco et al.*, 2006; *Gibson and Murphy*, 2010; *Kim et al.*, 2007; *Langley et al.*, 2009; *Qi et al.*, 2004; *Ren et al.*, 2004; *Yildirim et al.*, 2008]. Currently, the development of new derivatives exhibiting decreased toxicity, high potency, blood brain barrier permeability and improved selectivity is subject to intensive investigation [*Li et al.*, 2013].

So far, no clinical trials employing epigenetic modifiers have been conducted in ischemia. In various cancers, however, HDAC inhibitors are in different stages of clinical trials or have already been approved [*Schweizer et al.*, 2013] and some trials were conducted in neurological pathologies such as amyotrophic lateral sclerosis [*Cudkowicz et al.*, 2009] or Huntington's disease [*Hogarth et al.*, 2007].

2.3.2. Histone methylation in neurological pathologies and ischemia

Dysregulation of histone de-/methylating enzymes has recently been observed in neurological contexts. Mutations in a repressive H3K4me3/2 demethylase (JARID1C) and aberrant H3K4 methylation have been associated with X-linked retardation [*Iwase et al.*, 2007; *Jensen et al.*, 2005] and cases of autism spectrum disorder [*Adegbola et al.*, 2008; *Shulha et al.*, 2012]. Mutations or increased expression of the H3K9 methyltransferase GLP have been linked to mental retardation [*Kleefstra et al.*, 2006] and schizophrenia [*Chase et al.*, 2013] . In Huntington's disease increased levels of H3K9me3 coincide with elevated expression of the methylstransferase ESET [*Ryu et al.*, 2006]. Abnormal expression of the methyltransferase G9a influences addictive behaviour [*Feng and Nestler*, 2013]. In how far misregulation of target genes, or chromatin restructuring as a consequence of abnormal histone methylation are the

decisive factors for disease development is not fully understood. There is no doubt however, that a delicate balance of histone methylation marks in the brain is essential to function.

Concerning cerebral ischemia, knowledge on the role of histone methylation is limited. A repressor complex - repressor-element-1-transcription-factor (REST)- that is induced upon stroke was found to include the repressive histone demethylase LSD1 [*Lee et al.*, 2005] and the histone methyltransferase G9a among further repressive elements. In hippocampal CA1 neurons the activation of this repressive complex is followed by binding to target genes, such as the AMPA receptor subunit GluA2 and subsequent epigenetic remodelling and gene silencing [*Noh et al.*, 2012]. Few more studies exist that analysed methylation signatures of single gene promoters differentially regulated after ischemia, such as the silenced gene OPRM1 (μ- opioid receptor 1 or MOR-1) showing enriched H3K9me2 [*Formisano et al.*, 2007] and the induced neuroprotective genes, iNOS and HIF-1α, with marked increases of H3K4me2 together with a decrease of H3K9me2 levels - a typical activation signature [*Rana et al.*, 2012]. Taken together, changes in histone methylation marks in ischemia seem to be in line with the current knowledge on epigenetic signatures and crosstalk.

3. Hypothesis and Objectives

The occurrence of crosstalk between epigenetic levels suggests the hypothesis that histone methylation – same as DNA methylation and histone acetlyation - is involved in ischemic damage development as well as in protective and regenerative pathways.
Neuronal survival following ischemia might be promoted by altering transcriptional regulation on the level of histone methylation (**Fig. 6**).

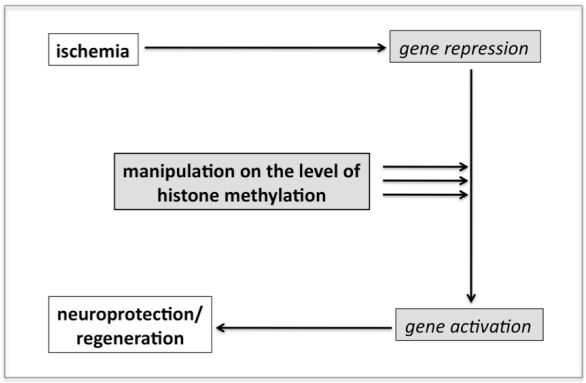

Figure 6 Graphic representation of the hypothesis
Ischemia induces a global state of gene repression. Manipulation on the epigenetic level (DNMT1 repression/HDAC inhibition) induces active gene transcription and a state of neuroprotection. Accordingly, interventions on the level of histone methylation might as well influence cell survival post ischemia.

3.1. Topics of investigation

3.1.1. Global histone methylation states in experimental ischemia

Altered epigenetic patterns are part of the ischemic pathology. Observed were elevated global DNA methylation levels post ischemia [*Endres et al.*, 2000; *Endres et al.*, 2001] as well as decreased global H4 acetylation levels [*Langley et al.*, 2008; *Xuan et al.*, 2012; *Yildirim et al.*, 2008], both epigenetic marks of gene repression. Whether signs of gene repression can be monitored on the level of histone methylation post ischemia remains uninvestigated so far.

3.1.2. HIF regulation of histone de-/methylases in hypoxia

The transcription factor HIF regulates a large number of important genes involved in the endogenous response to ischemia and mediates multiple transcriptional changes. Does it directly influence histone methylation by up- or downregulating selected histone methyltransferases or histone demethylases?

3.1.3. The manipulation of selected histone de-/methylases, neuronal survival post OGD and novel neuroprotective agents

A general transcriptional repression is observed after stroke and the manipulation of epigenetic marks towards increased transcription ameliorates outcome according to various studies. The question arises whether the manipulation (knockdown/ overexpression) of single enzymes involved in histone methylation can produce any effect – be it protection, or exacerbation of damage - under conditions of experimental stroke, by influencing the transcriptional activity. According to knowledge from other epigenetic levels, the induction of a transcriptional activator, as well as the inhibition/knockdown of enzymes acting as transcriptional repressors can protect neurons subjected to OGD and vice versa (**Fig. 6**).
The pharmacological inhibition of histone deacetylases is neuroprotective in ischemia. Do pharmacological inhibitors of histone de-/methylating enzymes exist, that are able to confer protection to neurons subjected to OGD? Addressing this question might provide a chance to discover novel neuroprotective agents.

3.1.4. The manipulation of selected histone de-/methylases and the transcription of target genes post OGD

If histone methylation can be manipulated to yield neuroprotection in experimental stroke, it would be interesting to investigate over which downstream target genes and pathways the effect is mediated. Are promoter histone modifications altered together with expression levels of candidate genes in the ischemic versus a protected state?

3.2. Challenge: the selection of candidate enzymes

A straightforward hypothesis can be formed according to knowledge based on DNA methylation and histone acetyaltion in stroke (**Fig. 6**). However, a much a higher complexity has to be faced in the young field of histone methylation, were marks and enzymes are both numerous and extremely specific. It is impossible to target all enzymes acting as transcriptional repressors/activators at once, as feasible with pan-

HDAC inhibitors on the level of histone acetylation. As a consequence, a more narrow approach involving few candidate enzymes has to be pursued studying histone methylation. Studies from more advanced fields regarding histone methylation, cancer and developmental research, helped to tackle the difficult question of the choice of candidate enzymes. Finally, 5 enzymes, all expressed in cortical neurons, were chosen for a more extensive investigation in experimental ischemia: the histone demethylase KDM3A as example of a transcriptional activator, the four enzymes SUV39H1, G9a, LSD1 and ESET were chosen for the analysis of transcriptional repressors.

3.2.1. The histone demethylase KDM3A - a transcriptional activator

KDM3A (JMJD1A) belongs to the family of Jumonji-domain containing enzymes. It is a dioxygenase and requires the cofactors Fe(II) and alpha-ketoglutarate to specifically demethylate mono- and dimethyl-H3K9 [*Ozer and Bruick*, 2007; *Yamane et al.*, 2006]. KDM3A acts as transcriptional activator as it catalyses the switch of the repressive H3K9 dimethylation mark to the active marks of H3K9me1 and unmethylated H3K9, which can consequently be acetylated (H3K9ac) (**Fig. 7**).

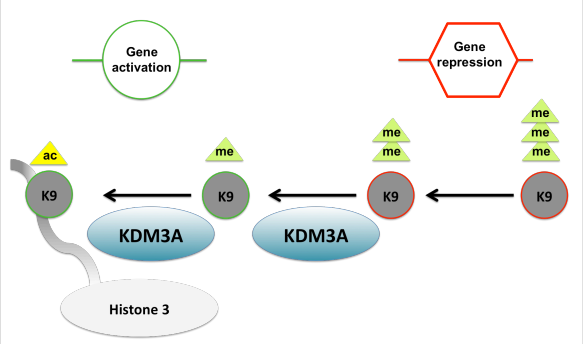

Figure 7 The histone demethylase KDM3A and H3K9 methylation

3.2.2. Transcriptional repressors: The histone methyltransferases SUV39H1, G9a and ESET

SUV39H1 (KMT1A), **G9a** (KMT1C) and **ESET** (KMT1E) are representatives of H3K9 methyltransferases each displaying distinct specificity, function and target regions as well as target genes (**Fig. 8**). Potentially, they all act as transcriptional repressors. ESET/SETDB1 has not yet been extensively characterized. In vivo it is responsible for the step from H3K9 dimethylation to H3K9 trimethylation, both repressive marks [*Ryu et al.*, 2006]. Biochemically the methyltransferases SUV39H1 and G9a are able to methylate H3K9me1/me2/me3. In vivo they show distinct

functions. SUV39H1 is the major KMT for H3K9 trimethylation at pericentric heterochromatin, while G9a is responsible for H3K9 mono- and dimethylation in euchromatic regions. It directly catalyzes the switch from repressive to activating H3K9 methylation marks [*Rice et al.*, 2003; *Tachibana et al.*, 2002].

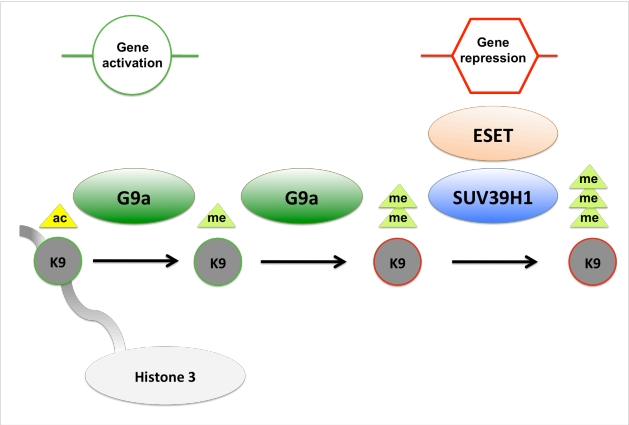

Figure 8 The histone methyltransferases ESET, SUV39H1 and G9a and H3K9 methylation

3.2.3. Transcriptional repressors: The histone demethylase LSD1

LSD1, the first identified histone demethylase, is a flavin-containing amino oxidase and catalyses the switch between H3K4me2/1/0 in a flavin and oxygen dependent manner. H3K4me2 and me1 are marks correlating with actively transcribed genes - LSD1 can hence act as transcriptional repressor by eradicating the activating methylation marks [*Forneris et al.*, 2005; *Forneris et al.*, 2008; *Shi et al.*, 2004] (**Fig. 9**).

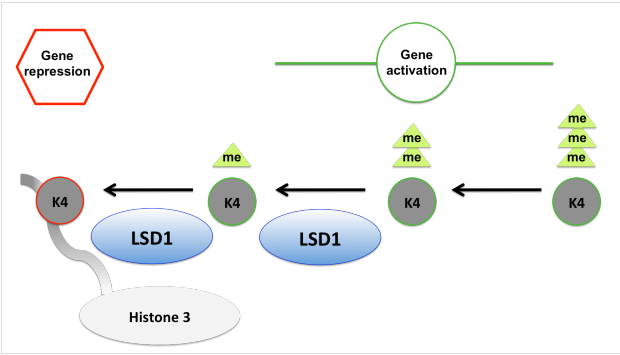

Figure 9 The histone demethylase LSD1 and H3K4 methylation

4. Materials and Methods

4.1. Materials

4.1.1. Cell culture media and supplements

B27 Supplement	Gibco (Karlsruhe, Germany)
Dulbecco's modified Eagle's medium (DMEM) (FG 0435)	Biochrom (Berlin, Germany)
Dulbecco's modified Eagle's medium (DMEM) high glucose	Biochrom (Berlin, Germany)
Dulbecco's phosphate-buffered saline (DPBS)	Biochrom (Berlin, Germany)
Fetal calf serum (FCS)	Biochrom (Berlin, Germany)
Fetal calf serum, Gold (FCS.Gold)	PAA (Linz, Austria)
Glutamate	Sigma (Taufkirchen, Germany)
HEPES	Biochrom (Berlin, Germany)
L-Glutamine	Biochrom (Berlin, Germany)
MEM-Earle	Biochrom (Berlin, Germany)
Neurobasal medium (NBM)	Gibco (Karlsruhe, Germany)
Non-essential amino acids	Sigma (Taufkirchen, Germany)
Penicillin/ Streptomicin	Biochrom (Berlin, Germany)
Poly-L-Lysine (PLL)	Biochrom (Berlin, Germany)
Sodium Pyruvate	Biochrom (Berlin, Germany)

4.1.2. Chemicals

Agarose	Sigma (Taufkirchen, Germany)
Ammonium persulphate (NH4)2S2O8	Sigma (Taufkirchen, Germany)
b-mercaptoethanol	Merck (Darmstadt, Germany)
b-NADH	Sigma (Taufkirchen, Germany)
Bacto-tryptone	Sigma (Taufkirchen, Germany)
Bacto-yeast extract	Sigma (Taufkirchen, Germany)
Bromphenol blue	Sigma (Taufkirchen, Germany)
Bovine serum albumin powder	Serva (Heidelberg, Germany)
Calcium chloride (CaCl2)	Sigma (Taufkirchen, Germany)
Chloroform	Merck (Darmstadt, Germany)
Chaetocin ($C_{30}H_{28}N_6O_6S_4$)	Sigma (Taufkirchen, Germany)
Coomassie brilliant blue G	Fluka (Munich, Germany)
Diethylpyrocarbonate	Sigma (Taufkirchen, Germany)
Dimethylsulphoxide (DMSO)	Sigma (Taufkirchen, Germany)
Dipotassium phosphate (K2HPO4)	Sigma (Taufkirchen, Germany)
DTT	Bio-mol (Hamburg, Germany)
Ethylenediaminetetraacetic acid (EDTA)	Sigma (Taufkirchen, Germany)

Ethanol	J.T. Baker (Deventer, Holland)
Ethyleneglycoltetraacetic acid (EGTA)	Sigma (Taufkirchen, Germany)
Glycerol	Merck (Darmstadt, Germany)
Glycine	Sigma (Taufkirchen, Germany)
Hydrochloric acid (HCl)	Sigma (Taufkirchen, Germany)
Isofluorane (Forene)	Abbott (Switzerland)
Isopropanol	Roth (Karlsruhe, Germany)
K252a	Sigma (Saint Louis, Missouri)
Lithium chloride (LiCl)	Sigma (Taufkirchen, Germany)
Lauryl sulphate (SDS)	Sigma (Taufkirchen, Germany)
LDH-standard TruCal-U Greiner,	DiaSys (Flacht, Germany)
Magnesium chloride ($MgCl_2$)	Serva (Heidelberg, Germany)
Magnesium sulphate, heptahydrate	Sigma (Taufkirchen, Germany)
Methanol	Roth (Karlsruhe, Germany)
Milk powder (blocking grade)	Roth (Karlsruhe, Germany)
Mithramycin ($C_{52}H_{76}O_{24}$)	Sigma (Taufkirchen, Germany)
Monosodium phosphate (NaH2PO4)	Sigma (Taufkirchen, Germany)
Monopotassium phosphate (KH2PO4)	Sigma (Taufkirchen, Germany)
N- Lauryl-Sarcosine ($CH_3(CH_2)_{10}CON(CH_3)CH_2COOH$)	Sigma (Taufkirchen, Germany)
Nonidet P 40 (NP40)	Sigma (Steinheim, Germany)
Phenelzine ($C_8H_{12}N_2 \cdot H_2SO_4$)	Sigma (Taufkirchen, Germany)
Phosphate buffered saline (PBS)	Life technologies (Darmstadt, Germany)
Ponceau S solution	Sigma (Taufkirchen, Germany)
Potassium chloride (KCl)	Sigma (Taufkirchen, Germany)
Potassium dihydrogenphosphate (KH_2PO_4)	Merck (Darmstadt, Germany)
Potassium monohydrogenphosphate(K_2HPO_4)	Merck (Darmstadt, Germany)
Propidium iodide	Sigma (Steinheim, Germany)
Rotiphorese gel (30% acrylamid, 0,8% bisacrylamid)	Sigma (Taufkirchen, Germany)
Redsafe Nucleic Acid Stain	Intron Biotechnology (Korea)
Sodium butyrate($CH_3CH_2CH_2COONa$)	Sigma (Taufkirchen, Germany)
Sodium bicarbonate ($NaHCO_3$)	Sigma (Taufkirchen, Germany)
Sodium chloride (NaCl)	Roth (Karlsruhe, Germany)
Sodium deoxycholate ($C_{24}H_{39}NaO_4$)	Sigma (Taufkirchen, Germany)
Sodium fluoride (NaF)	Sigma (Taufkirchen, Germany)
Sodium orthovanadate (Na_3VO_4)	Sigma (Taufkirchen, Germany)
Sodium pyruvate ($CH_3COCOONa$)	Sigma (Taufkirchen, Germany)
TEMED	Sigma (Taufkirchen, Germany)
Tranylcypromine ($C_9H_{11}N \cdot HCl$)	Sigma (Taufkirchen, Germany)
Trichostatin A (TSA) (T8552)	Sigma (Schnelldorf, Germany)
Trizma-base	Sigma (Steinheim, Germany)
Trizma-HCl	Sigma (Taufkirchen, Germany)
Triton x-100	Sigma (Taufkirchen, Germany)
Trypsin/EDTA	Biochrom (Berlin, Germany)
Tween-20	Sigma (Taufkirchen, Germany)
UNC 0638	Sigma (Taufkirchen, Germany)

4.1.3. Antibodies, enzymes, reagents and kits

2log marker	NEB (Frankfurt am Main, Germany)
BCA protein assay kit (23225)	Thermo Scientific Pierce, Bonn (Germany)
BCA protein assay kit, reducing agent compatible (23250)	Pierce (Bonn, Germany)
Benzonase Nuclease	Novagen, Merck Millipore (Germany)
BsrGI	NEB (Frankfurt, Germany)
BLOCK-iT Pol II miR Expression Vector Kit (K493-00)	Life Technologies (Darmstadt, Germany)
CalPhos™ Mammalian Transfection Kit (631312)	Clontech (Saint-Germain-en-Laye, France)

dNTPs	Roche (Mannheim, Germany)
Donkey anti-rabbit HRP-linked (NA934)	GE Healthcare (Buckinghamshire, UK)
Dynabeads protein G	Novex life technologies (Darmstadt, Germany)
Glyogen	Roche (Mannheim, Germany)
Hoechst 33258, bis-benzimide	Sigma (Taufkirchen, Germany)
LightCycler-FastStartDNA-Master-Sybr-GreenI	Roche (Mannheim, Germany)
M-MLV-RT 200U/µl	Promgea (Madison, USA)
M-MLV-RT reaction buffer 5x	Promgea (Madison, USA)
MscI	NEB (Frankfurt, Germany)
Mouse anti NeuN	Chemicon (Temecula, CA, USA)
NEBNext ChIP-seq Library Prep Master Mix	NEB (Frankfurt am Main, Germany)
Nucleobond Extra Midi EF/Maxi EF Kit (740420.50)	Machery-Nagel GmbH6Co (Düren, Germany)
NucleoSpin Gel and PCR Clean-up Kit (740609.250)	Machery-Nagel GmbH6Co (Düren, Germany)
NucleoSpin RNA clean-up KIT (740948.250)	Machery-Nagel GmbH6Co (Düren, Germany)
PEG-it™ Virus Precipitate Solution	Systems Biosciences (Heidelberg, Germany)
Plasmid DNA Purification Kit (740615.250)	Machery-Nagel GmbH6Co (Düren, Germany)
Precision Plus Standard	Kaleidoscope Bio-rad (Munich, Germany)
Primer Mix	Roche (Mannheim, Germany)
Protease inhibitor cocktail	Roche (Mannheim, Germany)
Rabbit anti-acetylated histone H3 lysine 9 (9649)	Cell Signalling (Frankfurt am Main, Germany)
Rabbit anti-ß-actin (4967)	Cell Signalling (Frankfurt, Germany)
Rabbit anti-di-methyl-histone3 lysine 9 (4658)	Cell Signalling (Frankfurt, Germany)
Rabbit anti-di-methyl-histone3 lysine 4 (9725)	Cell Signalling (Frankfurt, Germany)
Rabbit anti- G9a (3306)	Cell Signalling (Frankfurt, Germany)
Rabbit anti- LSD1 (2184)	Cell Signalling (Frankfurt, Germany)
Rabbit anti-myc (2272)	Cell Signalling (Frankfurt, Germany)
Rabbit anti- SUV 39H1 (8729)	Cell Signalling (Frankfurt, Germany)
Rabbit anti-tri-methyl-histone3 lysine 9 (9754)	Cell Signalling (Frankfurt, Germany)
Rabbit anti-tri-methyl-histone3 lysine 4 (9751)	Cell Signalling (Frankfurt, Germany)
Rabbit Igg (2729)	Cell Signalling (Frankfurt, Germany)
RNA-Sin 40U/µl	Promgea (Madison, USA)
RQ1 RNase-free DNase	Promgea (Madison, USA)
RQ1 RNase-free DNase 10x reaction buffer	Promgea (Madison, USA)
T4 Ligase	NEB (Frankfurt, Germany)
Trizol	Ambion (Darmstadt, Germany)
Western- Lightning -Plus enhanced chemiluminesce Reagent	Perkin Elmer (Rodgau, Germany)
XBal	NEB (Frankfurt, Germany)

4.1.4. Tools and equipment

Bioruptor	Diagenode (Seraing, Belgium)
Blotting chamber Trans-Blot Semi-Dry Transfer Cell,	Biorad (Munich, Germany)
Camera DFC 360 X	Leica (Wetzlar, Germany)
Cell culture incubator	Nuaire, COTECH (Berlin, Germany)
Centrifuge, Universal 30 RF	Thermo Electron (Oberhausen, Germany)
Centrifuge, Sigma 3K30	Thermo Scientific (Osterode Harz, Germany)

Criterion cassettes	Bio-rad (Munich, Germany)
Criterion precast gel, 4-15% Tris HCL	Bio-rad (Munich, Germany)
Electrophoresis chamber Criterion,	Biorad (Munich, Germany)
Fluorescent microscope, DMRA2	Leica (Wetzlar, Germany)
Fluorescent microscope, DMI 6000 B	Leica (Wetzlar, Germany)
Illumina Sequencer HighSeq 1500	Illumina (San Diego, USA)
Inverted contrasting microscope, DM IL	Leica (Wetzlar, Germany)
Lightcycler 2.0	Roche (Mannheim, Germany)
Matercycler gradient	Eppendorf (Köln, Germany)
Multi-well cell culture plates	Falcon (Franklin Lakes, NJ, USA)
Nanodrop 2000 Spectrophotometer	Peqlab (Erlangen, Germany)
Nitrocellulose membrane	Bio-rad (Munich, Germany)
Nucleofactor Amaxa	Lonza (Kölln, Germany)
OGD chamber, Concept 400	Ruskinn Technologies (Bridgend, UK)
pH metre, pH100	VWR International (Darmstadt, Germany)
Plate reader MRX Revelation,	Thermo Labsystems (Dreieich, Germany)
Power supply, Power Pack 200	Bio-rad (Munich, Germany)
Sonicator, Sonorex Super 10P	Bandelin Electronic (Berlin, Germany)
Whatman paper	Biometra (Göttingen, Germany)

4.1.5. Animals and cells

HEK 293 FT Pseudoviral Particle Producer Cell Line	Invitrogen
One Shot™ STBL3 chemically competent *E.Coli*	Life technologies (Darmstadt, Germany)
One Shot® TopTen™ chemically competent *E.Coli*	Life technologies (Darmstadt, Germany)
Wistar rat (E17-18)	Forschungseinrichtungen für experimentelle Medizin (FEM), Charite (Berlin, Germany)

4.2. Methods

4.2.1. Primary cortical neuron cultures

Animal experiments were performed according to institutional and international guidelines approved by the local authorities. Primary rat cortical neurons were derived from Wistar rats (E17), seeded in culture plates previously incubated with poly-L-lysine (5µG/ml in PBS w/o) for 1 hour at room temperature, and subsequently rinsed twice with PBS. Cells were seeded at a density of 175000 cells/cm^2 and cultivated in supplemented neurobasal medium (Starter) in 24 (for OGD, LDH, cell count and WB experiments), or 6-well plate (for mRNA and ChIP). Cultures were kept at 36.5°C and 5% CO_2 and were fed on DIV 4 with cultivating medium (starter medium without glutamate = "B27") by replacing half of the medium. Cultures treated with lentiviral constructs as well as neurons transfected for overexpression experiment had a slightly different feeding paradigm (see below).

The condition of the cultures was routinely assessed by light microscopy, prior to experiments. Cells transduced/transfected with constructs expressing fluorescent marker

protein were additionally analysed with the help of microscopic images taken pre and post ischemic injury. All OGD experiments were carried out on DIV 9, harvests of protein/mRNA/DNA took place between DIV 9 and 10 according to the time points of interest.
In every experiment sister colonies were used as control plates. All culture plates were handled in the same manner regarding routine cell culture procedures. In our primary cortical cell culture system, neuronal purity was always higher than 90% until DIV 14 with less than 10% astrocytes until DIV 14 and less than 1% microglia until DIV 28 as as previously demonstrated by immuno-cytochemistry [*Lautenschlager et al.*, 2000].

4.2.2. Culture of human embryonic kidney cells

Human embryonic kidney cells (HEK) cell cultures were used as producer cells for lentiviral constructs carrying miRNA constructs. HEK 293FT cells were purchased from Invitrogen and cultured in DMEM high glucose medium (+10% FCS, 1% Pen/strep, 1% sodium pyruvate, 1% Glutamine, 1% non-essential amino acids). According to density cells were with trypsinized, passaged to new culturing flasks and used for lentiviral production from passage 4 to p 15.

4.2.3. Chemicals and drug administration

Chemicals were purchased from Sigma Aldrich, Germany. **(Phenelzine** P6777; **Tranylcypromine** P8511; **BIX-01294** B9311; **Mithramycin** M6891**; Chaetocin** C9492 (lot 078K4137) and (lot 062M4099V); UNC0638 U4885). The BDNF blocker K252a was purchased from Sigma, Saint Louis. Apart from Tranylcypromine, which was solved in PBS in a 1 mM stock concentration, all other inhibitors were solved in dimethyl sulfoxide (DMSO) in 3 mM stock solutions and stored in aliquods at -20°C. With dilutions in PBS, dose –response curves were performed for each treatment the first time of usage by applying different concentration to neuronal cultures on DIV 8, 24 h prior to OGD followed by LDH level measurements from supernatants on DIV 10. The actual experiments were carried out with the respective non-toxic concentration of each inhibitor with diverse pretreatment times before OGD on DIV 9. Vehicle treated cultures received the dissolvent dilution corresponding to the concentrations of the reactive agent.
Applied end concentrations were: Mithramycin 10 nM, Chaetocin 30 nM, BIX-01294 at 100 nM, UNC0638 1 µM, Phenelzine at 100 µM and Tranylcypromine 10 µM, K252a 50 nM. The iron chelator Desferrioxamine (DFO) was applied in a 150 µm concentration for a duration of 48 h before mRNA harvest on DIV 10.

4.2.4. Oxygen-glucose deprivation as in vitro injury paradigm

As paradigm of experimental ischemia, we used combined oxygen-glucose deprivation (OGD), a widely used in vitro model. OGD experiments were performed on DIV 9. The length of the deprivation experiments was 130±5 min depending on the state of the culture assessed by light microscopy. The procedure took place as follows: culture medium was removed from cells and preserved in order to be able to apply "conditioned medium" after injury (1:1 collected medium and fresh culturing medium). In case cells had received a treatment, preserved collected medium without treatment was employed. Cells were then rinsed with PBS, placed in OGD chamber (a humidified, temperature controlled (36+/-0.5°C) chamber at PO2 < 2 mmHg). There, PBS was replaced by warmed balanced salt solution (BSS0), which was supplied to the chamber around 12 hours prior to the performance of the OGD experiment. OGD was terminated by taking the culture plates out of the OGD chamber and replacing BSS0 by warmed conditioned medium [*Bruer et al.*, 1997; *Harms et al.*, 2004]. Subsequently, culture plates were reoxygenated under normoxic conditions in the cell culture incubator. As OGD controls, served sister colonies remained under normoxic cell culture conditions in the incubator the whole time, but were subjected to the same medium exchange once OGD cultures were taken out of the OGD chamber. The condition of the cells at various time points after OGD was determined morphologically by phase contrast microscopy. 24 h post OGD aliquots of the medium were saved for the analysis of LDH activity.

4.2.5. miR-shRNA mediated knock down of target genes

4.2.5.1. Lentiviral miR-shRNA constructs

Interfering RNA target sequences were designed using the internet applications of Invitrogen (http://www5.invitrogen.com/custom-genomic-products/tools/mirna/). Diverse seed sequences consisting of 21 bases were selected per target gene and eventually tested for knockdown efficiency. For SUV39H1 knockdown two different seed sequences targeting the open reading frame were tested (5'-CTAGCCAAGCTTTCTTGTCCT-3´ = *mi-SUV39H1* and 5'-AGCAGGAGTATTACC TGGTTA-3´ = *mi2-SUV39H1*) of which the first was chosen for functional experiments. For G9a knockdown, tests of the following three sequences were undertaken (open reading frame: 5'-AAGTCTGAAGTCGAAGCTCTA-3´ = *mi-G9a;* 5'-TGACTTCAGCCTGTACTATGA-3´ = *mi2-G9a* and 5'-CGTGAGAGAGGATGAT TCTTA-3´ = *mi3-G9a*). Again the first sequence was chosen for functional tests and finally for LSD1 six different constructs were tested (targeting open reading frame: 5'-CACAAGGAAAGCTAGAAGA-3´ = *mi-LSD1*; 5'-TGTCGTCAGCAAACAAGTAA

A-3′ = *mi2-LSD1*; 5'-TAGACTTCAACGTCCTCAATA-3′ = *mi3-LSD1* and 5'-GGATGGGATTTGGCAACCTTA-3′ = *mi4-LSD1*; targeting 3' untranslated region: 5'-AGAGAGGAACTCACCCATTGA-3′ = *mi5-LSD1*; 5'-GTGGTGTAAGATAACCT CTTA-3′ = *mi6-LSD1*) of which the first seed sequence was chosen according to a publication reporting successful knock-down [*Metzger et al.*, 2005] and eventually employed for functional experiments.

Selected seed sequences were BLAST-searched against rat and mouse genome sequences to ensure target match with the genes of interest and to exclude unspecific targets. A non-targeting "scrambled" construct was used as control (AAATGTACTGCGCGTGGAGAC). The diverse seed sequences were designed as longer oligos, where they were embedded in a short hairpin loop structure (shRNA) (**Fig. 10 A**). With the help of the BLOCK-iT Pol II miR Expression Vector Kit (Invitrogen), microRNA-embedded short hairpin RNA (miR-shRNA) constructs were generated containing the respective oligos in microRNA cassettes within a simple intermediate expression vector. Excision of the whole micro RNA cassette (225 base pairs) was then performed with the help of the restriction enzymes XbaI and BsrGI and finally cloned into a third-generation lentiviral vector, based on Addgene plasmid 27232 (Dittgen 2004). The vector was slightly modified with the following changes: microRNA delivery was driven by a ubiquitin promoter and the reporter protein was exchanged with a myc-tagged red fluorescent protein (RFP) resulting in a vector of 10229 base pairs including the microRNA cassette (**Fig. 10 B**). The insertion of the microRNA cassette into the construct was first tested with the help of restriction digests with the enzyme MscI yielding three bands (795, 2632 and 6802 base pairs) and the correct base sequence was further verified by Sanger sequencing (primers: fw: AAGTTGGACATCACCTCCCACAAC; rev: AGCAGCGTATCCACATAGCG).

4.2.5.2. Lentivirus production

Lentivirus production took place in the producer cell line HEK 293 FT cultured as described above. The lentiviral vector with the respective miR-shRNA construct was cotransfected into HEK 293FT cells (Invitrogen) together with the packaging vectors psPAX (Addgene 12259) and 7.5pMD2G (Addgene 12260) with the calcium phosphate transfection method as described in Dull 1998. Cells were seeded in 175 cm^2 culture flasks and transfected the following day at 60-70% confluency. Viral harvest took place at 48 and 72 hours post transfection by collecting the supernatant. Concentration steps were carried out with PEG-it Virus Precipitation Solution (System Biosciences) and viral pellets were taken up in phosphate buffered saline (PBS) with magnesium and calcium and subsequently stored at -80°C in small aliquots.

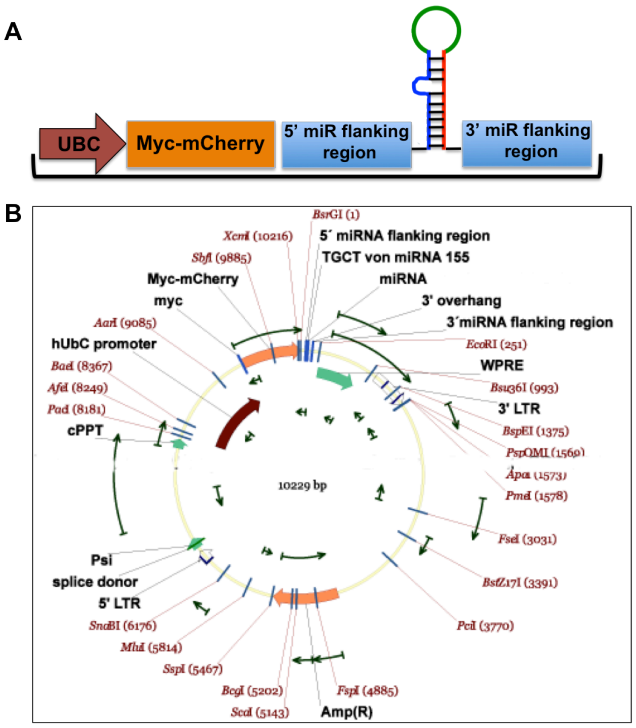

Fig. 10 Lentiviral miR-shRNA expression vector

A: Model of the construct: a ubiquitin promoter (UBC) drives the expression of a myc-tagged red fluorescent protein (mCherry) and the microRNA cassette, which consists of the interfering RNA containing short-hairpin construct (shRNA) within the 5'-3' micro RNA flanking sequences, which is based on the murine microRNA 155.

B: The whole lentiviral expression vector is depicted, displaying the microRNA cassette (upper part), restriction sites (red) and structures necessary for cloning, such as an Ampicillin resistance (Amp(R))or expression such as the long terminal repeat (LTR) for viral regulation of expression as well as the woodchuck hepatitis virus posttranscriptional response element (WPRE) to enhance expression.

4.2.5.3. Lentiviral titration and application

For titration neuronal cultures were transduced with viral solution on late DIV 1. Transduction efficiencies were determined and calculated from serial dilutions in neuronal cultures using RFP as a reporter for microscopic evaluation after 96 hours.
Regarding functional experiments, following viral application on late DIV 1, cells were fed fresh B27 medium on DIV 2 and 7 and in between a complete medium exchange was carried out on DIV 4. Oxygen glucose deprivation (OGD) was performed on DIV 9 and LDH measured 24 hours later on DIV 10. Included in the statistical analysis were experiments with transduction efficiencies above 80% assessed by comparing cell counts from phase contrast microscopy and RFP-positive neurons.

4.2.5.4. Evaluation of cell survival: cell counts

On DIV 9 pre OGD, as well as on DIV 10, 24 hours post OGD, epifluorescent microscopic images were taken with a Leica DMI 6000B microscope combined with a Leica DFC 360 FX camera and a computerized software program (Leica Application Suite V3.3.0). Ten regions of interest (ROIs) were preselected per well and repeatedly analysed at a 40x magnification, maintaining identical settings for all experiments. Red fluorescent protein-positive cells were counted in a blinded manner. Of the ten ROIs means were calculated per well ($N = 1$) and ratios from cell survival counts on DIV 10

compared to DIV 9 were calculated to assess the effect of enzyme knockdown on cell viability post OGD. Pre OGD, around 60 cells were counted per ROI. Per miRNA-shRNA construct an average of 10800 cells were analysed (60 x 10 ROIs x 9 wells x 2 OGD/CTRL condition) before OGD.
For microscopic visualization of neuronal survival, emitted fluorescence was pseudo-coloured in green in pre OGD images and in red 24 hours post OGD. Images were merged indicating the surviving neurons post OGD in yellow in the overlay image [*Datwyler et al.*, 2011].

4.2.6. Evaluation of cell damage: Lactate dehydrogenase assay

A colorimetric assay was used to quantitatively assess cytolysis 24 h after the injury paradigm. The cytosolic enzyme lactate dehydrogenase (LDH) is released into the supernatant by dying cells with damaged plasma membranes. LDH activity in the supernatant is hence proportional to the number of cells undergoing cell death. In the assay, the substrate of LDH, pyruvate, and its cofactor ß-NADH are added to the supernatant inducing catalytic activity. During the reaction the cofactor ß-NADH is reduced to NAD+, a turnover that can be assessed photometrically by excitation with 340 nm wavelength [*Koh and Choi*, 1987]. Accordingly, 50 µl of culture medium were pipetted in duplicates into 96-well plates. 200µl of ß-NADH solution (0.15mg/ml) were added and the reaction started by adding pyurvate (25 µl of a 22.7 mM solution). 10 repeated optical density measurements took place at 340nm with 30 sec intervals in a microplate reader. Results were evaluated using an LDH-Standard (Greiner). In a second step, the same procedure was applied after total lysis of cells using 0.5% Triton-X for 30 minutes at 37°C. Ratios of the units of LDH activity per ml per well and the maximum LDH activity per well after total lysis were calculated and data presented as percentage of cell death/injury.

4.2.7. Overexpression of target genes

4.2.7.1. Plasmid DNA for overexpression experiments

For overexpression experiments neurons were transfected with pCAG-MCSn1 plasmids [*Mergenthaler et al.*, 2012]. They were previously derived from pDRIVE-CAG (Invivogen) by removing LacZ and inserting a multiple cloning site (MCS) from pEGFP-N1 (Clontech). Two different vectors were subcloned carrying either the green fluorescent protein EGFP from pEGFP-N2 (Clontech), or mOrange from pRSET-B-mOrange, a bright orange fluorescent protein (gift from R. Tsien, University of California, La Jolla, CA).

Further subcloning took place were the diverse target genes were cloned into the pCAG-MCSn1 vector, driven by the strongly expressing cytomegalo virus (CMV) promoter, same as with the fluorescent proteins. The target genes employed were KDM3A (purchased), SUV39H1 (Open Biosystems: MMM1013-7512706), LSD1 (Open Biosystems: MMM 1013-9335032) and BCL-XL as positive CTRL (PCR amplified from a murine neuronal cDNA library).
All plasmids were amplified in Escherichia-coli cells (One Shot Top 10, Life technologies) and purified with an endotoxin free DNA purification kit (Nucleobond, Machery-Nagel). To verify DNA sequence accuracy constructs were sequenced with the following primers: forward: 5' TTCGGCTTCTGGCGTGTGAC-3' reverse: 5' GTGGTTTGTCCAAACTCATC-3' targeting sites on the pCAG-MCSn1 vector surrounding the respective constructs.

4.2.7.2. Paradigm of overexpression experiments in OGD

Primary neurons were prepared and immediately transfected via electroporation using a nucleofactor (Amaxa) reaching transfection rate of approximately 30%. $3x10^6$ cells were either cotransfected with 5 µg mOrange plasmid DNA and 5 µg of the empty pCAG-MCSn1 plasmid DNA, or with 5 µg EGFP plasmid DNA and 5 µg DNA of the respective target gene, or the empty pCAG-MCSn1 vector as negative CTRL [*Mergenthaler et al.*, 2012]. Cells were seeded at usual densities into 24-well plates cocultivating orange fluorescent protein expressing cells and cells expressing EGFP and the target gene half and half in each well. The cultivating medium directly after transfection was based on high glucose DMEM (+10% FCS, 1% Pen/Strep, 25 µM glutamate). Four hours later a complete medium exchange took place using 1/3 of the same fresh medium and 2/3 of collected medium (same recipe, but collected from neuronal cultures and preserved especially for the purpose). 24 hours post transfection on DIV 1 a second complete medium exchange was conducted replacing the medium with 1/3 fresh and 2/3 collected neurobasal medium (+B27 supplement, 1% Pen/Strep, 0,5 mM glutamine). Cultures were fed DIV 4 and 7. On DIV 9, pre OGD, epi-fluorescent microscopic images were taken with a Leica DMI 6000B microscope combined with a Leica DFC 360 FX camera and a computerized software program (Leica Application Suite V3.3.0). Eighteen regions of interest (ROIs) were preselected per well and analysed at a 40x magnification. 24 hours post OGD, on DIV 10, cells were microscopically reanalysed using the same settings. Subsequently, green and orange fluorescing cells were counted per well in a blinded manner (around 280 fluorescent cells of each colour per well). Each experiment consisted of 3 wells for each

condition: negative CTRL (pCAG-MSCn1/EGFP and pCAG-MSCn1/mOrange); positive CTRL (BCL-XL/EGFP and pCAG-MSCn1/mOrange); target gene (KDM3A/EGFP and pCAG-MSCn1/mOrange), (LSD1/EGFP and pCAG-MSCn1/mOrange), (SUV39H1/EGFP and pCAG-MSCn1/mOrange). Survival of transfected neurons post OGD was assessed by calculating ratios of red and green fluorescing cells (**Fig. 11**).

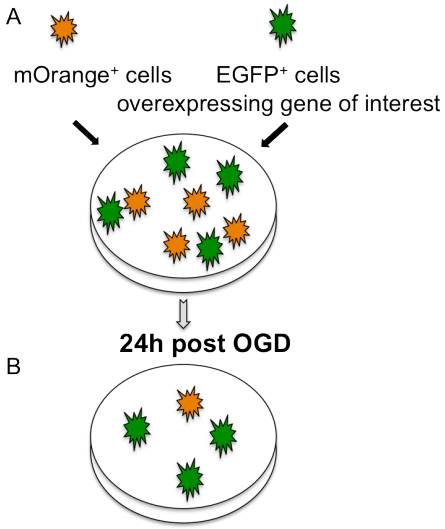

Figure 11 Cotransfection paradigm for overexpression experiments in OGD

A: Transfected cells expressing the gene of interest and a green fluorescent protein are cocultivated together with the same amount of orange fluorescing cells, which serve as controls. Pre OGD, cells are counted. A cell count ratio of 1 indicates equal amounts of green and orange cells. B: 24h post OGD surviving cells are recounted. Again, a cell count ratio of 1 indicates equal amounts of green and orange cells and is thus a sign that the overexpression of the candidate gene does not impact survival. Increased survival of green fluorescing cells results in a ratio higher than 1.

4.2.8. Gene expression analysis: immunoblots

For whole cell protein extraction cell cultures were lysed in ristocetin-induced platelet agglutination buffer (RIPA) (50mM Tris pH 7.4, 150 mM NaCl, 0.1% sodium dodecyl sulfate (SDS), 1% Triton x-100, 1% sodium deoxycholate; protease inhibitor cocktail (Roche) and 0.1% Benzonase Nuclease (Novagen)). 4 wells of a 24-well plate were harvested in 100 µl RIPA buffer, incubated on ice for 15 min, sonified for 1 min and centrifuged for 5 min at 4°C for removal of cellular debris. Protein concentration in the supernatant was determined by using a bicinchoninic acid protein assay kit (BCA) (Pierce) and supernatants stored at -80°C for further analysis using separation by gel electrophoresis (Biorad criterion electrophoresis chamber with precast gels 4-15%). Per probe, 30 µg of protein were denatured by boiling at 95°C in an equal volume of sample buffer (4% SDS, 0.2% bromphenol blue, 20% glycerol, 200 mM Dithiothreitol, Tris pH 6.8), loaded for SDS-PAGE, transferred to a nitrocellulose membrane under semi-dry blotting conditions, blocked in blocking buffer (5% milk in tris-buffered-saline solution with 0.1% Tween 20 (TBST)) for one hour at room temperature. Primary antibodies were applied in 5% bovine serum albumin (BSA) in TBST at 0.2-1 µg/ml and incubated

over night at 4°C under gentle agitation. Following short washing steps in distilled water, membranes were exposed to secondary horseradish-peroxidase-conjugated anti-rabbit antibody (GE Healthcare) diluted 1:5000 in 5% milk in TBST for 2 hours at room temperature und gentle agitation. Following three 10 min washing steps in TBST, protein detection took place by using an enhanced chemiluminscence assay (Perkin Elmer) and a Canon ES-78 camera together with a computerized software program (ProLine). As loading control anti-ß-actin (CS 4967) was employed. Primary antibodies for Western Blot were purchased from Cell Signalling (G9a: CS 3306; SUV39H1: CS 8729; LSD1: CS 2184; Myc: CS 2272; H3K9me3: CS 9754; H3K9me2: CS 4658, H3K9ac: CS 9649, H3K4me3: 9751, H3K4me2: CS 9725). For Western blot quantification ImageJ software (NIH) was used.

4.2.9. Gene expression analysis: polymerase chain reaction

For mRNA expression analysis, quantitative real time Polymerase Chain Reaction (qRT-PCR) was performed using LightCycler 2.0 (Roche). Briefly, whole cell mRNA was harvested in Trizol (1ml per 3 Mio cells) and stored at -20°C. Following chloroform extraction, RNA containing pellets were solved in diethylpyrocarbonate treated water. After DNase digest, PCR-inhibitors were removed with the help of NucleoSpin RNA clean-up KIT (Macherey Nagel). RNA concentration was measured using Nanodrop and probes were uniformly diluted. RNA was reverse transcribed to complementary DNA (cDNA) with M-MLV reverse transcriptase and random hexamers. For qRT-PCR the LightCycler-FastStartDNA-Master SYBR-Green-I Kit (Roche) was used. Amplification and detection relied on LightCyclerRelative Quantification Software (Roche Molecular Biochemicals). All PCRs were performed in duplicate. The relative expression of each gene of interest (GOI) was calculated compared to a reference gene (ref) by the delta Cp (crossing point) method with efficiency correction using the equation $E_{(GOI)}^{-Cp(GOI)} / E_{(ref)}^{-Cp(ref)}$. Mean values of duplicates were determined. The reference genes gene ß-actin and reep5 with the most stable expression patterns in OGD were chosen in a previously performed methodological study using NormFinder Software (ref). In all experiments, PCRs for both reference genes were performed and similar results obtained with either reference. Amplification efficiencies (E) were determined for each primer pair by a serial dilution curve and calculated using LightCycler 2.0 software.

Thermal cycling conditions and amplification efficiencies for each primer pair are listed in the table below.

Gene	Sequence 5'-3' fw. And rev.	Annealing temperature (Celsius)	Melting curve temperature (Celsius)	Elongation time (Celsius/sec)	Efficiency
ß-Actin	Acccacactgtgcccatcta Gccacaggattccataccca	68°	82°	72°/15	1.86
REEP5	Ctgataggtttcggatacccag Gactcgtgcttcaggaagatgg	68°	84°	72°/15	1.97
SUV39H1	Cgtgtagtccagaaaggcatcc Ccacgtagtccaggtcaaagag	68°	84°	72°/15	1.94
G9a	Tagcaacggacagcctccaatc Cttcagacttgctgtcagagtcc	68°	86°	72°/15	1.98
ESET	Gacccaaacatgtgcacaaatc Tgcaaagtactcatcacccatc	66°	82°	72°/15	1.99
LSD1	Gcctcagcagacacagaagg Gttataaggtgcttctaactgc	64°	80°	72°/15	2.06
KDM3A	Cagactcccccagcccggaa Gggcagctgtgccacgatgt	59°	81°	72°/15	1.94
BDNF	Cgtggggagctgagcgtgtg Tgcccctgcagccttccttc	66°	82°	72°/10	2.14
BCL-XL	Cctggcacctggcggatagc Gcgcttgcttcactgctgcc	66°	84°	72°/10	2.18
VEGF	Gctttactgctgtacctccacc Ctttggtctgcattcacatctgc	68°	84°	72°/15	2.14
GRIA	Gacaccccatatcgacaatttg Gatgaaggacacatggagtgtc	64°	77°	72°/15	2.11

4.2.10. Chromatin immunoprecipitation and sequencing (ChIP-Seq)

Around 50 million rat cortical neurons per condition (Chaetocin and vehicle treated, each pre and post OGD) were cultivated, pretreated with 30 nM Chaetocin/vehicle (see above) on DIV 8 and harvested on DIV 9. Cells were crosslinked in 1% formaldehyde in growth media for 10 min at 4°C, and the reaction stopped with 125 mM glycine. Cultures were rinsed in cold PBS, scraped, centrifuged and washed twice with PBS, and the pellet snap frozen in liquid nitrogen. Resuspension took place in a first lysis buffer (50 mM HEPES-KOH, pH7.5, 140 mM NaCl, 1 mM EDTA, 10% glycerol, 0,5% NP-40, 0,25% Triton X-100, freshly added protease inhibitors) for 10 min at 4°C followed by centrifugation and uptake in a second lysis buffer (10 mM Tris-HCl, pH 8.0, 200 mM NaCl, 1 mM EDTA, 0.5 mM EGTA) for 10 min, RT. The pelleted chromatin was solubilized (10 mM Tris-HCl, pH 8.0, 100 mM NaCl, 1 mM EDTA, 0.5 mM EGTA, 0,1% Na-Deoxycholat, 0,5% *N*-Lauroylsarcosine) and sheared by pulsed sonication for 40 min at 4°C in a bioruptor (Diagenode) to a bulk DNA reduction to less than 400 bp [*Lee et al.*, 2006]. Sheared chromatin was clarified by centrifugation at 20,000 g for 10 min. Per Immunoprecipitation 15 µg of DNA were used with 5 µg of H3K9ac antibody/IgG. Immune complexes were blocked with magnetic Dynabeads in RIPA +

0,25% BSA for 4h while rotating at 4°C, rinsed five times with cold RIPA and the precipitated complexes finally separated from the beads with elution buffer (50 mM Tris-HCl, pH8.0, 10 mM EDTA, 1.0% SDS) for 30 min at 65°C followed by centrifugation and collection of the supernatant. Crosslink reversal took place by adding 5 M NaCl at 65°C overnight. DNA was purificatied and precipitatitated with ethanol. Library preparation was conducted using NEBNext ChIP-seq Library Prep Master Mix for Illumina (New England Biolabs) according to manufacturer's protocol. Sequencing of 50 bp single reads was performed on an Illumina HiSeq 1500 using TruSeq v3 chemistry. Read mappping against rat genome rn5 reference genome was performed using BWA (version 0.5.9-r16) [*Li and Durbin*, 2009] allowing up to two mismatches per read. Non-uniquely mapped reads were discarded and redundant reads were removed using SAMtools rmdup [*Li et al.*, 2009]. Read counts in regions of interest were determined using BEDtools [*Quinlan and Hall*, 2010]. Different regions of analysis were selected per gene of interest and absolute read counts per region were normalized to total reads x 1,000,000.

Gene	Chromo-some	TSS	-1 kb	-3 kb	+1 kb	+2kb	Accession Nr	Position
Bmi1	17	87087687	87086687	87084687	87088687	87089687	NM_001107368.2	chr17:87087687-87091418
Hmox1	19	25622556	25621556	25619556	25623556	25624556	NM_012580.2	chr19:25622556-25629377
Gria2	2	199113059	199114059	199116059	199112059	199111059	NM_001083811.1	chr2:198991676-199113059
Bdnf	3	107371329	107370329	107368329	107372329	107373329	NC_005102.3	chr3:107371329-107421906
Bdnf	3	107372531	107371531	107369531	107373531	107374531	NM_001270631.1	chr3:107372531-107421906
Bdnf	3	107390141	107389141	107387141	107391141	107392141	NM_001270638.1	chr3:107390141-107421906
Bcl2l1	3	154715277	154716277	154718277	154714277	154713277	NM_001033671.1	chr3:154662586-154715277
Bcl2l1	3	154715412	154716412	154718412	154714412	154713412	NM_031535.2	chr3:154713126-154715412
Bcl-Xl	3	154716802	154717802	154719802	154715802	154714802	NM_001033670.1	chr3:154662586-154716802
Casp12	8	2681125	2680125	2678125	2682125	2683125	NM_130422.1	chr8:2681125-2708341
Vegfa	9	16232415	16231415	16229415	16233415	16234415	NM_031836.3	chr9:16232415-16247657
Vegfa	9	16239839	16238839	16236839	16240839	16241839	NM_001110336.1	chr9:16239839-16247657

To calculate significant differences between sequence reads the following assumtions were made: Given are two datasets for two conditions C1 and C2 consisting of N1 and N2 uniquely mapped reads. In a given genomic region for C1 and C2 we observe k1 and k2 mapped reads, repectively. Assuming that the reads for C1 and C2 are more or less equally distributed across the genome the difference between k1 and k2 only depends on N1 and N2. Different signal-to-noise-ratios for C1 and C2 are irrelevant in this context. The probability is modelled as a series of n = k1 + k2 Bernoulli experiments

with probability of success of p = N1/(N1 + N2). The probabilities follow the Binomial distribution:

$$\Pr(X = k_1) = \binom{n}{k_1} p^{k_1} (1-p)^{n-k_1}$$

For the calculation of the P-values the probabilities were summed up:

$$\text{P-value} = \sum_{i=k_1}^{n} \binom{n}{i} p^{i} (1-p)^{n-i}$$

4.2.11. Statistical analysis

Data are presented bar graphs, dot blots and box plots, with the bars representing mean ± 95 % confidence interval. Using SPSS (IBM) and GraphPad Prism (GraphPad, San Diego, CA, USA), t-tests, one-way and two-way ANOVAs (analysis of variance) were carried out with Tukey's *post hoc* analysis where indicated according to the experimental paradigm [*Schlattmann and Dirnagl*, 2010]. Experiments were at least performed in triplicate if not stated otherwise. *P*-values $\leq$ 0.05 were considered statistically significant.

5. Results

5.1. Global histone methylation post ischemia

In order to find out whether a global pattern of repression can be discerned on the level of histone methylation, selected histone methylation sites were analysed post oxygen glucose deprivation (OGD) - the in vitro model of stroke. Neuronal cultures were subjected to OGD on DIV 9, followed by whole cell protein harvest at various points in time between 0 and 24 h post injury. In immunoblots, protein levels of the diverse methylation states were compared to corresponding undamaged control cultures. On DIV 10 lactate dehydrogenase (LDH) levels of sister colonies were analysed in order to compare the cellular damage post OGD. Only protein of experiments with comparable ischemic damage was compared in immunoblots (LDH data not shown).

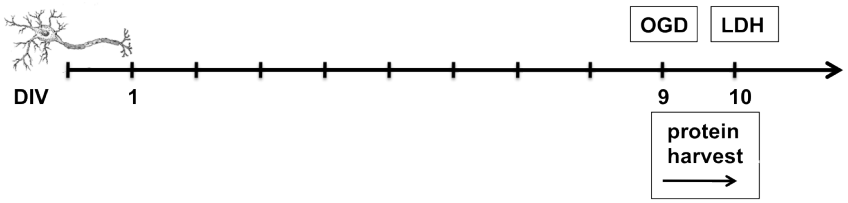

5.1.1. No discernable change in global histone methylation post OGD

To detect typical marks of repression, antibodies against H3K9me3 and me2 were applied. To assess a possible reduction in activating marks, H3K9me1, H3K9ac as well as H3K4me2 and me1 levels were analysed. A selection of representative immunoblots is shown in **Fig. 12** However, in spite of minor changes in few samples, no recurrent pattern in global H3K9me2/me3, H3K9me1/ac, or H3K4me3/me2 levels could be discerned in repeated experiments.

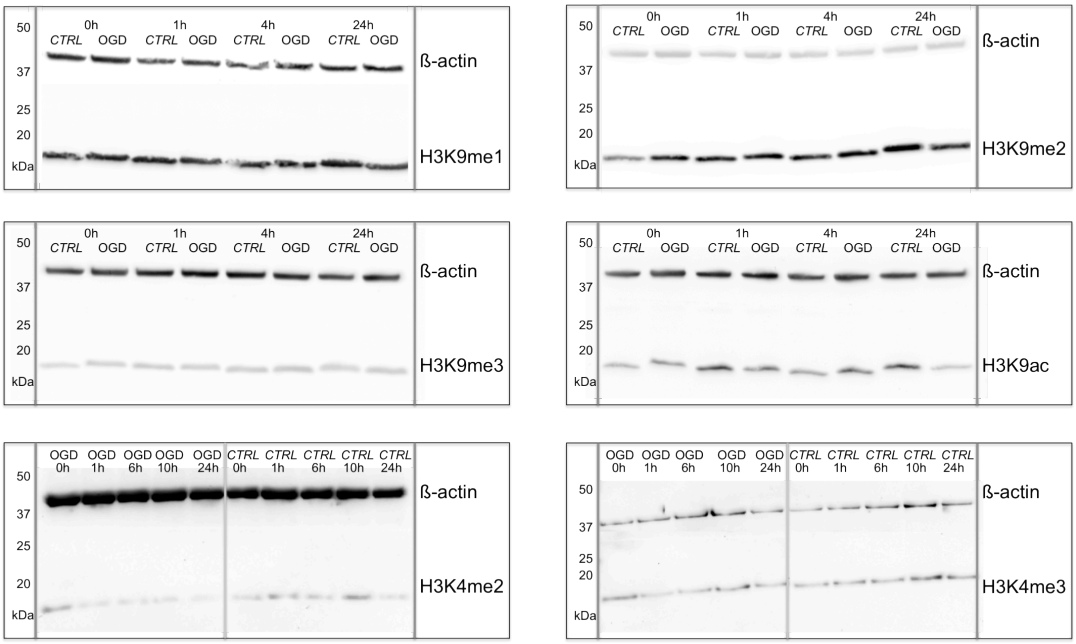

Figure 12 Immunoblot analysis of histone methylation marks (OGD versus CTRL)
6 representative immunoblots: whole cell protein of neuronal cultures subjected to OGD/CTRL harvested 0, 1, 4, 24 h /0, 1, 6, 10, 24 h post OGD (DIV 9), incubated with antibodies targeting H3K9me1, me2, me3, H3K9ac and H3K4me2, me3 to detect global epigenetic changes post OGD; loading control: ß-actin

5.2. HIF-dependency of selected histone de-/methylases

A typical signalling cascade of neuroprotection in ischemia is mediated by the transcription factor HIF1α, regulating a number of genes relevant for the cellular response to hypoxia. Whether the candidate histone de-/methylases SUV39H1, G9a, ESET, LSD1, or KDM3A are among the target genes of HIF1α was tested. On DIV 7, cortical neurons were subjected to a 48 h treatment with PBS or the iron chelator Desferrioxamine (DFO), a hypoxic mimetic and inductor of HIF1α. Cellular RNA and protein were harvested on DIV 9 and mRNA expression levels of the candidate genes were analysed compared to PBS treated controls.

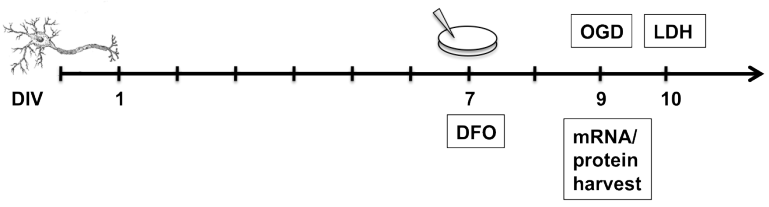

5.2.1. HIF increases mRNA and protein levels of KDM3A, bot not SUV39H1, G9a, ESET and LSD1

HIF1α accumulation led to a nearly five-fold induction of KDM3A mRNA expression levels (**Fig. 13 A**) and a significant increase in KDM3A protein levels upon DFO exposure (**Fig. 13 B**) . Global H3K9me2 levels, the target of KDM3A, however, show no changes upon HIF mediated KDM3A induction. The mRNA levels of SUV39H1, G9a, ESET and LSD1 were not affected by HIF1α induction (**Fig. 13 A**).

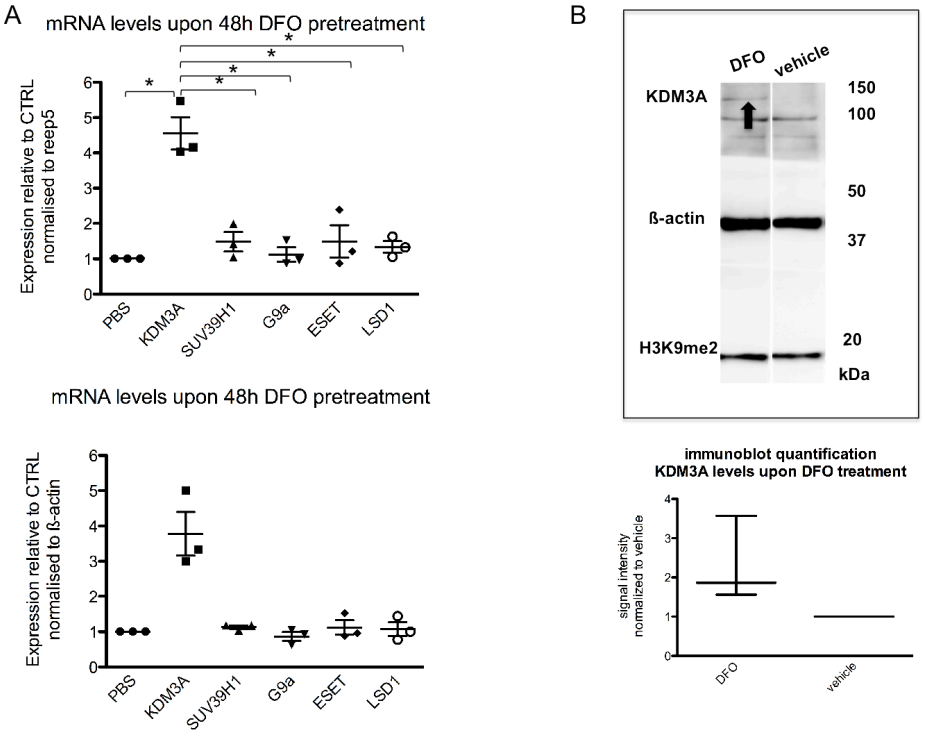

Figure 13 HIF dependency of diverse histone de-/methylating enzymes.
Neurons were subjected to 48 hours DFO treatment prior to mRNA/protein harvest.
A: mRNA levels of diverse histone de-/methylating enzymes are depicted normalised to reep 5 (upper graph), and to ß-actin (lower graph). All mRNA experiments were analysed using these two reference genes. As NormFinder rated reep5 even higher, only reep5 and the corresponding statistics will be depicted in the following plots. According to both reference genes, the histone demethylase KDM3A is significantly upregulated upon HIF induction, while SUV39H1, G9a, ESET and LSD1 show no change in expression. A one-way Anova was conducted to compare the effect of DFO treatment on mRNA levels of histone de-/methylases. There was a significant difference: $N = 3$, $F_{(5,12)} = 19.26$, $p < 0.001$. Post-hoc comparisons using Tukey's HSD test indicated that the mean score for KDM3A mRNA levels ($M = 4.55$, $SD = 0.79$) were significantly different from that of all the other groups (vehicle/ PBS: $M = 1$, $SD = 0$; SUV39H1: $M = 1.49$, $SD = 0.48$; G9a: $M = 1.12$, $SD = 0.36$; ESET: $M = 1.50$, $SD = 0.80$; LSD1: $M = 1.34$, $SD = 0.29$).
B: Exemplary immunoblot and blot quantification of KDM3A protein levels ($N = 3$); loading ctrl: ß-actin; H3K9me2 = KDM3A target

5.3. The manipulation of histone de-/methylases and neuronal survival post OGD

5.3.1. Overexpression of histone de-/methylating enzymes

To elucidate the role of selected histone de-/methylating enzymes in OGD, the effect of overexpression of the respective genes of interest was analysed. Neurons were cotransfected with an expression vector carrying the gene of interest and a vector expressing green fluorescent protein EGFP. These green fluorescent cells were cocultivated with orange fluorescent "control" cells (cotransfected with an empty expression vector and a vector expressing an orange fluorescent protein) in the same well (**Fig. 11**). Microscopic images were taken directly pre and 24 hours post OGD and fluorescing neurons were counted. Ratios of green and red fluorescent cells were calculated.

5.3.1.1. Overexpression of a transcriptional activator: KDM3A

Assumption: A surplus of KDM3A in the cell might shift repressive H3K9 methylation states towards the active marks (H3K9me1/H3K9ac) (**Fig. 14**) and thus influence the transcription of target genes and potentially mediate neuroprotection in OGD.

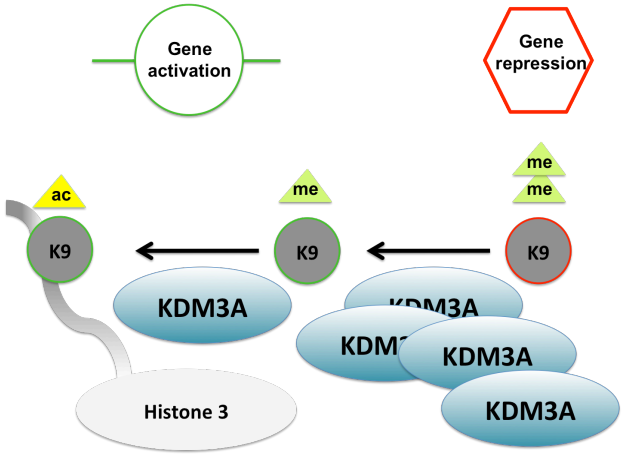

Figure 14 Hypothesis: overexpression of the histone demethylase KDM3A

Observation: Overexpression of the KDM3A gene yielded elevated KDM3A protein levels on DIV 9 but no global changes in H3K9me2 levels (**Fig. 15 A**). KDM3A overexpression did not impact neuronal survival 24 hours post OGD (**Fig. 15 B**).

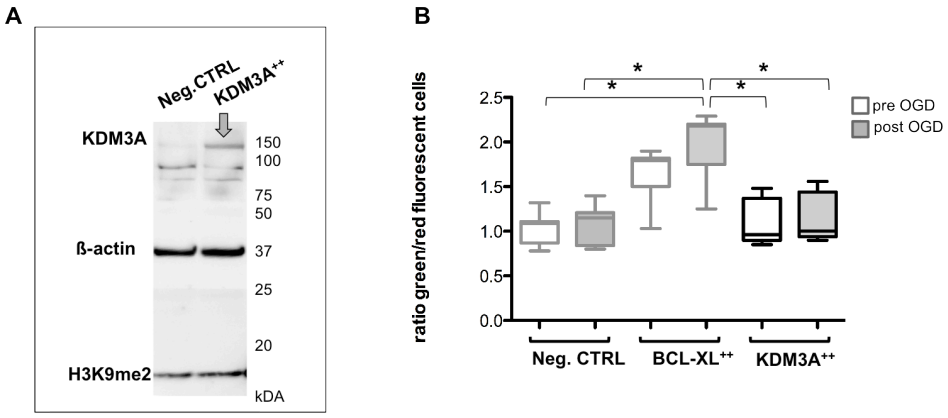

Figure 15 Overexpression of KDM3A in cortical neurons
A: Immunoblot: KDM3A overexpression, loading ctrl: ß-actin, KDM3A target: H3K9me2
B: Survival ratio of blinded cell counts of overexpression experiment with BCL-XL overexpression serving as positive CTRL; N = 7; mean ratios: Neg. CTRL: pre: 1.05; post: 1.08; BCL-XL**: pre: 1.63; post: 2.0; KDM3A^{++}: pre: 1.07; post: 1.13.

A two-way repeated measurements ANOVA was carried out that examined the effect of overexpression and time on neuronal survival in OGD. There was a significant interaction between overexpression and time $F_{(2,\ 18)} = 11.94$ with $p < 0.001$ Bonferroni posttest revealed a significant difference between positive CTRL (BCL-XL) overexpression and neg. CTRL values.

Source of Variation	DF	Sum of Squares	Mean Square	F	P
overexpression	2	5.011	2.506	18.38	<0.001
time	1	0.2469	0.2469	24.69	<0.001
overexpression x time	2	0.2389	0.1194	11.94	<0.001
Residual	18	0.1800	0.00999		
Total	41	8.130			

5.3.1.2. Overexpression of transcriptional repressors: SUV39H1 and LSD1

Assumption: The overexpression of selected transcriptional repressors could increase cell death post OGD, by reducing gene activation further (**Fig. 16**). The transcriptional repressors SUV39H1 and LSD1 were overexpressed using the same paradigm described above.

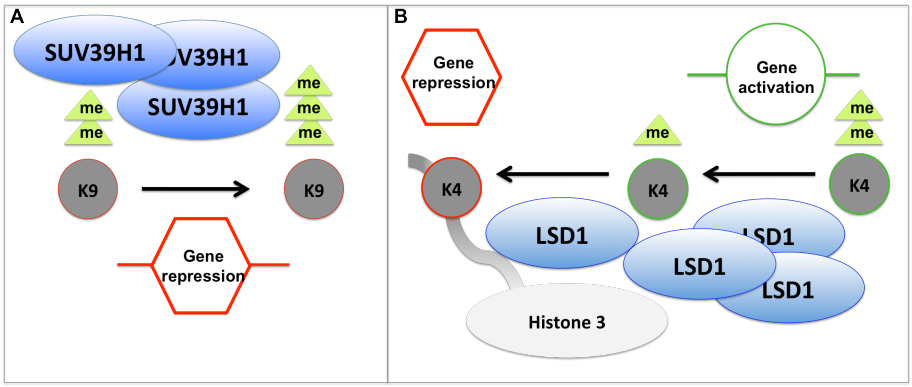

Figure 16 Hypothesis: overexpression of SUV39H1 and LSD1

Observation: SUV39H1 protein levels were increased in neurons on DIV 9 upon SUV39H1 overexpression (**Fig. 17 A)**, as well as LSD1 protein levels following exogenous LSD1 overexpression (**Fig. 17 C**). Neither SUV39H1, nor LSD1 overexpression impacted neuronal survival 24 hours post experimental stroke (**Fig. 17 B, D**).

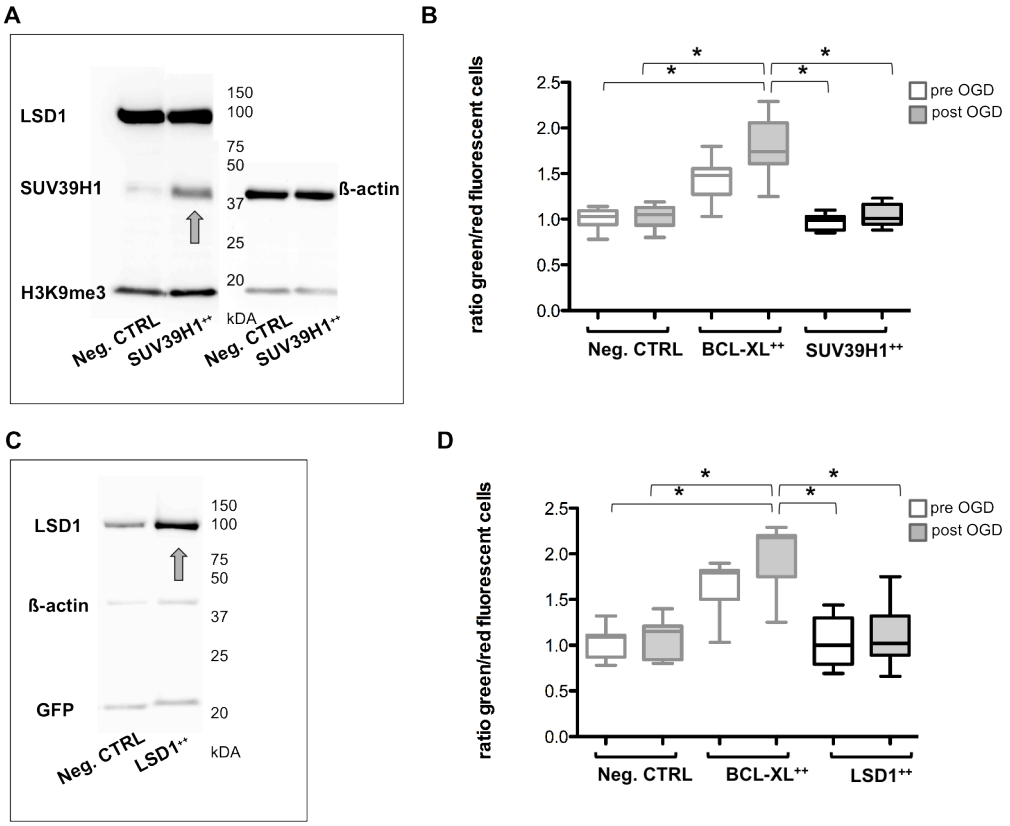

Figure 17 Overexpression of SUV39H1 and LSD1 in cortical neurons
A: Immunoblot: SUV39H1 overexpression, loading ctrl: LSD1 and ß-actin, SUV39H1 target H3K9me3
B: SUV39H1 overexpression: *N* = *9*; mean ratios: neg. CTRL: pre: 1.01; post: 1.0; pos. CTRL = BCL-XL: pre: 1.44; post: 1.79; SUV39H1: pre: 0.96; post: 1.04; 3
C: Immunoblot: LSD1 overexpression, loading ctrl: ß-actin, GFP = green fluorescent protein expression
D: LSD1 overexpression: *N* = 7; mean ratios: neg. CTRL: pre: 1.05; post: 1.08; : pos. CTRL = BCL-XL: pre: 1.63; post: 2.00; LSD1: pre: 1.02; post: 1.10;
B, D: Two-way repeated measurement analyses were carried out as with KDM3A described in Fig. 15. with significant interaction between overexpression and time but no significant difference in the groups of interest LSD1 /Suv39H1 versus neg. CTRL. Statistical details not shown.

5.3.2. Pharmacological inhibitors of repressive histone de-/methylases

Pharmacological inhibition of HDACs, which act as transcriptional repressors, leads to significant protective and regenerative effects in multiple neurological pathologies including ischemia [*Schweizer et al.*, 2013]. Certain inhibitors are considered as treatment option and being tested in clinical trials of other neurological pathologies [*Cudkowicz et al.*, 2009; *Hogarth et al.*, 2007].

Here, we aimed at investigating new inhibitors of selected repressive histone de-/methylating enzymes in the context of ischemic injury. Pharmacological inhibitors of KMTs/KDMs that are applicable in vivo are not easily found as yet, as histone methylation as a field of research is not older than a decade [*Copeland et al.*, 2010; *Spannhoff et al.*, 2009; *Wigle and Copeland*, 2013].

First toxicity tests of different concentrations of each inhibitor were conducted. Rat cortical neurons were pretreated with the respective inhibitor on DIV 8, 24 hours before injurious OGD for 130±5min on DIV 9. 24 hours post OGD, lactate deydrogenase (LDH) release into the supernatant was measured per well in order to indirectly assess cell damage via increase of LDH activity. A second LDH measurement took place after total cell lysis. The percentage of cell death was calculated per well by quantifying the first LDH measurement relative to the amount of LDH release after total lysis.

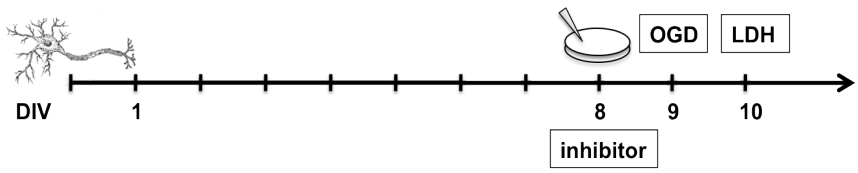

Following dose-response testing, functional experiments were conducted with non-toxic concentrations of each inhibitor by using the same paradigm of pretreatment on DIV 8, OGD on DIV 9 and LDH measurements 24 hours post injury in repeated experiments. Mean values of three wells per condition were formed in each independent experiment.

5.3.2.1. Pharmacological inhibition of histone methyltransferases

- Chaetocin –

Chaetocin is an alkaloid with antibacterial and cytostatic activity produced by *Chaetronium minutum [Hauser et al., 1970]*. The fungal metabolite was the first inhibitor of a KMT to be discovered. It was suggested to specificically inhibit SUV39 family members with the strongest inhibitory effect against SUV39H1 and to a lesser

extent against G9a [*Greiner et al.*, 2005; *Iwasa et al.*, 2010]. In vivo Chaetocin treatment induced a loss of H3K9 trimethylation at specific promoters together with an increase in H3K9 acetylation and gene expression [*Bernhard et al.*, 2011; *Cherrier et al.*, 2009].

Assumption: In experimental stroke, Chaetocin treatment could reduce repressive H3K9me2 and H3K9me3, induce gene exression and be protective (**Fig. 18**).

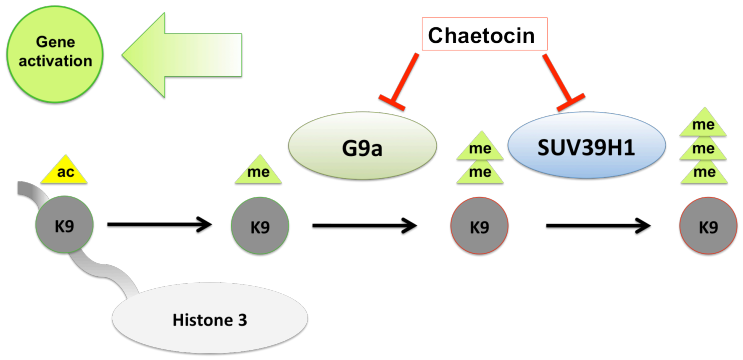

Figure 18 Hypothesis: Chaetocin inhibition of SUV39H1 and G9a

Chaetocin: dose-response testing

Chaetocin dose-response testing revealed low toxicity below 60 nM dosage (**Fig. 19 A**) as well as a tendency towards decreased cell death in ischemia upon pretreatment with 3 - 100 nM. A concentration of 30 nM showed the strongest protection (**Fig. 19 B**).

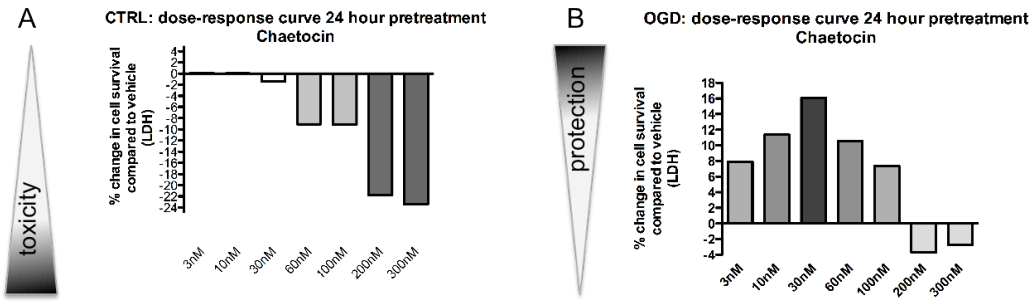

Figure 19 Dose-response testing: Chaetocin
LDH measurements of Chaetocin versus vehicle treated neuronal cultures
A: Chaetocin toxicity in CTRL cultures. (- 5% = 5% more cells died in inhibitor treated group compared to vehicle treated group)
B: Chaetocin protection in OGD cultures. (+5% = 5% more cells survived OGD in inhibitor treated group compared to vehicle treated group)

Chaetocin: functional experiments

24 hours pretreatment with 30 nM Chaetocin significantly protected neurons post OGD (**Fig. 20**). 44.8% of neurons died in the vehicle treated group versus 35.1% in the Chaetocin treated group after experimental stroke. Cellular survival in control cultures at normoxia was not affected by Chaetocin administration. Chaetocin could hence be identified as novel neuroprotective agent.

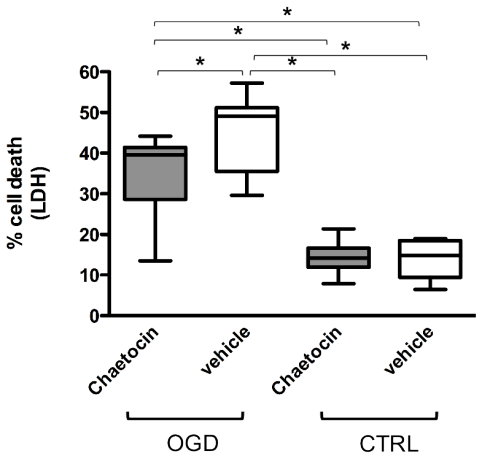

Figure 20 Pretreatment with 30 nM Chaetocin induces neuroprotection in OGD

Rat cortical neurons treated with Chaetocin/ vehicle on DIV 8, subjected to OGD on DIV 9, LDH measurements on DIV 10
N = 10; Chaetocin: Mean (*M*) = 35.096, *SD* = 8.750; vehicle: *M* = 44.804, *SD* = 9.724
A two-way ANOVA was conducted that examined the effect of OGD and treatment on cell survival. There was a significant interaction between effects of OGD and treatment: $F_{(1,\ 36)} = 4.714$ with $p = 0.037$ for interaction.
To isolate significant differences between groups a Tukey post-hoc analysis was performed. Significant effects are indicated in the figure * = $p < 0.005$

Tests of Between-Subjects Effects

Dependent Variable: LDH

Source	Type III Sum of Squares	df	Mean Square	F	Sig.
OGD	6567.688	1	6567.688	128.399	0.000
treatment	230.16	1	230.16	4.5	0.041
OGD * treatment	241.13	1	241.13	4.714	0.037
Error	1841.422	36	51.151		
Total	38335.442	40			

- BIX-01294 -

Library scans resulted in the discovery of BIX-01294 (diazepin-quinazolin-amine derivative), a novel specific inhibitor of G9a [*Chang et al.*, 2009; *Kubicek et al.*, 2007].

Assumption: In experimental ischemia, the inhibition of G9a through BIX-01294 treatment could reduce repressive H3K9me2, induce gene activation and protect neurons (**Fig. 21**).

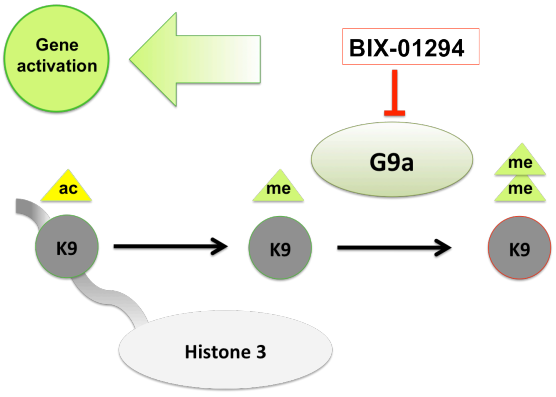

Figure 21 Hypothesis: BIX-01294: inhibition of G9a

BIX-01294: dose-response testing

BIX-01294 shows no signs of toxicity at concentrations of 50 nM to 100 nM. Toxicity starts at dosages of 200 nM and higher. As a very slight protective tendency could be assessed upon treatment with 100 nM BIX-01294, functional tests were extended with this concentration in OGD (**Fig. 22**).

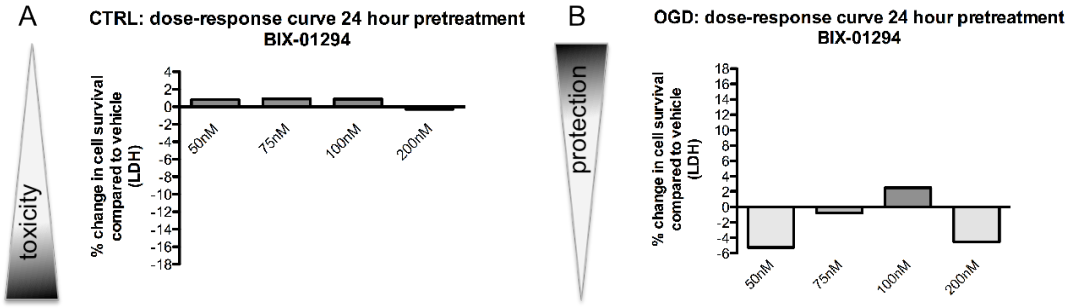

Figure 22 Dose-response testing: BIX-01294
LDH measurements of BIX-01294 versus vehicle treated neuronal cultures
A: BIX-01294 toxicity in CTRL cultures (explanation see Fig. 19)
B: BIX-01294 protection in OGD cultures

BIX-01294: functional experiments

24 hour pretreatment of neurons with 100 nM BIX-01294 showed no significant protective effect upon neuronal survival in OGD (**Fig. 23**). The difference between BIX-01294 treated cells versus vehicle treated cells amounts to 2.57% with a mean percentage of cell death of 25.69 in the treated versus 28.22 in the vehicle treated group subjected to OGD.

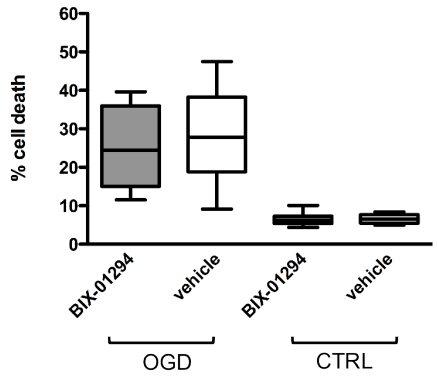

Figure 23 100 nM BIX-01294 pretreatment does not promote neuronal survival in OGD

Rat cortical neurons treated with BIX-01294/ vehicle on DIV 8, subjected to OGD on DIV 9, LDH measured on DIV 10
N = 10; BIX-01294: *M* = 25.69, *SD* = 10.43
vehicle: *M* = 28.22, S*D* = 12.45
A two-way ANOVA was conducted that examined the effect of OGD and treatment on cell survival. There was no significant interaction between effects of OGD and treatment: $F_{(1,\ 36)} = 0.204$ with $p = 0.654$ for interaction.

Tests of Between-Subjects Effects

Dependent Variable: LDH

Source	Type III Sum of Squares	df	Mean Square	F	Sig.
OGD	4191.847	1	4191.847	62.59	0.000
treatment	18.469	1	18.469	0.276	0.603
OGD * treatment	13.642	1	13.642	0.204	0.654
Error	2411.036	36	66.973		
Total	17813.986	40			

- UNC0638 -

Based on the structural knowledge of BIX-01294, new inhibitors were designed with optimized potency, increased specificity as well as low toxicity. The most recent was UNC0638 [*Vedadi et al.*, 2011].

Assumption: In experimental ischemia, G9a inhibition with UNC0638 treatment could reduce repressive H3K9me2, induce gene activation and protect neurons (**Fig. 24).**

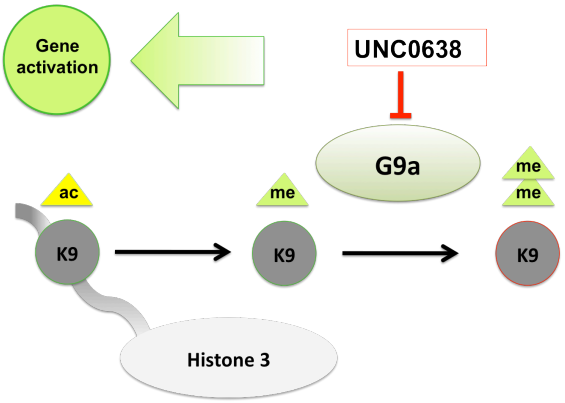

Figure 24 Hypothesis: UNC0638, an inhibition of G9a

UNC0638: dose-response testing

Dose-response tests with UNCO638 revealed an increasingly toxic effect upon pretreatment from 0.1 to 10 µM concentration. No clear protective tendency could be assessed with any concentration (**Fig. 25**).

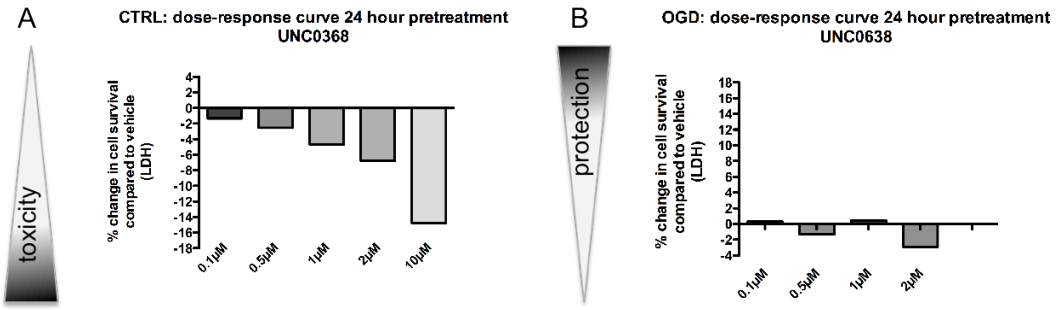

Figure 25 Dose-response testing: UNC0638
LDH measurements of UNC0638 versus vehicle treated neuronal cultures
A: UNC0638 toxicity in CTRL cultures
B: UNC0638 protection in OGD cultures

UNC0638: functional experiments

Several concentrations were evaluated in functional OGD experiments. Representative experiments with a 1 µM dosage of UNC0638 are shown. No concentration with low toxicity showed any tendency towards neuronal protection in OGD **(Fig. 26)**.

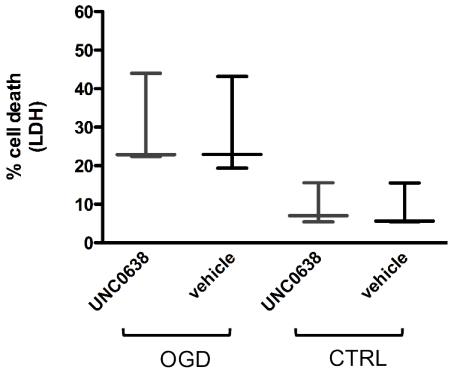

Figure 26 1 µM UNC0638 pretreatment does not affect neuronal survival in OGD

Rat cortical neurons treated with UNC0638/ vehicle on DIV 8, subjected to OGD on DIV 9, LDH measured on DIV 10
N = 3; UNC0638: *M* = 29.76, S*D* = 12.30; vehicle: *M* = 28.49, S*D* = 12.81
A two-way ANOVA was conducted that examined the effect of OGD and treatment on cell survival. There was no significant interaction between effects of OGD and treatment: $F_{(1, 8)} = 0.005$ with $p = 0.945$ for interaction.

Tests of Between-Subjects Effects

Dependent Variable: LDH

Source	Type III Sum of Squares	df	Mean Square	F	Sig.
OGD	1202.509	1	1202.509	12.676	0.007
treatment	2.224	1	2.224	0.023	0.882
OGD * treatment	0.489	1	0.489	0.005	0.945
Error	758.938	8	94.867		
Total	6351.140	12			

- Mithramycin -

The polyketide Mithramycin is a clinically approved antitumor antibiotic produced by the soil bacteria *Streptomyces agrillaceu*m with inhibitory effects against the histone methyltransferase ESET.

Assumption: ESET inhibition by Mithramycin could reduce repressive H3K9me3 and confer neuroprotection to cortical neurons in OGD (**Fig. 27**).

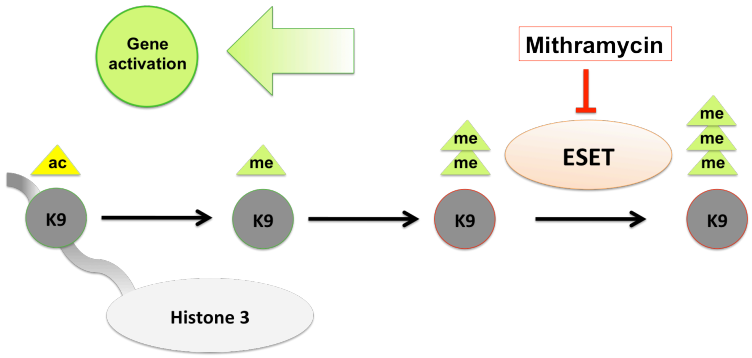

Figure 27 Hypothesis: Mithramycin inhibition of ESET

Mithramycin: dose-response testing

Dose-response tests with Mithramycin revealed an increasingly toxic effect upon pretreatment from 40 to 80 nM concentration. A protective tendency around 10-20 nM could be assessed (**Fig. 28**).

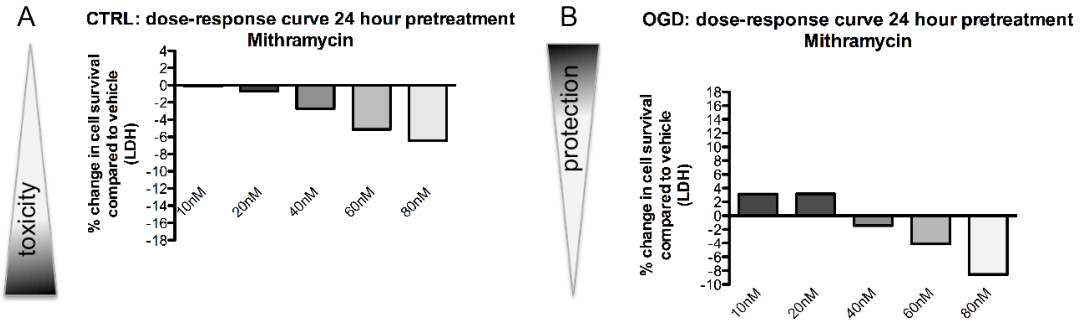

Figure 28 Dose-response testing: Mithramycin
LDH measurements of Mithramycin versus vehicle treated neuronal cultures
A: Mithramycin toxicity in CTRL cultures
B: Mithramycin protection in OGD cultures

Mithramycin: functional experiments

24 h Mithramycin pretreatment at a 10 nM concentration significantly decreased neuronal cell damage in an in experimental ischemia without showing basal toxicity at normoxic control conditions **(Fig. 29**). The mean percentage of cell death in the Mithramycin treated group was 23.95 % versus 32. 34 % in the vehicle treated group.

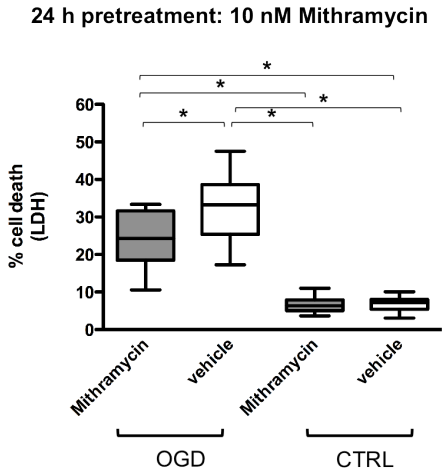

Figure 29 10 nM Mithramycin pretreatment confers protection to neurons in OGD

Rat cortical neurons treated with Mithramycin/ vehicle on DIV 8, subjected to OGD on DIV 9, LDH measured on DIV 10
N = 10; Mithramycin: *M* = 23.95, S*D* = 8.27
vehicle: *M* = 32.34, S*D* = 9.42
A two-way ANOVA was conducted that examined the effect of OGD and treatment on cell survival. There was a significant interaction between effects of OGD and treatment: $F_{(1, 36)} = 4.097$ with $p = 0.05$ for interaction.
To isolate significant differences between groups a Tukey post-hoc analysis was performed. Significant effects are indicated in the figure * = $p < 0.005$

Tests of Between-Subjects Effects

Dependent Variable: LDH

Source	Type III Sum of Squares	df	Mean Square	F	Sig.
OGD	4625.348	1	4625.348	111.081	0.000
treatment	18.627	1	181.627	4.362	0.044
OGD * treatment	170.588	1	170.588	4.097	0.050
Error	1499.021	36	41.639		
Total	18574.026	40			

5.3.2.2. Pharmacological inhibition of the histone demethylase LSD1

- Phenelzine -

Phenelzine, a clinically approved MAO antidepressant agent, was found to be strongly neuroprotective in ischemia in 2006 [*Wood et al.*, 2006]. The mechanism of protection was then explained by Phenelzine's ability to sequester reactive aldehydes. In 2010 Phenelzine, was discovered to be a most potent inhibitor of LSD1 [*Culhane et al.*, 2010].

Assumption: Phenelzine could in part confer neuroprotection by inhibiting LSD1 and hence maintaining active H3K4me1 and H3K4me2 marks and gene expression in experimental stroke (**Fig. 30**).

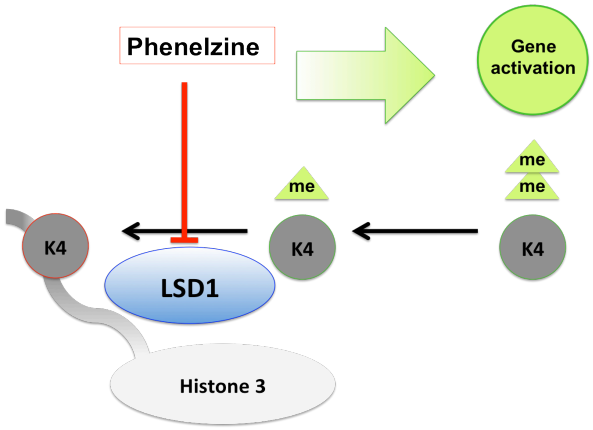

Figure 30 Hypothesis: Phenelzine inhibition LSD1

Phenelzine: dose-response testing

Phenelzine dose response tests showed an increasing toxicity from 50 µM to 100 µM together with an increased protective tendency in OGD upon dosage increase (**Fig. 31).**

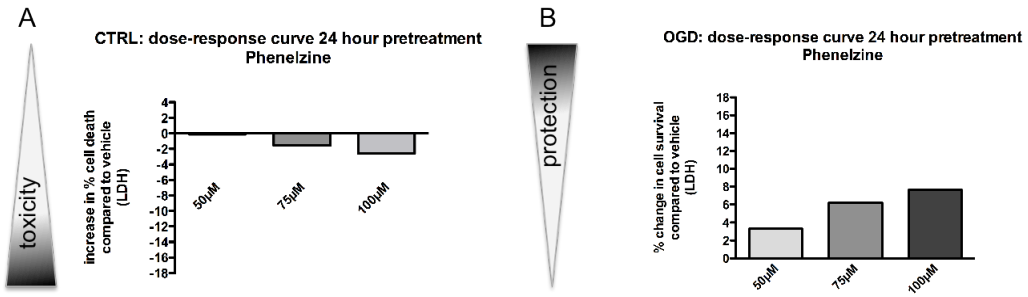

Figure 31 Dose-response testing: Phenelzine
LDH measurements of Phenelzine versus vehicle treated neuronal cultures
A: Phenelzine toxicity in CTRL cultures
B: Phenelzine protection in OGD cultures

Phenelzine: functional experiments

24 h pretreatment with 100µM Phenelzine significantly protected cortical neurons in OGD (**Fig. 32 A**). The mean percentage of cell death in the Phenelzine treated group was 23.39 % versus 37. 56 % in the vehicle treated group. H3K4me2 levels, the target of LSD1, showed an elevation assessed in immunoblots from protein harvested 24h post 100 µM Phenelzine/ vehicle treatment on DIV 9 (**Fig. 32 B**). A second paradigm was used, where cells were incubated with Phenelzine 48 hours pre OGD and subsequently Phenelzine was washed out by a complete medium exchange 24h/16h pre OGD.

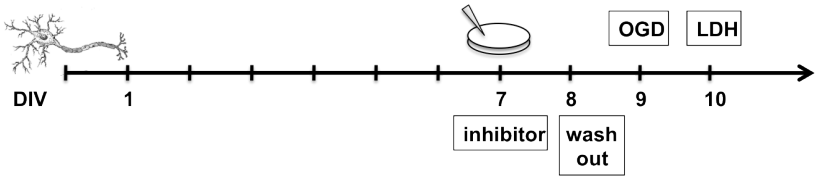

In this experiment, cytoprotection was still discernable 24 hours post OGD (**Fig. 32 C**). (Groups with an additional medium exchange showed a general decrease in cell death as it corresponds to an additional feeding and dead cells are washed out.

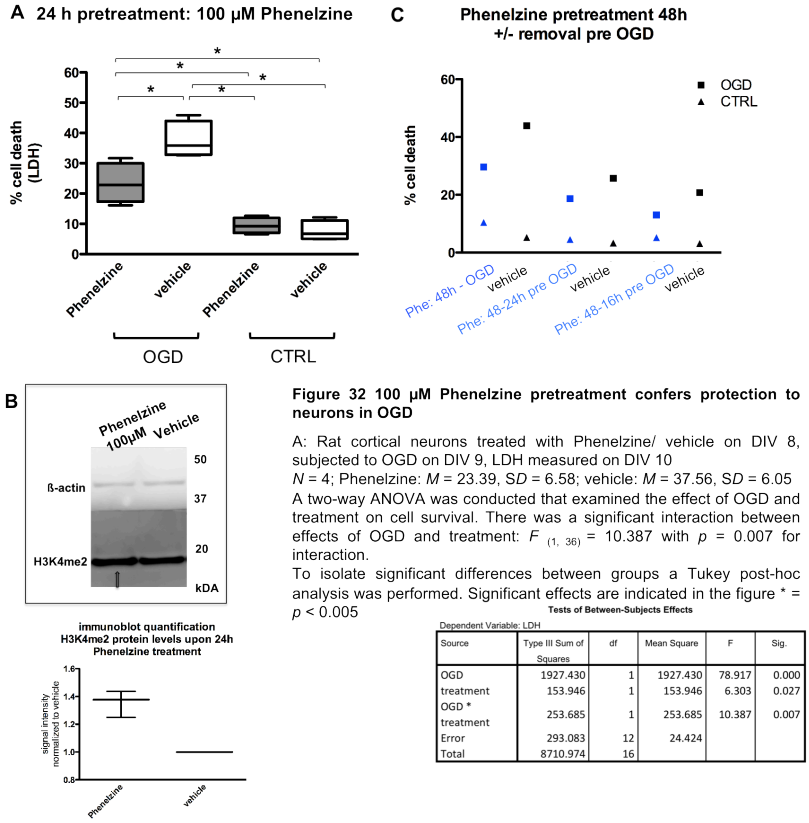

Figure 32 100 µM Phenelzine pretreatment confers protection to neurons in OGD

A: Rat cortical neurons treated with Phenelzine/ vehicle on DIV 8, subjected to OGD on DIV 9, LDH measured on DIV 10
N = 4; Phenelzine: *M* = 23.39, *SD* = 6.58; vehicle: *M* = 37.56, *SD* = 6.05
A two-way ANOVA was conducted that examined the effect of OGD and treatment on cell survival. There was a significant interaction between effects of OGD and treatment: $F_{(1,\ 36)} = 10.387$ with $p = 0.007$ for interaction.
To isolate significant differences between groups a Tukey post-hoc analysis was performed. Significant effects are indicated in the figure * = $p < 0.005$

Tests of Between-Subjects Effects

Dependent Variable: LDH

Source	Type III Sum of Squares	df	Mean Square	F	Sig.
OGD	1927.430	1	1927.430	78.917	0.000
treatment	153.946	1	153.946	6.303	0.027
OGD * treatment	253.685	1	253.685	10.387	0.007
Error	293.083	12	24.424		
Total	8710.974	16			

B: Immunoblot and quantification of H3K4me2 levels upon 24 h pretreatment with 100µM Phenelzine. H3K4me2 levels are elevated in the treated group (*N* = 3).

C: 48 h 100 µM Phenelzine pretreatment with subsequent washout 24h/16h pre OGD. Phenelzine washout was performed by a medium exchange.

- Tranylcypromine -

Tranylcypromine, or *Parnate* (2-phenylcyclopropylamine), was the first known inhibitor of LSD1 [*Schmidt and McCafferty*, 2007; *Yang et al.*, 2007] apart from being an irreversible inhibitor of monoamine oxidases and in clinical use as antidepressant.

Assumption: Tranylcypromine could confer neuroprotection by inhibiting LSD1, maintaining active H3K4me1 and H3K4me2 marks and gene expression in experimental stroke (**Fig. 33**).

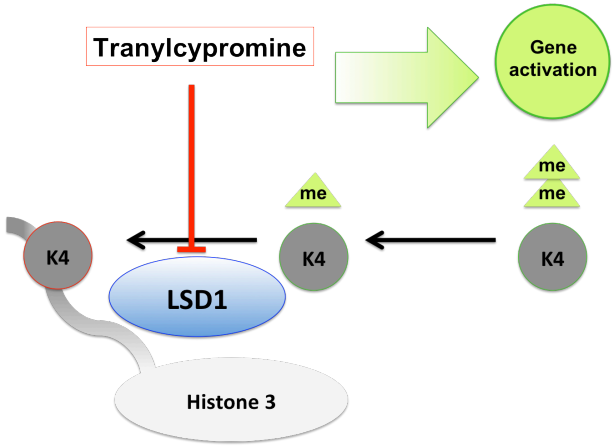

Figure 33 Hypothesis: Tranylcypromine inhibition of LSD1

Tranylcypromine: dose-response testing

Dose-response testing with 24hour pretreatment of Tranylcypromine showed a low tendency towards toxicity starting from 50 µM to 200 µM usage. A tendency towards neuroprotection in OGD could be assessed in first trials upon employment of a 10 µM concentration (**Fig. 34**).

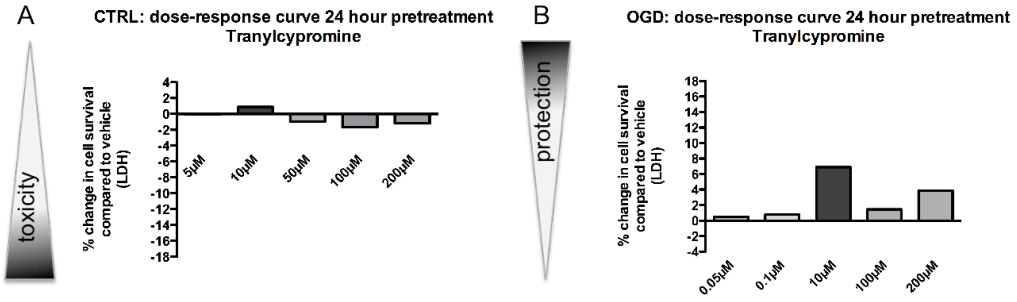

Figure 34 Dose-response testing: Tranylcypromine
LDH measurements of Tranylcypromine versus vehicle treated neuronal cultures
A: Tranylcypromine toxicity in CTRL cultures
B: Tranylcypromine protection in OGD cultures

Tranylcypromine: functional experiments

Despite a slight reduction in cell death recurring in every experiment upon Tranylcypromine pretreatment (mean value 4.14%), no significant effect could be reached with mean cell death values of 26.34% in the Tranylcypromine treated group versus 30.48 in the vehicle group following OGD (**Fig. 35**).

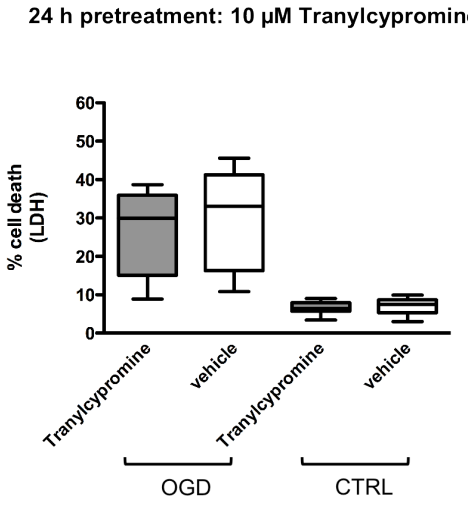

Figure 35 10 µM Tranylcypromine pretreatment does not promote neuronal survival in OGD

Rat cortical neurons treated with Tranylcypromine/ vehicle on DIV 8, subjected to OGD on DIV 9, LDH measured on DIV
N = 10; Tranylcypromine: *M* = 26.33, S*D* = 11.06; vehicle: *M* = 30.47, S*D* = 12.74
A two-way ANOVA was conducted that examined the effect of OGD and treatment on cell survival. There was no significant interaction between effects of OGD and treatment: $F_{(1, 36)} = 0.47$ with $p = 0.497$ for interaction.

Tests of Between-Subjects Effects

Dependent Variable: LDH

Source	Type III Sum of Squares	df	Mean Square	F	Sig.
OGD	4669.057	1	4669.057	63.836	0.000
treatment	52.075	1	52.075	0.712	0.404
OGD * treatment	34.410	1	34.410	0.470	0.497
Error	2633.078	36	73.141		
Total	19783.948	40			

5.3.3. Genetic inhibition of selected histone de-/methylases

The assumption that the blockade of transcriptional repressors conferred protection in ischemia was confirmed by some results with pharmacological inhibitors of histone de-/ methylating enzymes in OGD. The next step to test the hypothesis was a more specific genetic approach to elucidate the role of selected candidate enzymes. In post-mitotic neurons, stable knockdown was achieved through lentiviral delivery of microRNA embedded short hairpin (miR-shRNA) constructs targeting the candidate enzymes SUV39H1, G9a and LSD1. Knockdown efficiency was tested on the mRNA and protein level. Primary neuronal cultures were transduced on DIV 1 reaching transduction efficiencies around 80% - 90%. mRNA/protein was harvested on DIV 9 to check knockdown capacities of the diverse miR-shRNA constructs.

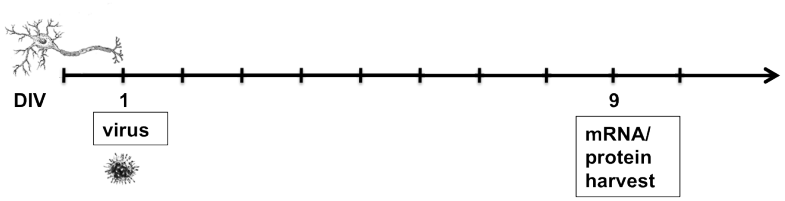

5.3.3.1. Knockdown efficiency

- Knockdown of SUV39H1 -

For the knockdown of SUV39H1, two different miR-shRNA constructs complementary to the open reading frame sequence of SUV39H1-mRNA were tested (mi-SUV39H1 and mi2-SUV39H1). On the mRNA level only very slight reductions of SUV39H1 were visible upon treatment with either construct compared to cultures treated with a non-targeting scrambled control plasmid (**Fig. 36 A**). Western blot analysis however revealed a robust knockdown of SUV39H1 protein levels upon administration of mi-SUV39H1, subsequently chosen for experimental use (**Fig. 36 B** and **C**). No significant changes of global H3K9me3 levels were observed upon SUV39H1 knockdown compared to the scrambled ctrl.

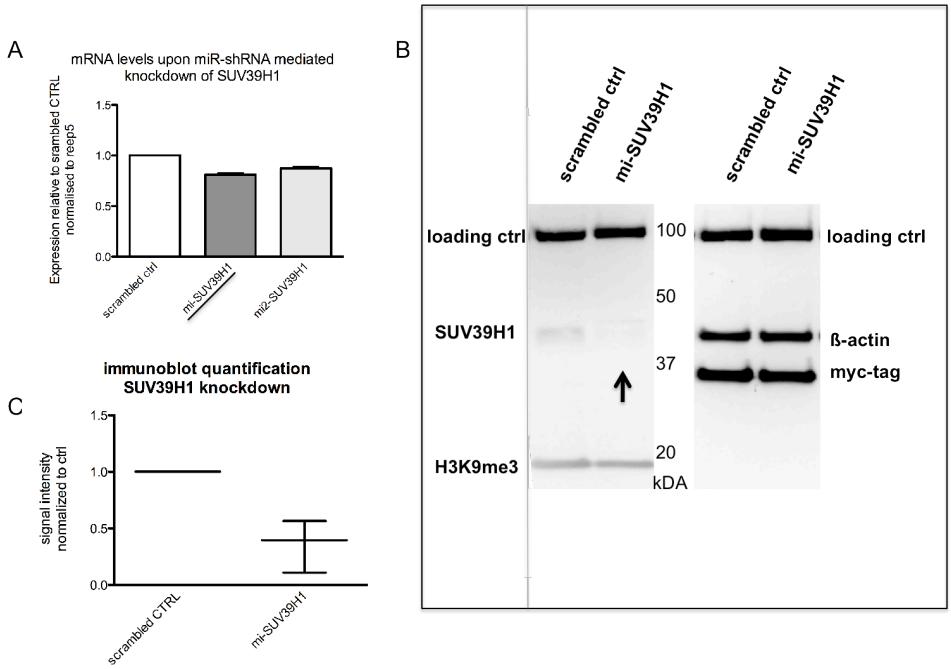

Figure 36 Knockdown efficiency of miR-shRNA constructs targeting SUV39H1
Neuronal cultures transduced with 2 different miR-shRNA constructs targeting SUV39H1 and a scrambled control construct
A: 2 different miR-shRNA constructs against SUV39H1 were tested with a qPCR.
B: Knockdown efficiency of the selected mi-SUV39H1 construct knocking down SUV39H1 in a representative immunoblot. As loading controls were ß-actin and an additional loading ctrl running at 100 kDA to ensure equal loading; myc-antibody taregts the myc-tag on the lentiviral expression vector to show equal lentiviral transduction efficiency
C: Quantification of SUV39H1 protein levels of neurons transcduced with the mi-SUV39H1 show successful knockdown compared to scrambled ctrl (*N* = 3).

- Knockdown of G9a -

Three different miR-shRNA constructs targeting the open reading frame of G9a mRNA were tested (mi-G9a, mi2-G9a, mi3-G9a), among which the most efficient, mi-G9a, was chosen for functional experiments. It induced both, a stable reduction in G9a mRNA (**Fig. 37 A**) and protein levels on DIV 9 compared to the scrambled control (**Fig. 37 B** and **C**). To assess the effect of G9a knockdown on its histone target, H3K9 was analysed in immunoblots. No stable changes in global H3K9me2 levels were observed. H3K9ac levels however, marking active transcription, were significantly elevated following G9a knockdown (**Fig. 37 C**).

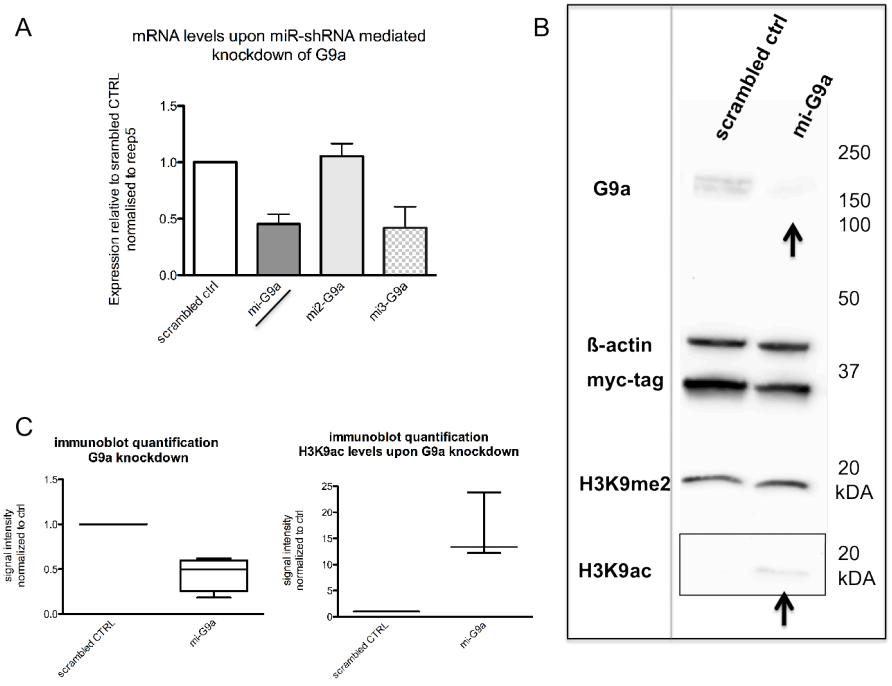

Figure 37 Knockdown efficiency of miR-shRNA constructs targeting G9a
Neuronal cultures transduced with different miR-shRNA constructs targeting G9a and a scrambled ctrl
A: 3 different miR-shRNA constructs against G9a tested with qPCR, of which 2 (mi-G9a, mi3-G9a) show a reduction in mRNA levels compared to the scrambled ctrl construct (mi-G9a was selected for functional experiments).
B: Knockdown efficiency of the selected mi-G9a, stably reducing G9a protein levels in an immunoblot; loading ctrl: ß-actin; identification of equal transduction efficiency: myc-tag; target of G9a: H3K9me2; indirect: H3K9ac
C: Quantification of G9a protein levels of neurons transcduced with mi-G9a *(N* = 4); Quantification of H3K9ac levels upon G9a knockdown (*N* = 3).

- Knockdown of LSD1 -

For LSD1, six different constructs targeting different regions of the LSD1 mRNA (open reading frame and 3' UTR, the target of endogenous miRNAs) were tested. One construct reduced LSD1 mRNA efficiently (mi5-LSD1) on the mRNA level (**Fig. 38 A**), but did not affect the protein level (data not shown). One mi-LSD1 construct, selected for functional experiments, significantly reduced LSD1 protein levels in neurons (**Fig. 38 B** and **C**). Further a significant drop in H3K4me2 levels was observed upon knockdown of LSD1 (**Fig. 38 B** and **C**).

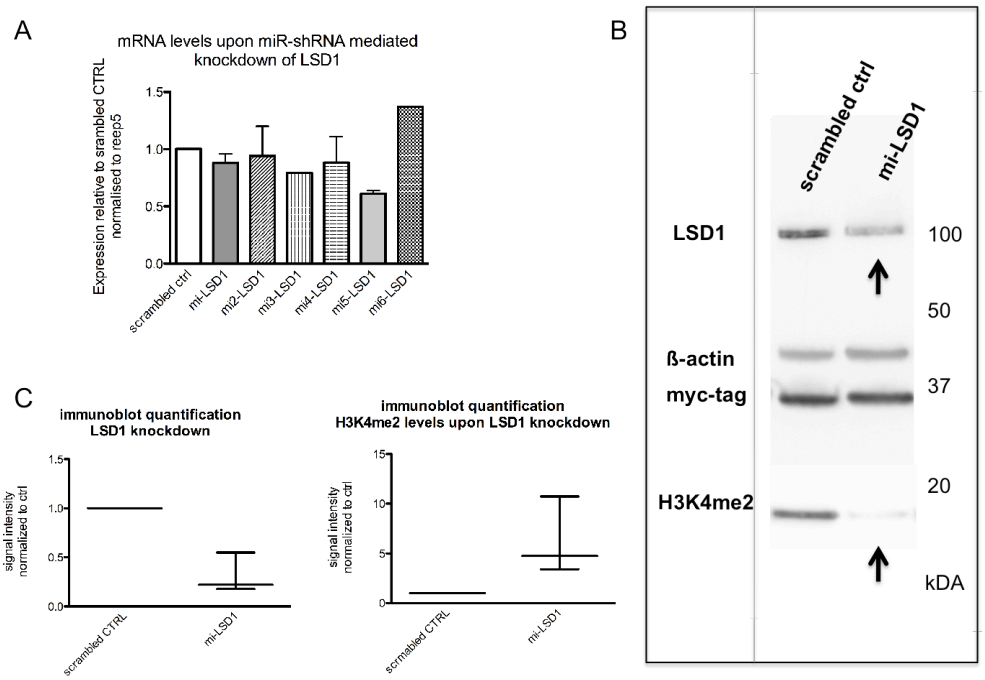

Figure 38 Knockdown efficiency of miR-shRNA constructs targeting LSD1
Neuronal cultures transduced with different miR-shRNA constructs targeting LSD1 anda scrambled ctrl
A: With qPCR 6 different miR-shRNA constructs against LSD1 were tested
B: Representative immunoblot of LSD1 knockdown with selected construct;. loading ctrl: ß-actin; equal transduction efficiency: myc; target of LSD1: H3K4me2
C: Quantification of LSD1 protein levels of neurons transcduced with mi-LSD1 or scrambled ctrl construct (*N* = 3); H3K4me2 level quantification following LSD1 knockdown *(N* = 3).

5.3.3.2. Cell survival after knockdown of histone de-/methylating enzymes in OGD

To analyse the effect of knockdown of the transcriptional repressors SUV39H1, G9a, or LSD1 on neuronal survival post OGD, cell cultures were transduced with the respective constructs (mi-SUV39H1, mi-G9a, or mi-LSD1 and scrambled ctrl) on DIV 1. Cultures were subjected to a 135 ± 5 min OGD on DIV 9. To assess cell survival two methods were applied: LDH levels were measured on DIV 10 and microscopic images were

taken for cell counts, on DIV 9 before OGD and 24 h after the insult on DIV 10, before measuring LDH.

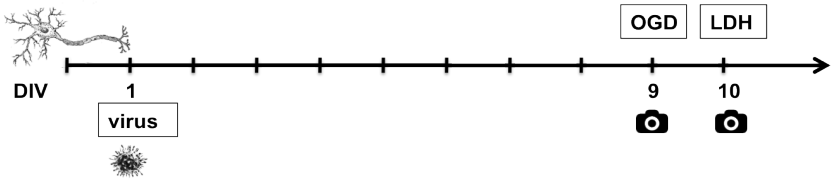

For cell count assessment, the same regions of interest were repeatedly photographed pre and post OGD. Subsequent cell counts of RFP positive cells were conducted in a blinded manner. Representative images of the knockdown groups SUV39H1/G9a/LSD1 as well as the CTRL culture are shown in **Fig. 39**. **Column 1** shows the RFP expression (pseudo-coloured in green) of cultures on DIV 9 pre OGD (scrambled ctrl, mi-SUV39H1, mi-G9a, mi-LSD1). The same region of interest 24 h post injury is depicted in **column 2**. Overlay images of DIV 9 and DIV 10 images were formed and show surviving neurons in yellow (**Fig. 39, column 3**). Considerably less surviving neurons (yellow) are found in the group treated with the scrambled ctrl construct compared to the knockdown groups and especially thoses treated with mi-SUV39H1 or mi-G9a (**Fig. 39, rows 1-4**). In the LSD1 knockdown group the effect is less pronounced.

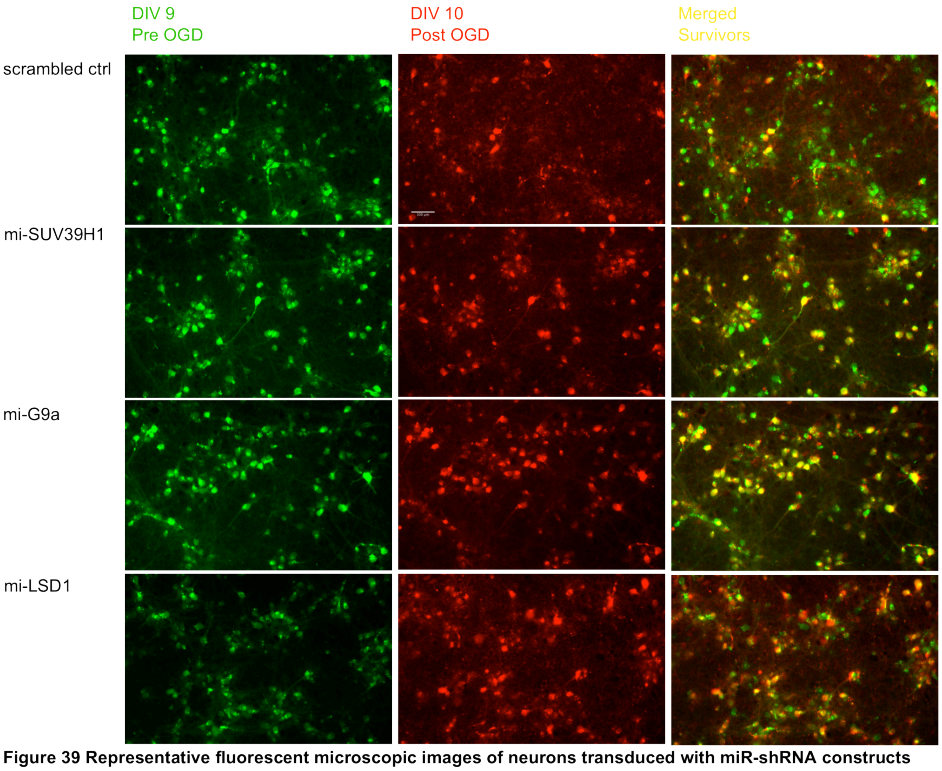

Figure 39 Representative fluorescent microscopic images of neurons transduced with miR-shRNA constructs
Column 1: RFP fluorescence of cortical neurons pre OGD (DIV 9) pseudocoloured in green
Column 2: RFP fluorescence of cortical neurons post OGD (DIV 10)
Column 3: merged images pre and post OGD show surviving neurons in yellow

Knockdown of the histone methyltransferases SUV39H1, and G9a induces significant neuroprotection in OGD

Knockdown of SUV39H1 or G9a in cortical neurons reduced cell death significantly in OGD. LDH levels were markedly decreased in the knockdown groups compared to the cultures treated with a scrambled control construct (**Fig. 40 A**). Further, cell counts showed an increased cell viability following OGD in the knockdown groups. As indicated by a lower survival ratio, a much lower percentage of cells survived in the scrambled control group (**Fig. 40 B**).

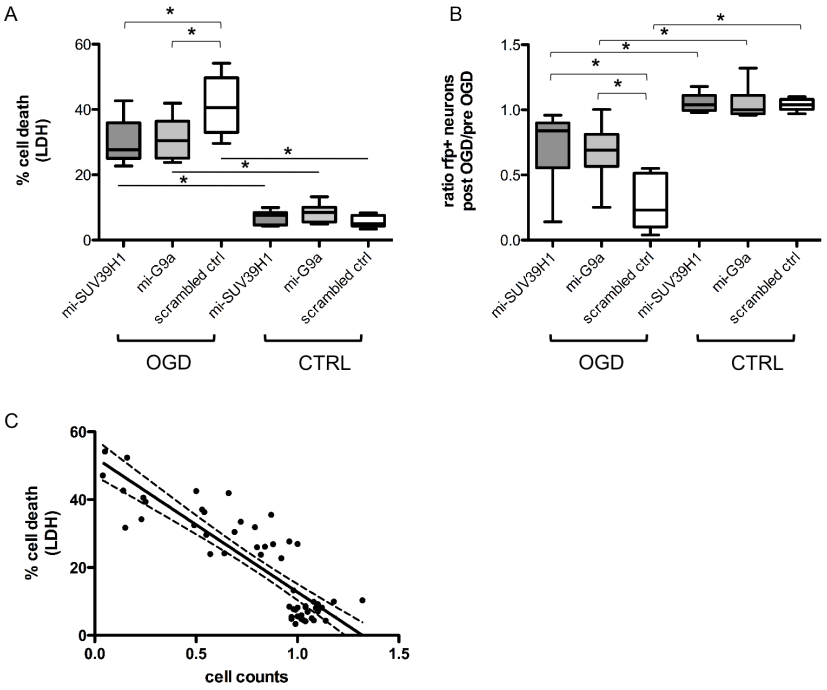

Figure 40 Knockdown of SUV39H1 and G9a induces neuroprotection post OGD

A: Percentage of cell death following SUV39H1 or G9a knockdown in OGD compared to scrambled ctrl, assessed with LDH assay; *N* = 9; mi-SUV39H1: *M* = 30.42; mi-G9a: *M* = 30.96; scrambled ctrl *M* = 41.04

A two-way ANOVA was conducted that examined the effect of OGD and microRNA treatment on cell survival. There was a significant interaction between effects of OGD and microRNA application, $F_{(2, 48)} = 7.7$ with $p = 0.001$ for interaction. To isolate significant differences between groups a Tukey post hoc analysis was performed. Significant effects are indicated in the figure * = $p < 0.001$.

Tests of Between-Subjects Effects

Dependent Variable: LDH

Source	Type III Sum of Squares	df	Mean Square	F	Sig.
OGD	9938.246	1	9938.246	334.494	< 0.001
miRNA	220.589	2	110.294	3.712	0.032
OGD * miRNA	455.145	2	227.573	7.659	0.001
Error	1426.141	48	29.711		
Total	12040.122	53	227.172		

B: Cell survival following SUV39H1 or G9a knockdown in OGD assessed by cell count ratios pre and post OGD. Survival ratios of 1 represent a 100% survival rate (ratio post/pre OGD mi-SUV39H1: *M* = 0.72; mi-G9a: *M* = 0.67; scrambled ctrl: *M* = 0.27). There was a significant interaction between effects of OGD and microRNA application, $F_{(2, 48)} = 8.7$ with $p < 0.001$ for interaction. To isolate significant differences between groups a Tukey post hoc analysis was performed. Significant effects are indicated in the figure * = $p < 0.001$.

Tests of Between-Subjects Effects

Dependent Variable: cell counts

Source	Type III Sum of Squares	df	Mean Square	F	Sig.
OGD	3.276	1	3.276	111.666	< 0.001
miRNA	0.592	2	0.296	10.083	< 0.001
OGD * miRNA	0.513	2	0.256	8.742	< 0.001
Error	1.408	48	0.0293		
Total	5.788	53	0.109		

C: Cell counts correlate inversely with LDH measurements, Person's $r = (54)$ -.87, $p < 0.001$.

The knockdown of SUV39H1/G9a alone did not impact cell viability in general as indicated by the equally low percentage of cell death assessed by LDH measurements and a stable cell count ratio around 1 in the healthy CTRL cultures (**Fig. 40 A** and **B**). Cell survival analysis results obtained from both LDH measurements and cell counts in neuronal cultures (OGD and CTRL) correlated significantly, which corroborates the robust neuroprotective effect upon knockdown of SUV39H1/G9a in OGD (**Fig. 40 C**).

Knockdown of LSD1 reveals a slight trend towards decreased cell death in OGD

Upon knockdown of LSD1 a slight decrease in cell death could be monitored compared to scrambled control cultures 24 hours post OGD, it did however not reach significance. Cell count levels confirmed the same effect on cell viability – a slight tendency towards increased survival, however not reaching significance. Again the healthy CTRL cultures displayed no signs of toxicity upon mi-LSD1 application (**Fig. 41**).

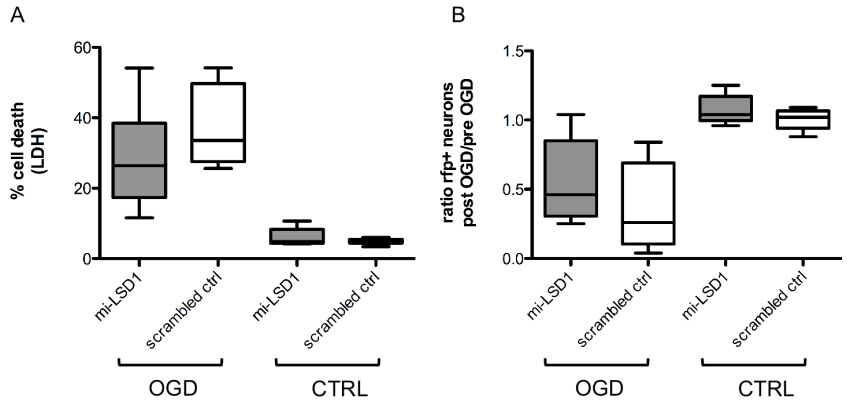

Figure 41 Knockdown of LSD1 shows tendency towards decreased cell death in OGD

A: Percentage of cell death (LDH) following LSD1 knockdown compared scrambled controls post OGD; *N* = 9; mi-LSD1: *M* = 29.67 versus scrambled ctrl: *M* = 37.94.
A two-way ANOVA was conducted that examined the effect of OGD and microRNA treatment on cell survival. There was no significant interaction between effects of OGD and microRNA application, $F_{(1, 32)} = 2.563$ with $p = 0.119$ for interaction.

B: Cell count levels following knockdown of LSD1 in OGD; *N* = 9; mi-LSD1: *M* = 0.56 versus scrambled ctrl: *M* = 0.37.
A two-way ANOVA was conducted that examined the effect of OGD and microRNA treatment on cell survival. There was no significant interaction between effects of OGD and microRNA application, $F_{(1, 32)} = 0.710$ with $p = 0.406$ for interaction.

Tests of Between-Subjects Effects

Dependent Variable: LDH

Source	Type III Sum of Squares	df	Mean Square	F	Sig.
OGD	7189.103	1	7189.103	88.199	0.000
miRNA	107.617	1	107.617	1.320	0.259
OGD * miRNA	208.939	1	208.939	2.563	0.119
Error	2608.320	32	81.510		
Total	24054.675	36			

Tests of Between-Subjects Effects

Dependent Variable: cell counts

Source	Type III Sum of Squares	df	Mean Square	F	Sig.
OGD	2.964	1	2.964	61.485	0.000
miRNA	0.156	1	0.156	3.236	0.081
OGD * miRNA	0.034	1	0.034	0.710	0.406
Error	1.543	32	0.048		
Total	24.902	36			

5.4. Changes in gene transcription upon SUV39H1 and G9a inhibition with Chaetocin

As the targeted manipulation of epigenetic players on the level of histone methylation conferred protection to neurons subjected to experimental ischemia, it remained to be investigated whether this effect was based on changes in gene transcription and, more precisely, an increase in gene activation. To analyse changes in gene transcription upon SUV39H1 and G9a inhibition two methods were employed. First, chromatin immunoprecipitation was conducted, followed by a genome wide sequencing step to analyse changes in H3K9 promoter modifications upon Chaetocin/vehicle pretreatment in OGD. Subsequently, mRNA levels of selected genes were analysed upon Chaetocin/vehicle treatment followed by experimental ischemia.

5.4.1. Changes in promoter signatures upon Chaetocin treatment

Successful inhibition of the repressive histone methyltransferases SUV39H1 and G9a should yield a reduction of repressive H3K9 methylation marks and an increase of activating H3K9 acetyltion in promoter regions of target genes. Neuronal cultures were pretreated with Chaetocin or vehicle on DIV 8, subjected to OGD on DIV 9 and chromatin was harvested 1 hour post reoxygenation. LDH levels of sister colonies were taken on DIV 10 in order to ensure OGD quality (data not shown).

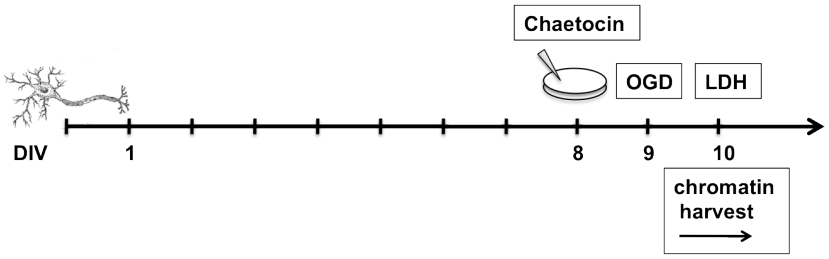

Chromatin immunoprecipitation (ChIP) was carried out followed by genome-wide sequencing to compare post-translational histone modifications upon Chaetocin versus vehicle treatment in OGD. ChIP-Seq was successfully carried out with an H3K9ac antibody, whereas the employment of 4 different H3K9 methylation antibodies did not produce valuable sequencing data. Promoter H3K9 acetylation was analysed in selected genes of interest chosen according to two parameters: one group consisted of genes known to be involved in important pathways of neuroprotection, that additionally showed an upregulation upon HDAC administration in experimental ischemia (BCL2, BCL-XL, HMOX1, VEGF, and BDNF) [*Faraco et al.*, 2006; *Hu et al.*, 2006; *Kim et*

al., 2009; *Kim and Chuang*, 2014; *Langley et al.*, 2008; *Lanzillotta et al.*, 2012; *Marinova et al.*, 2009; *Wang et al.*, 2012]; to the second group belonged genes described to be target genes of G9a (BMI1, GRIA, VEGF) [*Clifford et al.*, 2012; *Kubicek et al.*, 2007; *Noh et al.*, 2012]. Transcription start sites (TSS) of the respective genes were selected as starting points and two different promoter regions sizes were analysed per TSS, one stretching from -1kb to +1kb around the TSS and a larger one ranging from -3kb to +2kb around the TSS. For some genes several TSS were analysed (BDNF, BCL2, VEGFa).

Upon SUV39H1 and G9a inhibition via Chaetocin treatment the following genes show a significant increase in promoter acetylation compared to vehicle treated sister colonies subjected to OGD: HMOX1, GRIA2, BDNF1, BDNF2, BDNF3, BCL 2/1, BCL2/1 BCL-XL, VEGFa1 (**Fig. 42 A, B**). This enrichment of the activating H3K9ac mark is significant independent of selected region size (small region: **Fig. 42 A**; larger region **Fig. 42 B**). In contrast, H3K9ac is not significantly altered in analysed promoter regions of the genes BMI1, CASP 12 and VEGFa2 (**Fig. 42 C, D**).

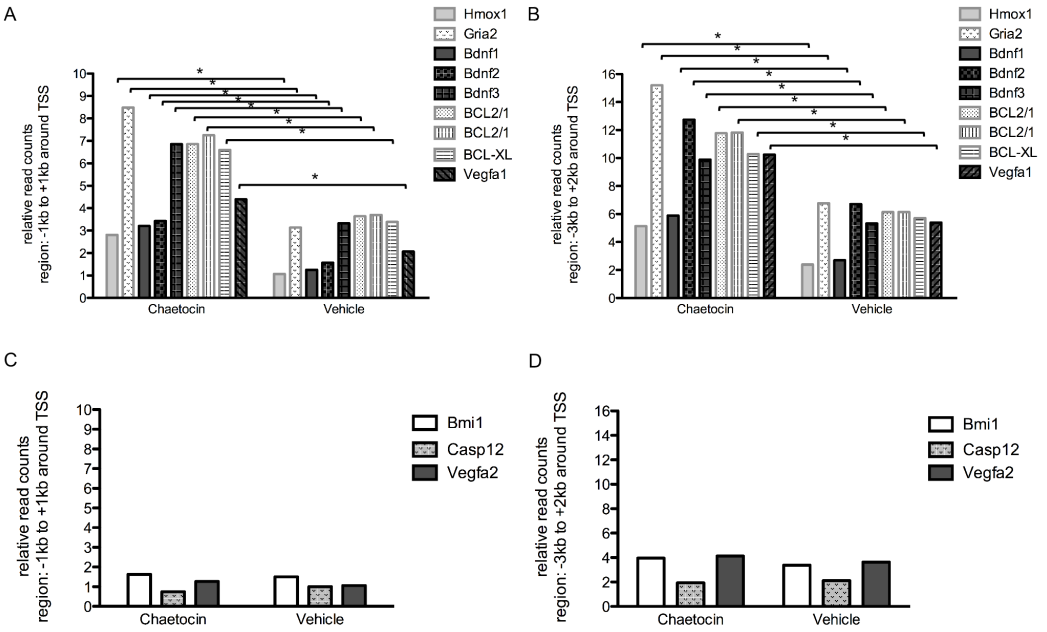

Figure 42 Promoter histone acetyltion of Chaetocin treated neurons following OGD
Rat cortical neurons pretreated with 30 nM Chaetocin/vehicle on DIV 8, subjected to OGD on DIV 9, chromatin harvest one hour post reoxygenation, immunoprecipitation with H3K9ac antibody, sequencing of 50 bp single reads.
Analysis of two region sizes per selected transcription start site (TSS) of candidate genes: smaller region: -1kb to +1kb around TSS (**A, C**); larger region: -3kb to +2kb around TSS (**B, D**). Several TSS were analyzed per gene promoter in BDNF, VEGFa, BCL2/1.
N = 1; Absolute read counts per region were normalized to total reads * 1000000. Read counts of DNA harvested from Chaetocin pretreated cells subjected to OGD was compared to read counts of precipitated DNA from vehicle treated cell using t-statistics. Significant effects are indicated in the figure * = $p < 0.05$.
Candidate genes are grouped according to H3K9 enrichment:
A, B: candidate genes with significant increase of H3K9 promoter aceytlation in Chaetocin treated neurons
C, D: : candidate genes showing no significant change of H3K9ac in Chaetocin treated neurons

5.4.2 Changes on the mRNA level upon Chaetocin treatment

Using RT-qPCR transcriptional changes of selected genes were analysed on the mRNA level upon 24 h Chaetocin/vehicle treatment on DIV 8 and subsequent OGD on DIV 9. The mRNA of neurons subjected to OGD as well as of the corresponding control cultures was harvested at reoxygenation (0h) as well as 1h, 4h and 24h post OGD (DIV 10). Included were all experiments that showed comparable cell damage and protection upon Chaetocin treatment according to LDH levels (data not shown).

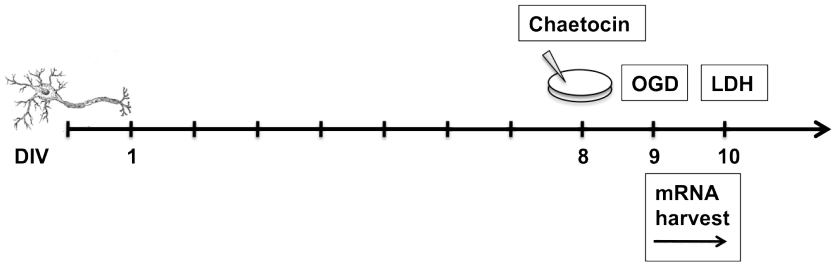

Analysed were 4 genes of interest (BDNF, VEGF, BCL-XL, GRIA2), that showed a significant increase in activating H3K9ac upon Chaetocin treatment in OGD according to ChIP-Seq data.

The neurogenic genes BDNF and VEGF showed a significant upregulation of mRNA levels in the Chaetocin treated group subjected to OGD versus the CTRL group relative to vehicle treated cells: BDNF mRNA was increased 1, 4 and 24 h post OGD (**Fig. 43 A**) and VEGF mRNA was increased 1 and 4 h post OGD (**Fig. 43 B**). In contrast to this the transcriptional level of BCL-XL and GRIA2 was not significantly altered as a consequence of Chaetocin treatment in OGD (**Fig. 43 C, D**).

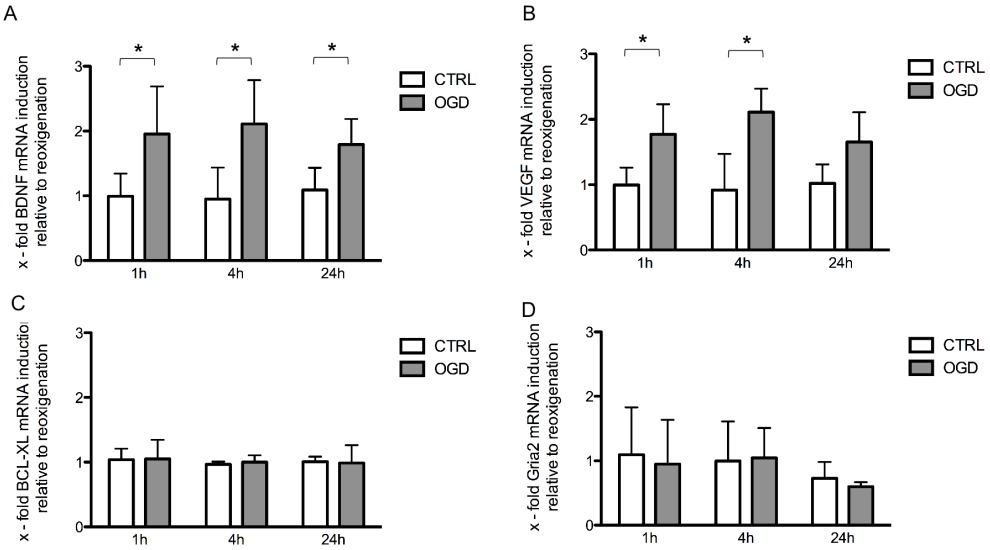

Fig. 43 Changes in mRNA levels upon inhibition of SUV39H1 and G9a with Chaetocin
Neurons pretreated with 30 nM Chaetocin/vehicle on DIV 8, subjected to OGD on DIV 9, mRNA harvests: reoxygenation (0 h), 1 h, 4 h and 24 h post OGD.
Reep 5 served as gene reference gene. To depict the relative increase of mRNA levels upon reoxygenation mRNA values of Chaetocin treated cells were normalized to values of the respective vehicle treated cells and subsequently related to the onset of reoxygenation (0 h). A two-way ANOVA was conducted to evaluate transcriptional changes of candidate genes over time. A Tukey post hoc analysis was further employed to evaluate group differences. Significant effects are indicated in the figure * = $p < 0.05$.

A: Relative induction of BDNF mRNA in Chaetocin treated cells 1 h, 4 h and 24 h post reoxygenation; $N = 5$; CTRL: 1h: $M = 0.99$, $SD = 0.351$, 4h: $M = 0.95$, $SD = 0.488$, 24h: $M = 1.09$, $SD = 0.344$; OGD: 1h: $M = 1.95$, $SD = 0.735$, 4h: $M = 2.11$, $SD = 0.680$, 24h: $M = 1.79$, $SD = 0.395$; There is no significant interaction of OGD and time $p = 0.610$. However, the factor OGD versus CTRL differs significantly with $p < 0.001$.

Source of Variation	DF	Sum of Squares	Mean Square	F	P
OGD	1	6.363	6.363	24.356	<0.001
Time	2	0.039	0.0195	0.0746	0.928
OGDx time	2	0.263	0.132	0.504	0.610
Residual	23	6.008	0.261		
Total	28	12.707	0.454		

B: Relative induction of VEGF mRNA in Chaetcoin treated cells 1 h, 4 h and 24 h post reoxygenation; $N = 3$; CTRL: 1h: $M = 1.00$, $SD = 0.266$, 4h: $M = 0.92$, $SD = 0.552$, 24h: $M = 1.02$, $SD = 0.292$; OGD: 1h: $M = 1.77$, $SD = 0.460$, 4h: $M = 2.11$, $SD = 0.357$, 24h: $M = 1.65$, $SD = 0.454$; There is no significant interaction of OGD and time $p = 0.492$. However, the factor OGD versus CTRL differs significantly with $p < 0.001$.

Source of Variation	DF	Sum of Squares	Mean Square	F	P
OGD	1	3.377	3.377	20.156	<0.001
Time	2	0.103	0.0513	0.306	0.742
OGDx time	2	0.252	0.126	0.753	0.492
Residual	12	2.011	0.168		
Total	17	5.743	0.338		

C: Relative induction of BCL-XL mRNA in Chaetcoin treated cells 1 h, 4 h and 24 h post reoxygenation; $N = 3$; CTRL: 1h: $M = 1.04$, $SD = 0.170$, 4h: $M = 0.97$, $SD = 0.042$, 24h: $M = 1.01$, $SD = 0.076$; OGD: 1h: $M = 1.05$, $SD = 0.295$, 4h: $M = 1.00$, $SD = 0.105$, 24h: $M = 0.99$, $SD = 0.278$; There is no significant interaction of OGD and time $p = 0.927$ and the factor OGD versus CTRL does not differ significantly.

Source of Variation	DF	Sum of Squares	Mean Square	F	P
OGD	1	0.0003	0.0003	0.009	0.927
Time	2	0.013	0.006	0.177	0.840
OGDx time	2	0.002	0.001	0.035	0.966
Residual	12	0.424	0.035		
Total	17	0.439	0.026		

D: Relative induction of GRIA2 mRNA in Chaetcoin treated cells 1 h, 4 h and 24 h post reoxygenation; $N = 3$; CTRL: 1h: $M = 1.09$, $SD = 0.734$, 4h: $M = 0.00$, $SD = 0.614$, 24h: $M = 0.73$, $SD = 0.254$; OGD: 1h: $M = 0.95$, $SD = 0.687$, 4h: $M = 1.05$, $SD = 0.464$, 24h: $M = 0.60$, $SD = 0.069$; There is no significant interaction of OGD and time $p = 0.939$ and the factor OGD versus CTRL does not differ significantly.

Source of Variation	DF	Sum of Squares	Mean Square	F	P
OGD	1	0.02555	0.02555	0.063	0.939
Time	2	0.5135	0.2567	0.092	0.767
OGDx time	2	0.03509	0.01755	0.920	0.425
Residual	12	3.349	0.2791		
Total	17	3.924			

5.5. BDNF upregulation is essential to Chaetocin-induced neuroprotection

In order to investigate whether the transcriptional activation of BDNF as a consequence of SUV39H1 and G9a inhibition is essential to Chaetocin-induced cytoprotection in OGD, we blocked BDNF-TrkB signalling by applying K252a [*Tapley et al.*, 1992]. Rat cortical neurons were pretreated with Chaetocin/ vehicle/ Chaetocin + K252a/ K252a on DIV 8. Neurons underwent OGD on DIV 9 and cell survival was monitored by measuring LDH on DIV 10.

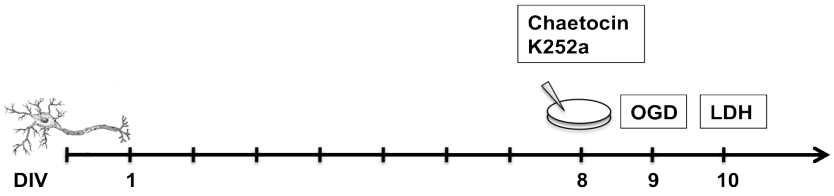

As demonstrated above, Chaetocin pretreatment protected neurons significantly from OGD-induced cell death (**Fig. 44**). The administration of BDNF-TrkB blocker K252a together with Chaetocin attenuated Chaetocin-induced protection of neurons subjected to OGD. BDNF-TrkB blockade with K252a alone had no significant exacerbating effect on cellular survival upon OGD.

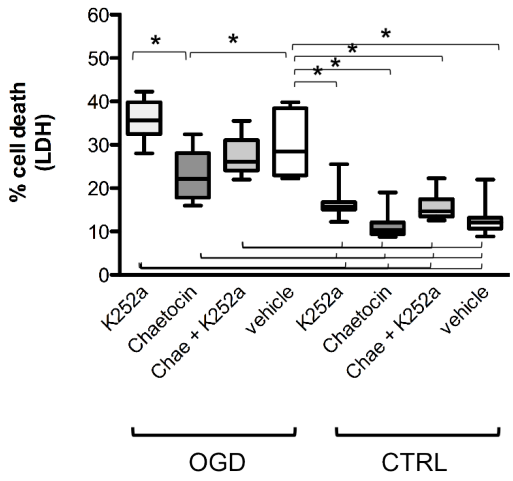

Figure 44 BDNF-TrkB blockade attenuates Chaetocin-induced neuroprotection

Neurons treated with K252a/ Chaetocin/ Chaetocin +K252a/ vehicle on DIV 8, subjected to OGD on DIV 9, LDH measurement on DIV 10. Ten independent experiments were conducted, each consisting of 3 wells per condition; *N* = 10; OGD: K252a: *M* = 35.84, *SD* = 4.510; Chaetocin: *M* = 23.22, *SD* =6.035; Chaetocin + K252a: *M* = 27.49, *SD* = 4.455; vehicle: *M* = 30.66, *SD* =7.297; CTRL: K252a: *M* = 16.42, *SD* = 3.474; Chaetocin: *M* = 11.16, *SD* =2.998; Chaetocin + K252a: *M* = 15.56, *SD* =2.935; vehicle: *M* = 12.73, *SD* = 3.553)
A two-way ANOVA was conducted that examined the effect of OGD and treatment on cell survival. There was a significant interaction between effects of OGD and treatment, $F_{(3,72)} = 3.546$ with $p = 0.019$ for interaction. To isolate significant differences between groups a Tukey post hoc analysis was performed. Significant effects are indicated in the figure with * = $p < 0.05$.

Source of Variation	DF	Sum of Squares	Mean Square	F	P
OGD	1	4704.318	4704.318	218.611	<0.001
treatment	3	798.869	266.29	12.375	<0.001
OGDx treatment	3	228.897	76.299	3.546	0.019
Residual	72	1549.376	21.519		
Total	79	7281.459	92.17		

6. Discussion

The administration of HDAC inhibitors in experimental stroke is highly neuroprotective according to multiple studies. The effect is based on the attenuation of transcriptional repression following ischemia. An increase in histone acetylation levels leads to gene transcription and importantly, the transcriptional activation of neuroprotective genes. It was the aim of this study to elucidate the role of histone methylation in this context. It was demonstrated that the epigenetic level of histone methylation was involved in ischemic damage development as well as neuroprotection. Neuronal survival following ischemia was successfully promoted by the manipulation of selected histone de-/ methylating enzymes. Especially promising results were obtained by inhibiting the histone methyltransferases Suv39H1 and G9a either genetically, or pharmacologically with Chaetocin. As hypothesized, the neuroprotective effect induced by the inhibition of transcriptional repressors on the level of histone methylation was based on the transcriptional activation of protective genes, such as the neurotrophin BDNF.

6. 1. Global histone methylation in experimental ischemia

To find out whether alterations in global histone methylation occur in experimental stroke, primary neuronal cultures exposed to OGD were analysed by immunoblotting. No global changes in single methylation marks at H3K9, or H3K4 could be identified in the 24 hours following experimental ischemia in this study (**Fig. 11)**.

In the literature global amounts of DNA methylation are reported to be elevated post ischemia [*Endres et al.*, 2000; *Endres et al.*, 2001]. Similarly, global H3 acetylation [*Faraco et al.*, 2006; *Kim et al.*, 2007; *Lanzillotta et al.*, 2012; *Ren et al.*, 2004; *Wang et al.*, 2011] as well as H4 acetylation levels [*Langley et al.*, 2008; *Xuan et al.*, 2012; *Yildirim et al.*, 2008] drop following experimental stroke, all signs of gene silencing. Given these observations, the lack of any change in global histone methylation levels monitored in this study seems surprising. However, it does not necessarily imply that no post-translational modifications on the histone methylation level occur at promoters of single genes. The analysis of transcriptional changes through the detection of changes in

global histone methylation patterns by immunoblotting bears different complexities, that lie in the complex nature of histone methylation, the technical challenge that such complexity brings with it and the conclusions that can be drawn from such observations. Unlike DNA methylation and histone acetylation, that characterize an "on" or "off" state of gene transcription, histone methylation marks can denote states of active transcription as well as gene silencing depending on site specificity as well as methylation state. While a global analysis of histone acetylation is possible for a whole histone protein (H3/H4), which includes several acetylation sites at once (H3K4, H3K9, H3K14, H3K18, H3K23,…), histone methylation can only be observed targeting one single site (e.g. H3K9 or H3K4) and taking the particular methylation state (mono-/di-/ trimethylation) into consideration (H3K9me1 = active transcription; H3K9me2 = gene silencing). This does not allow to visualise a cumulative effect of several repressive marks together in an immunoblot using one antibody as possible for histone acetylation. At the very specific level of single methylation marks (e.g. H3K9me2), the probability to see pronounced effects in immunoblots is lower and effects could be harder to detect. Additionally, the very basic question of antibody quality might hamper a successful detection of global changes in single methylation marks. Problems with high cross-reactiviy as well as the inhibition of antibodies by PTMs close to the primary one of interest are a matter of discussion in the field [*Bock et al.*, 2011]. In our study antibodies of different companies were tested (data not shown) but did not yield different results.

According to the literature global changes in single histone methylation sites have been observed in different contexts. A significant increase in repressive H3K9me3 marks was detected in Huntington's disease by immunoblotting [*Ryu et al.*, 2006]. Nitric and hypoxic stress situations, that also contribute to ischemic damage, were analysed in cancer studies. In breast cancer cells prolonged nitric oxide exposition elevated global H3K9me2 levels [*Hickok et al.*, 2013]. In human lung carcinoma cells subjected to prolonged hypoxic conditions an increase of repressive global H3K9me2 levels and a decrease of activating H3K9me1 and H3K9ac marks was detected [*Chen et al.*, 2006]. On the other hand no changes in global H3K9me2/me3 levels could be detected upon hypoxia in Hela cells [*Beyer et al.*, 2008; *Pollard et al.*, 2008; *Sar et al.*, 2009; *Wellmann et al.*, 2008]. The effect of HDAC inhibitors on global histone methylation marks also yielded inconsistent results regarding conclusions about transcriptional activity. A global increase of activating H3K4me2 and me3 levels could be assessed in healthy neurons and astrocytes following HDAC inhibitor treatment [*Marinova et al.*, 2009; *Marinova et al.*, 2011]. Contrary to this idea the use of a HDAC inhibitors was also shown to induce repressive H3K9me2 levels in hypoxia [*Chen et al.*, 2006]. These inconsistencies render a statement about the general state of gene transcription difficult.

A recent study further confirms that the assessment of global levels of histone methylation is not suitable to draw conclusions about a general state of gene transcription as global histone methylation levels do not necessarily reflect trends on the promoter level of single genes. In this study rat brains were preconditioned with cortical spreading depression. It resulted in a global decrease of activating H3K4me2 and me1 compared to control cultures, unchanged H3K4me3 levels and an almost 60% increase of repressive global H3K9me2 levels [*Passaro et al.*, 2010]. Subsequent promoter methylation analysis of induced neuroprotective genes, however, showed methylation changes just contrary to those assessed upon global analysis. A closer look at non-sequencing long interspersed sequences (LINEs) showed that preconditioning led to H3K4me2 decrease and H3K9me2 increase in these non-coding regions, a pattern that exactly reflected the state of histone methylation observed in global analysis [*Rana et al.*, 2012]. It is unclear, which biological function these non-coding repeat sequences serve and what these changes in methylation signatures imply for the cell/organism.

However, to analyse the state of gene transcription it makes sense to observe histone methylation changes occurring on a gene- and promoter-specific level rather than assessing global patterns. To capture these subtle changes a more specific approach than immunoblotting is necessary. To understand epigenetic signatures in cellular processes, current research aims at analysing several modifications of different epigenetic levels at once, combining chromatin immunoprecipitation analyses with genome wide sequencing. The vast array of epigenetic modifications is being investigated in different mammalian cell types in order to elucidate whether typical sets of patterns can be ascribed to active/repressed promoters, enhancer regions, or elongation sites [*Bernstein et al.*, 2007; *Gifford et al.*, 2013; *Kouzarides*, 2007; *Mikkelsen et al.*, 2007].

Around 850 combinatorial patterns recurring at > 0.1 % in the genome have been suggested by analysing combinations of histone acetylation and methylation marks in a human cell population [*Linghu et al.*, 2013; *Ucar et al.*, 2011]. Taking into consideration that the vast amount of proposed patterns further recruit very specified regulatory elements reading these combinatorial patterns. More recent findings suggest a “much richer chromatin landscape beyond simple accessibility” [*Ernst and Kellis*, 2013].

Such an analysis is beyond the scope of this study. In summary, it can only be stated, that not seeing any reproducible global pattern in H3K9 and H3K4 methylation marks post OGD in immunoblots does not imply that no alteration in post-translational modifications occur at promoter levels of single genes or that gene transcription is unaffected.

6.2. Hypoxic regulation of histone de-/methylases

The transcription factor HIF plays a major role in the transcriptional response to ischemia. To address the question whether it regulates epigenetic players such as histone de-/methylases in order to mediate further transcriptional changes, mRNA levels of selected enzymes were analysed following HIF accumulation. We could show for the first time that HIF induces KDM3A mRNA and protein levels in primary cortical neurons (**Fig. 12**). The result is in line with the literature that identified KDM3A to be a direct target of HIF. KDM3A upregulation was assessed in several tumour cells and tissues upon hypoxia [*Beyer et al.*, 2008; *Pollard et al.*, 2008; *Sar et al.*, 2009; *Wellmann et al.*, 2008]. The functional impact of hypoxia-mediated KDM3A induction is currently under debate. There is some evidence that hypoxia actively induces several genes involved in growth and differentiation in cancer cells via KDM3A [*Krieg et al.*, 2010]. However, Jumonji dioxygenases require oxygen for the enzymatic reaction and low oxygen tension affects their activity. It has also been proposed that hypoxia-induced upregulation of Jumonji dioxygenases could be a necessary compensatory mechanism to maintain basal demethylase activity in spite of low oxygen levels [*Lee et al.*, 2014; *Xia et al.*, 2009]. Whether KDM3A induction upon hypoxia in primary neurons serves the purpose of basal transcriptional balance or active induction of target genes was not followed up in this study. Its upregulation, however, suggests an important role in the cellular response to hypoxia and identifies KDM3A as potentially interesting candidate enzyme in experimental ischemia.

The transcription of the enzymes SUV39H1, G9a, LSD1 and ESET remained unchanged upon HIF induction in primary neurons (**Fig. 12**). Nevertheless, these histone de-/methylases might play a role in hypoxic gene regulation independent of the HIF pathway. Hypoxic stress has been described to induce the methyltransferase G9a in human lung carcinoma cells. The findings suggest a rise in G9a nuclear protein levels and activity but not in mRNA levels [*Chen et al.*, 2006]. The latter is in accordance with our results observed in primary neurons.

6.3. Neuroprotection and the manipulation of histone de-/ methylases

6. 3.1. Overexpression of histone de-/methylating enzymes

6.3.1.1. Overexpression of a transcriptional activator: KDM3A

Due to the strongly enhanced expression of KDM3A in hypoxia (**Fig. 12**) this transcriptional activator was identified as interesting candidate enzyme for overexpression in OGD, assuming that the transcriptional activation of target genes might promote neuronal survival. However, KDM3A overexpression in cortical neurons did not affect cellular viability following OGD (**Fig. 15**). Different speculations are possible to explain the lack of effect upon KDM3A overexpression.

It is conceivable, that exogenous KDM3A has no direct impact on target gene expression as enzyme function is tightly regulated through other factors. Different enzymes involved in histone methylation might be necessary to catalyse steps preceding KDM3A catalytic activity (e.g. H3K9me3 demethylation). Moreover, KDM3A cofactors might play a role. Cofactors, such as Fe(II) and alpha-ketoglutarate might not be abundant in the cell and hence regulate, or mitigate KDM3A function. Further adding to the complexity is the lack of molecular oxygen under hypoxic conditions, as KDM3A requires oxygen for its catalytic activity. The exact range of required oxygen seems to diverge between cell types. While KDM3A demethylase activity is not lost at 1 % pO_2 in HELA cells, macrophages already show detectable H3K9me2/3 methylation increases at a pO_2 below 3% [*Beyer et al.*, 2008; *Tausendschon et al.*, 2011]. Concerning the specific oxygen requirements of KDM3A in primary neurons nothing is known so far. It remains unclear whether more KDM3A proteins in the cell can exert more action under hypoxic conditions.

Then again, KDM3A is anyway upregulated upon hypoxia in various cell types [*Beyer et al.*, 2008; *Mimura et al.*, 2011; *Pollard et al.*, 2008; *Sar et al.*, 2009; *Wellmann et al.*, 2008; *Xia et al.*, 2009] including primary cortical neurons (**Fig. 12**). A ceiling effect, where the enzyme-substrate reaction is saturated and a surplus of enzyme is not catalytically active is also imaginable. The exact impact of KDM3A upregulation under hypoxia and whether it always correlates to increased gene expression is still under debate. Some evidence for increased target gene expression upon hypoxia-induced KDM3A upregulation exists. In two cells lines (human umbilical vein endothelial cells and HEK293) an interaction of KDM3A and HIF1α under hypoxic conditions could be observed pointing at a HIF-dependent recruitment of KDM3A to target genes. Among the target genes was, for example *SLC2A3,* a gene encoding glucose transporter isoform 3, which is important for glucose uptake. HIF1 and KDM3A are suggested to be

induced in response to hypoxic stimuli in order to regulate genes involved in glycolysis as adaptation to anaerobic conditions [*Mimura et al.*, 2012]. Similarly, in renal cell and colon carcinoma cell lines, KDM3A is proposed to act as signal amplifier to facilitate hypoxic gene expression, for example of the genes adrenomedullin and growth and differentiation factor 15, by decreasing promoter histone methylation upon HIF1α induction [*Krieg et al.*, 2010]. On the other hand it is being discussed that increased KDM3A levels upon hypoxia do not serve to induce specific hypoxic response genes but to maintain epigenetic homeostasis under hypoxia and compensate for decreasing oxygen tension to ensure basal expression of genes [*Xia et al.*, 2009].
In cortical neurons KDM3A target genes are unknown. It hence remains unclear whether hypoxia leads to their increased expression, whether this contributes to the hypoxic response, or ensures basal function, or whether KDM3A target genes at all comprise genes relevant for neuronal survival in OGD. A closer analysis of KDM3A target genes and expression profiles comparing normoxic and hypoxic conditions in cortical neurons would be necessary to elucidate the issue further.
In summary, KDM3A overexpression in neurons did not affect survival post OGD in the applied paradigm. Many open questions about KDM3A basic function in neurons can be raised and without extensive inquiry, it is impossible to clearly relate the observed result to our hypothesis.

6.3.1.2. Overexpression of transcriptional repressors: SUV39H1 and LSD1

The overexpression of both transcriptional repressors SUV39H1 and LSD1 had no impact on survival of neurons subjected to OGD. The hypothesis that an increase in the activity of transcriptional repressors could deteriorate the state of cortical neurons in experimental stroke could not be corroborated by these experiments. Neither exogenous LSD1 expression nor SUV39H1 overexpression influenced cell viability. Again – as in the case of KDM3A overexpression – it remains unevaluated in how far the increase of protein levels of the enzyme impacts target gene expression – repression according to this paradigm. In the cases of SUV39H1 and LSD1, which both function in multiple repressor protein complexes [*Carbone et al.*, 2006; *Cherrier et al.*, 2009; *Humphrey et al.*, 2001; *Nicolas et al.*, 2003; *Reed-Inderbitzin et al.*, 2006; *Shi et al.*, 2005] the probability is very high that gene regulation is dependent on protein complex activity. The abundance of one single interaction partner might leave the overall complex function unaffected.
Another possibility that may explain the lack of effect upon SUV39H1/LSD1 overexpression in OGD is, that enzymes catalyzing further methylation steps are needed

before SUV39H1 or LSD1 can perform their catalytic function. LSD1 is able to demethylate the active mark H3K4me2 but not H3K4me3. A change in transcriptional state might be performed stepwise with different enzymes acting together in a sequential manner. On the other hand examples from the literature exist where exogenous expression of either enzyme influenced cell fate. Nothing is known about cortical neurons, however, in human embryonic kidney fibroblasts the promotion of cell cycle progression was observed upon exogenous LSD1 expression [*Cho et al.*, 2011b; *Hayami et al.*, 2011] as well as increased proliferation and migration of lung carcinoma cells following LSD1 overexpression [*Lv et al.*, 2012]. SUV39H1 overexpression inhibited apoptosis in colon carcinoma [*Mungamuri et al.*, 2012] and altered proliferation and differentiation in transgenic mice overexpressing SUV39H1 during embryogenesis [*Czvitkovich et al.*, 2001].
Without further experiments analysing changes in histone methylation states and transcriptional alterations following the overexpression of exogenous enzymes, a definite explanation for the observed results remains elusive.

6.3.2. Pharmacological inhibition of histone de-/methylases

As the pharmacological inhibition of HDACs proved beneficial in experimental ischemia, pharmacological inhibitors of selected histone de-/methylases acting as transcriptional repressors were tested in OGD. Among the six pharmacological inhibitors of histone de-/ methylating enzymes currently available, two substances could be identified as novel neuroprotective agents in experimental stroke: Chaetocin and Mithramycin (**Fig. 20, Fig. 29**). The protective effect of Phenelzine could further be confirmed in our study (**Fig. 32**).

6.3.2.1. The inhibition of SUV39H1 and G9a

Inhibiting the transcriptional repressors SUV39H1 and G9a with 24 h Chaetocin pretreatment conferred robust protection to rat cortical neurons in OGD (**Fig. 20**). Chaetocin was for the first time applied in a neurological context and identified as novel neuroprotective agent. Concurrently, SUV39H1 and G9a were identified as important players in experimental ischemia and neuroprotection.
The fungal metabolite Chaetocin interacts directly with the histone methyltransferases SUV39H1 and G9a [*Greiner et al.*, 2005]. The exclusive specificity towards SUV39 family members as well as the mechanism of action of Chaetocin are currently being discussed. The inhibitory potency against SUV39H1 and G9a, however, has been confirmed by different research groups [*Cherblanc et al.*, 2013a; *Cherblanc et al.*,

2013b; *Greiner et al.*, 2013]. According to the literature, (a cancer and an HIV study) Chaetocin induces a loss of H3K9 trimethylation and an increase in H3K9 acetylation at specific promoters with subsequent activation of gene expression [*Bernhard et al.*, 2011; *Cherrier et al.*, 2009].

In our study Chaetocin was similarly shown to induce H3K9 promoter acetylation in selected genes (**Fig. 42**) and to trigger the transcription of the neuroprotective genes BDNF and VEGF in OGD (**Fig. 43**), which confirmed our hypothesis regarding the benefit of transcriptional activation in ischemia (**Fig. 6**).

The consequences of Chaetocin treatment are similar to those of HDAC inhibitors, which suggests a similar mechanism of action set in motion on the level of histone methylation. Like HDAC inhibitors, Chaetocin treatment shows antitumor activity by inducing cell cycle arrest as has recently been monitored in different cancer pathologies [*Cherrier et al.*, 2009; *Tran et al.*, 2013; *Yokoyama et al.*, 2013]. On the other hand, Chaetocin's anticancer activity has also been attributed to an observed reactive oxygen species (ROS) induction upon Chaetocin administration [*Chaib et al.*, 2012; *Isham et al.*, 2012; *Tibodeau et al.*, 2009]. Investigations about off-target effects, such as ROS induction upon Chaetocin treatment, were not followed up in our study. ROS induction is endogenously triggered during ischemia and contributes considerably to neuronal damage development. [*Kostandy*, 2012]. Due to the absence of toxicity of Chaetocin at the employed 30 nM concentration in healthy neurons and the neuroprotective effect in OGD, ROS induction in primary rat cortical neurons seemed unlikely.

In contrast to the results obtained with Chaetocin treatment, the G9a inhibitors BIX-01294 and UNC0638 [*Chang et al.*, 2009; *Kubicek et al.*, 2007; *Vedadi et al.*, 2011] did not affect cell survival in OGD at non-toxic concentrations (**Fig. 23, Fig. 26**). It is very probable that the expected protection could not be produced due to a lack of potency of the inhibitors at the employed concentrations. In cells less sensitive for toxicity than neurons, such as embryonic stem cells, fibroblasts [*Kubicek et al.*, 2007] and cancer cells [*Cho et al.*, 2011a], BIX-01294 has been described to potently inhibit G9a. It was, however, demonstrated that the potency and toxicity of BIX-01924 are hardly separable [*Vedadi et al.*, 2011] (**Fig. 45**). In comparison to BIX-01294 UNC0638 was at first claimed to be more efficient [*Vedadi et al.*, 2011] (**Fig. 45**). Very recently, however, it also turned out "not useful" for in vivo settings due to poor pharmacokinetics [*Liu et al.*, 2013]. A number of new inhibitors are currently being designed based on the structural knowledge of BIX-01294, all postulating optimized potency, increased specificity as well as low toxicity: examples are UNC0224, a 2,4-Diamino-7-aminoalkoxy-quinazoline [*Liu et al.*, 2009], then UNC0321, the first G9a inhibitor with picomolar

potency [*Liu et al.*, 2010] then UNC0638, and lately UNC0642 apparently with improved in vivo activity [*Liu et al.*, 2013].

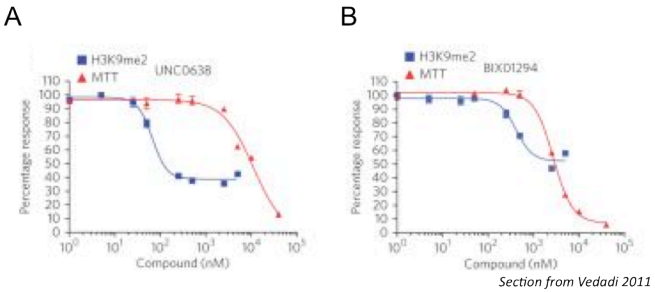

Figure 45 Potency and toxicity of the inhibitors UNC0638 and BIX-01294
The separation of functional potency (blue) and toxicity (red) of the two G9a inhibitors UNC0638 (**A**) and BIX-01294 (**B**); The functional potency is determined by H3K9me2 reduction, toxicity by an MTT assay measuring cell viability.

In spite of the difficulty of finding a suitable G9a inhibitor for actual experimental use, the importance of G9a in ischemic damage development and neuroprotection could be assessed by joint blockade of SUV39H1 and G9a with the pharmacological agent Chaetocin and specific kockdown of G9a with miRNA (**Fig. 40**). G9a even appears to be the more interesting candidate enzyme comparing the catalytic function of SUV39H1 and G9a. Biochemically SUV39H1 and G9a are both able to methylate H3K9me1/me2/me3. In vivo however, they show distinct functions. SUV39H1 is the major KMT for H3K9 trimethylation at pericentric heterochromatin and essentially involved in genomic stability [*Czvitkovich et al.*, 2001; *Melcher et al.*, 2000; *Peters et al.*, 2001; *Peters et al.*, 2003]. G9a has – unlike SUV39H1 – a more direct influence on gene transcription as it is mainly responsible for in vivo H3K9 mono and dimethylation in euchromatic regions [*Rice et al.*, 2003; *Tachibana et al.*, 2002]. As such, G9a plays a major role in catalyzing the switch of transcriptional states [*Gyory et al.*, 2004; *Tachibana et al.*, 2002]. Cells deficient of G9a show reduced levels of H3K9me2 but increases in activating H3K9 acetylation levels (unlike G9a+/+ or G9a+/- cells) [*Rice et al.*, 2003; *Tachibana et al.*, 2002]. According to our hypothesis this switch from a repressed transcriptional state to active transcription is the major step to induce neuroprotection in ischemia if epigenetic transcriptional repressors are inhibited.

6.3.2.2. The inhibition of ESET

In this study Mithramycin was for the first time observed to confer significant protection to neurons in experimental stroke (**Fig. 29**). A neuroprotective property has already been assessed in experiments where neuronal cell death due to oxidative stress was reduced upon mithramycin treatment [*Chatterjee et al.*, 2001] and in a model of Huntington's disease, where Mithramycin was reported to downregulate excessive

H3K9 trimethylation [*Ferrante et al.*, 2004; *Ryu et al.*, 2006]. As a mechanism of action reduced levels of the methyltransferase ESET were proposed [*Ferrante et al.*, 2004; *Ryu et al.*, 2006].
Mithramycin binds specifically to guanosine-cytosine-rich DNA [*Mir et al.*, 2003] and thus interferes with DNA binding of transcription factors of the Sp family to target promoters [*Blume et al.*, 1991]. The methyltransferase ESET is such a target gene of SP1 and its expression is inhibited upon Mithramycin administration in a dose-dependent manner [*Ferrante et al.*, 2004; *Ryu et al.*, 2006].
However, in spite of the reduction of ESET protein levels Mithramycin cannot be regarded as specific inhibitor of ESET. The blockade of SP1 transcription factor binding is a broad mechanism that affects transcription through the regulation of other enzymes as well. Recently, HDACs have been found to be reduced as a consequence of Mithramycin administration as well [*Liu et al.*, 2006; *Sleiman et al.*, 2011]. As no specific inhibitor of ESET exists as yet, this enzyme was not further analysed in the current study.

6.3.2.3. The inhibition of LSD1

LSD1 catalyses the switch of activating H3K4me2/me1 marks and the repressive H3K4me0 mark. An inhibtion of the demethylase was assumed to activate gene expression in OGD. The two inhibitors Phenelzine and Tranylcypomine were tested and yielded contradictory results (**Fig**. **32 A, Fig. 35**). While Phenelzine induced significant protection in OGD, Tranylcypromine administration led to a slight, but non-significant reduction in cell death in experimental ischemia. Adding to the complexity was again the lack of specificity of both inhibitors functioning as monoamine oxidase blockers. The neuroprotective effect of Phenelzine in ischemia is known since 2006. Then, it was explained to rely on Phenelzine's capacity to sequester reactive aldehydes, accumulating during ischemia [*Wood et al.*, 2006]. At the time however, its function as inhibitor of LSD1 was unknown. Further experiments conducted in our study to elucidate the role of LSD1 in Phenelzine-mediated protection in experimental stroke hint at an involvement of LSD1: H3K4me2 levels rose upon 24 h Phenelzine pretreatment (**Fig. 32 C**). This could be interpreted as a consequence of LSD1 inhibition through Phenelzine and point at transcriptional changes induced as a result. Phenelzine further induced neuroprotection in OGD upon an intermittent treatment paradigm (**Fig. 32 B**), which suggests that the protection is mediated by transcriptional changes in the cell rather than acute sequestration of reactive aldehydes during the hypoxic phase of

experimental stroke. However, definite evidence for a potential role of LSD1 in ischemia and neuroprotection could not be deduced from these experiments.

6.3.3. Genetic inhibition of repressive histone de-/methylases

Based on the knowledge gained from the blockade of selected histone de-/methylating enzymes with pharmacological inhibitors, the transcriptional repressors SUV39H1, G9a and LSD1 were chosen for knockdown experiments in order to investigate their role in ischemia and neuroprotection more closely.

6.3.3.1. SUV39H1 and G9a knockdown is neuroprotective in OGD

The neuroprotective effect observed upon pharmacological inhibition of SUV39H1 and G9a could be confirmed by knockdown of each of the repressive histone methyltransferases (**Fig. 40**).

The hypothesis that targeted manipulation on the epigenetic level of histone methylation can induce a state of neuroprotection in experimental ischemia could hence clearly be confirmed. For the first time two histone methyltransferases, SUV39H1 and G9a, were identified to play a role in the disease context.

Different contexts prove the importance of these enzymes regarding cell fate and cell survival. The knockdown of SUV39H1 or G9a has been demonstrated to inhibit cell growth in PC3 cancer cells [*Kondo et al.*, 2008] as well as proliferation in hepatocellular carcinoma [*Fan et al.*, 2013] and acute myelogenous leukemia [*Ma et al.*, 2013]. Interestingly, this phenomenon, that the knockdown of repressive epigenetic players induces fatal events for cancer cells while on the other hand displaying beneficial effects in neurological contexts has been observed before on the level of HDAC inhibition [*Langley et al.*, 2009]. Our results, showing that neuronal survival is increased upon SUV39H1/G9a knockdown, support this idea and emphasize the fact that epigenetic regulation is indeed largely dependent on cell type and cell function.

Further, the study confirms that histone methylation is not a secondary epigenetic phenomenon but marks a highly influential level of gene regulation by itself as well as through interaction with other levels. Both, SUV39H1 and G9a are known to interact with epigenetic regulators of other levels and multiple repressive elements [*Carbone et al.*, 2006; *Chen et al.*, 2009; *Cherrier et al.*, 2009; *Davis et al.*, 2006; *Fujita et al.*, 2003; *Gyory et al.*, 2004; *Mozzetta et al.*, 2014; *Nicolas et al.*, 2003; *Reed-Inderbitzin et al.*, 2006; *Roopra et al.*, 2004]. It is possible that the disruption of interaction with important partners and complexes upon knockdown of the histone methyltransferases actually influences the maintenance of repressive chromatin states and hence stroke outcome.

Generally, the formation and maintenance of repressed heterochromatic structures is based on an interplay of several important epigenetic players. Heterochromatin protein 1 (HP1) is one such crucial player and to function HP1 requires the establishment of H3K9 methylation as chromatin binding site [*Lachner et al.*, 2001]. A further prerequisite for HP1 recruitment to chromatin is its binding to SUV39h1 [*Stewart et al.*, 2005]. SUV39H1-HP1 directly interact with DNMT3A [*Lehnertz et al.*, 2003] establishing a link to repressive DNA methylation. A further link to DNA methylation exists. The maintenance of repressed chromatin states by SUV39H1 and G9a is partly sustained by direct binding to DNMT1 [*Esteve et al.*, 2006; *Fuks et al.*, 2003; *Ikegami et al.*, 2007; *Zimmermann et al.*, 2012]. In experimental stroke, reduction of DNMT1 levels leads to cytoprotection [*Endres et al.*, 2001]. One might speculate that this interplay between SUV39H1 or G9a and important interaction partners such as DNMT1 is disturbed upon inhibition of the histone methyltransferases. This might impact the establishment and maintenance of transcriptional repression. It might hold true for further interaction partners such as HP1 and DNMT3A as well.

Concerted action of SUV39H1 and HDAC1, 2 and 3 has also been observed [*Vaute et al.*, 2002]. Similarly, G9a was previously shown to orchestrate epigenetic remodelling and gene silencing in interaction with HDAC1 and 2 and other repressive elements at the promoters of target genes in the REST-CoREST complex [*Noh et al.*, 2012]. In the context of ischemia, not only pan-HDAC inhibition has proven to be a successful treatment strategy for neuronal survival [*Schweizer et al.*, 2013] but REST depletion was as well shown to restore gene expression and rescue hippocampal neurons in stroke [*Noh et al.*, 2012]. Again, it is possible, that G9a knockdown disturbs successful interaction with HDAC partners or the Co-REST complex and hence hampers the repressive effect of these interaction partners.

Apart from interactions with HDACs, DNMT1 and further repressive elements, SUV39H1 and G9a have recently been found in a mega complex consisting of the main H3K9 KMTs, namely SUV39H1, G9a, GLP and ESET. Interestingly, in cells depleted of SUV39H1, or G9a the remaining KMTs were destabilized on the protein level. Interdependency was further assessed on the functional level concerning the regulation of known G9a target genes. G9a target genes were not only abnormally expressed in G9a-/- cells but also in SUV39H1 -/- cells [*Fritsch et al.*, 2010]. This finding could explain the observed cytoprotection upon either SUV39H1 or G9a knockdown in OGD in spite of the different roles attributed to the two enzymes in vivo, where SUV39H1 is usually more important in heterochromatin formation and maintenance while the more direct influence on transcription is ascribed to G9a.

The influence of SUV39H1/G9a knockdown on epigenetic interaction partners was not further analysed this study. It was only observed that H3K9 acetylation is affected upon G9a knockdown (**Fig. 37**) and pharmacological inhibition of the histone methyltransferases by Chaetocin (**Fig. 42**). Genreally, it was demonstrated that the presence or absence of SUV39H1 or G9a alone plays an essential role in ischemia and neuroprotection.

6.3.3.2. LSD1 knockdown does not affect neuronal survival in OGD

The histone demethylase LSD1 shows many functional similarities to SUV39H1 and G9a. Its knockdown induces similar anticancer effects. Suppressed proliferation of bladder and lung cancer cell lines [*Hayami et al.*, 2011] was described upon LSD1 knockdown, as well as abrogated invasion of esophageal squamous carcinoma cells [*Yu et al.*, 2013] and decreased growth of neuroblastoma cells [*Schulte et al.*, 2009]. Likewise, LSD1 acts as transcriptional repressor [*Shi et al.*, 2004]. Just like SUV39H1 and G9a it interacts with many repressive elements. In interaction with DNMT1 for example, it plays a role in the stabilization of DNA methylation [*Wang et al.*, 2001]. It is also found in diverse repressor complexes, even together with G9a, in the Co-REST complex [*Humphrey et al.*, 2001; *Shi et al.*, 2005]. Above all, it is known to play a role in neuronal differentiation [*Ceballos-Chavez et al.*, 2012] and the development of the neuronal phenotype [*Zibetti et al.*, 2010].

In spite of all these functional similarities, LSD1 knockdown did not significantly influence survival in OGD in the experimental setup employed. Hence, LSD1 does not seem to be an essential player in the applied OGD paradigm. Its role as transcriptional repressor might be taken over by other enzymes upon knockdown of LSD1. The exact function of many histone de-/methylating enzymes is not fully characterized yet, several redundancies with further enzymes might exist. LSD1 and LSD2 functions can overlap [*Holmes et al.*, 2012]. Another option is, that LSD1 might regulate the transcription of genes that do not impact survival post OGD in cortical neurons in general, or in the in vitro experimental setup employed here that captures a particular time frame only.

Apart from explanations focusing on LSD1's irrelevance regarding neuronal survival post OGD, a further possibility has to be taken into account. In the experiments carried out as described above many different microRNAs targeting LSD1 were tested (**Fig. 38 A**) that did not seem to affect LSD1 protein levels at all, even upon prolonged viral incubation until DIV 14 (data not shown). This fact could be explained by non-potent microRNAs but also by protein stabilization or a very long half-life of the protein. No data is available on this fact up to now. The miR-shRNA construct that was finally

employed in the functional experiments does significantly diminish protein levels (**Fig. 38 B** and **C**), however basal levels still seem to be found in the cell as the lane in the immunoblot cannot be completely eradicated. This could imply that LSD1 is to a certain degree stabilized even upon reduction of levels due to mi-LSD1 application. In the cell, the enzyme could show sufficient functionality to ensure certain vital processes. In order to prove the complete absence of LSD1 activity upon mi-LSD1 application an activity assay would have been useful to fully exclude the possibility of functionality.

6.4. Changes in gene transcription upon SUV39H1 and G9a inhibition

According to our hypothesis epigenetic remodelling in stroke can confer protection to neurons through transcriptional derepression or activation (**Fig. 6**). The term "transcriptional activation" is used very broadly in this simplified model. Of interest are genes that, by being activated/derepressed, have the capacity to change cellular fate towards survival in experimental stroke – important neuroprotective players. Transcriptional activation upon epigenetic remodelling by Chaetocin treatment was assessed on two levels: an increase in H3K9ac at promoter regions and a rise in mRNA levels of the corresponding gene candidates in OGD.

6.4.1. Chaetocin alters promoter acetylation post OGD

Cells deficient of G9a show reduced levels of H3K9me2 but increases in activating H3K9 acetylation levels [*Rice et al.*, 2003; *Tachibana et al.*, 2002] and (**Fig. 37**). In order to locate a rise in activating epigenetic marks upon SUV39H1 and G9a inhibition via Chaetocin, ChIP was conducted with a H3K9ac antibody. In line with the hypothesis Chaetocin pretreated cells subjected to OGD showed significant H3K9ac enrichment in the promoter regions of, for example, HMOX1, GRIA2, BDNF, BCL 2, BCL-XL and one TSS of VEGFa (**Fig. 42 A, B**), while the promoter regions of BMI1, CASP 12 and VEGFa2 remained unaffected (**Fig. 42 C, D**). The induction of important neuroprotective and regenerative players upon epigenetic manipulation in experimental ischemia has been closely analysed in the context of HDAC inhibition. The genes showing active promoter signatures upon Chaetocin administration in OGD in our paradigm correlate with studies about epigenetic remodelling upon HDAC inhibition in experimental ischemia. Typical neuroprotective players such as BDNF [*Kim et al.*, 2009; *Kim and Chuang*, 2014; *Yasuda et al.*, 2009], VEGF [*Hu et al.*, 2006; *Kim and Chuang*, 2014], BCL 2 [*Faraco et al.*, 2006], BCL-XL [*Lanzillotta et al.*, 2012] and HMOX1 [*Wang et al.*, 2012] are reported to be induced upon HDACi in experimental

ischemia. As histone methyltransferases act in repressor complexes with HDACs [*Carbone et al.*, 2006; *Cherrier et al.*, 2009; *Davis et al.*, 2006; *Fujita et al.*, 2003; *Gyory et al.*, 2004; *Nicolas et al.*, 2003; *Noh et al.*, 2012; *Reed-Inderbitzin et al.*, 2006; *Roopra et al.*, 2004; *Unoki*, 2011; *Vaute et al.*, 2002] common target genes or pathways might be activated upon inhibition of repressive enzymes. The fact that both HDAC inhibition in experimental ischemia as well as the inhibition of the repressive histone methyltransferases SUV39H1 and G9a induces activating promoter signatures at common responsive genes strengthens the idea of orchestrated action. In line with the literature is also the enrichment of H3K9ac of GRIA2 upon G9a inhibition. GRIA2 codes for an AMPA receptor subunit and was found to be responsive to the repressor complex REST of which G9a is a member [*Noh et al.*, 2012]. Interestingly, not all TSS within a gene seem to be responsive to SUV39H1 and G9a inhibition. While two loci were analysed in VEGFa only one shows Chaetocin-induced H3K9ac enrichment upon OGD (**Fig. 42**). As the use of alternative promoters is important for differential regulation of genes this might be an example for the regulatory complexity that could mirror tissue specificity or adaptation to specific environmental stimuli [*Landry et al.*, 2003].

6.4.2. Chaetocin induces neuroprotective genes post OGD

Neuroprotective candidate genes were observed to respond to SUV39H1 and G9a inhibition via Chaetocin in OGD by an altered histone modification states. Interestingly, a rise in activating epigenetic marks, such as H3K9ac in promoter regions of selected genes, did not necessarily correlate with actual transcription of a gene in our experimental paradigm (**Fig. 43**). BCL-XL and GRIA2 that showed a significant H3K9ac enrichment upon Chaetocin administration in OGD 1 h post insult compared to vehicle treated cells did not display a significant augmentation in mRNA levels (1 h, 4 h 24 h) under the same conditions (**Fig. 43 C, D**). This divergence might be explained by the technical fact that ChIP data was only assessed once and would need validation, or by the functional aspect that transcriptional regulation takes place on various levels, histone modifications and chromatin remodelling being only one factor among others. Cooperative action of transcription factor binding, activators, enhancers but also negative regulators such as silencers and repressors is required for the complex regulation of active transcription. Hence in spite of a response of multiple genes on the level of posttranslational histone modifications upon SUV39H1/G9a inhibition, an actual upregulation on the mRNA level is not implied. This might be in line with an observation of Kondo et al. who, following a microarray analysis upon SUV39H1 and

G9a knockdown in PC3 cancer cells, report an actual upregulation of only "very few genes" [*Kondo et al.*, 2008].
However for VEGF, H3K9ac enrichment around one TSS correlated with significantly upregulated mRNA levels 1 and 4 hours post OGD (**Fig. 43 B**). The fact that only one TSS showed H3K9ac could not be related to a special transcript variant of VEGF, as the PCR primers in use were designed to multiply several transcript variants. However, that VEGF transcription can be G9a dependent has already been observed in an asthma model [*Clifford et al.*, 2012].
In ischemia, abundant evidence exists for the importance of VEGF in the mediation of protection [*Talwar and Srivastava*, 2014]. VEGF exerts its protective function not only via its angiogenic activity [*Sun et al.*, 2003; *Wang et al.*, 2005], a capacity neglectable in a neuronal cell culture, but also displays direct neuroprotective and plasticity-promoting properties [*Hermann and Zechariah*, 2009; *Storkebaum et al.*, 2004; *Sun et al.*, 2003]. Similarly, BDNF, that showed both significant H3K9ac enrichment and transcriptional activation on the mRNA level 1, 4 and 24 hours post OGD in Chaetocin-treated cells (**Fig. 42 A, B and 43 A**), is well known to promote protective and neurogenic developments in the ischemic brain [*Berger et al.*, 2004; *Chen et al.*, 2013; *Han et al.*, 2000; *Han and Holtzman*, 2000].

6.4.3. BDNF as key mediator of Chaetocin-induced neuroprotection

We identified the neurotrophin BDNF as transcriptionally responsive gene to Chaetocin treatment. Promoter regions were H3K9ac enriched upon SUV39H1 and G9a inhibition via Chaetocin in OGD and BDNF mRNA levels were significantly upregulated under the same conditions (**Fig. 42, 43**). BDNF regulation in the cell is complex. The gene is comprised of multiple exons, yields various transcripts [*Aid et al.*, 2007] and has eight promoter sequences that use multiple transcription start sites [*Liu et al.*, 2005; *West et al.*, 2014; *Zheng et al.*, 2012]. We analysed three different TSS in the BDNF gene (*BDNF1, BDNF2, BDNF3*) and all of them showed increased levels of H3K9ac upon Chaetocin treatment. The subsequent increase in mRNA levels was sustained up to 24 hours post OGD. Together with the knowledge that BDNF is involved in neuronal plasticity and survival [*D'Sa and Duman*, 2002; *Han et al.*, 2000; *Lee et al.*, 2002] and promotes post-ischemic survival [*Chen et al.*, 2013] these results suggest an important role for BDNF in Chaetocin-induced protection in OGD. This assumption was confirmed by the fact that BDNF-TrkB blockade attenuated Chaetocin-induced neuroprotection in OGD (**Fig. 44**). Again, this finding is in line with the current literature were abundant examples highlight the crucial role of BDNF-TrkB signaling in

neuroprotection and regeneration in diverse ischemic settings. Infarct volume decreases monitored upon administration of BDNF were shown to depend on BDNF-TrkB signalling [*Han and Holtzman*, 2000]. BDNF-TrkB blockade partially inhibited the protective effect of lithium in a model of glutamate excitotoxicity [*Hashimoto et al.*, 2002]. Further, BDNF-TrkB inhibition with K252a in ischemic brain slices blocked the protective effect of the plant extract PBI-05204 [*Van Kanegan et al.*, 2014]. Neurogenic effects of HDAC inhibitors were attenuated upon BDNF blockade with BDNF antibodies in neurons [*Hasan et al.*, 2013] as well as with K252a in a rodent model of ischemia: sodium butyrate-induced neurogenesis in various brain regions [*Kim et al.*, 2009] as well as oligodendrogensis and reduction of white matter injury were demonstrated to depend on BDNF-TrkB signaling [*Kim and Chuang*, 2014].

In summary, a body of literature argues for the importance of BDNF in mediating neuroprotective and regenerative processes in the ischemic brain. Our data corroborates these observations and additionally links BDNF expression to the regulation of the repressive histone methyltransferases SUV39H1 and G9a in experimental ischemia.

7. Conclusion

The most significant findings of this thesis could be summarized as follows:

1. No global changes in single methylation states at H3K9 or H3K4 could be assessed during 24 hours following experimental ischemia.
2. The transcriptional activator KDM3A showed a significant HIF-dependent induction on both the mRNA and protein level, which suggested a role for KDM3A in hypoxia. Exogenous KDM3A overexpression, however, did not influence neuronal survival post OGD.
3. Inhibiting the transcriptional repressors LSD1 and ESET with the pharmacological inhibitors Phenelzine and Mithramycin led to significant neuroprotection for rat cortical neurons subjected to OGD. Nevertheless, both inhibitors display a relatively broad mechanism of action and limited specificity towards the two histone de-/methylating enzymes. The significant protection could not be fully confirmed by LSD1 knockdown experiments, neither did LSD1 overexpression alter neuronal cell fate upon OGD.
4. The inhibition of the transcriptional repressors SUV39Ha and G9a, either by applying the fungal metabolite Chaetocin, or by knocking down each of the enzymes, significantly promoted neuronal survival in OGD. The inhibition of the two histone methyltransferases induced changes in H3K9 signatures over the promoters of several genes including neuroprotective players such as BCL-2, BCL-XL, VEGF and BDNF. A rise in H3K9ac, regarded as typical mark of gene activation could be noticed globally upon G9a knockdown and locally in various promoter regions upon OGD. Actual changes in gene transcription as a consequence of SUV39H1 and G9a inhibition were observed in the genes VEGF and BDNF, both growth factors, known to be involved in neuroprotective and regenerative cellular processes. BDNF blockade attenuated the protective effect of Chaetocin treatment for neurons subjected to OGD and could hence be identified as major mediator of Chaetocin-induced neuroprotection in experimental ischemia.

All in all, these findings confirm the hypothesis that the inhibition of transcriptional repressors on the epigenetic level of histone methylation can successfully change the fate of neurons destined to die of ischemic damage. The inhibition of repressive histone methyltransferases induces active gene transcription of important mediators of neuroprotection such as BDNF. Inhibitors like Chaetocin should be evaluated for their potential use in clinical trials for stroke.

8. Bibliography

Abel, T., and R. S. Zukin (2008), Epigenetic targets of HDAC inhibition in neurodegenerative and psychiatric disorders, *Current opinion in pharmacology*, *8*(1), 57-64.

Adegbola, A., H. Gao, S. Sommer, and M. Browning (2008), A novel mutation in JARID1C/SMCX in a patient with autism spectrum disorder (ASD), *American journal of medical genetics. Part A*, *146A*(4), 505-511.

Aid, T., A. Kazantseva, M. Piirsoo, K. Palm, and T. Timmusk (2007), Mouse and rat BDNF gene structure and expression revisited, *Journal of neuroscience research*, *85*(3), 525-535.

Auer, R. N. (1991), Excitotoxic mechanisms, and age-related susceptibility to brain damage in ischemia, hypoglycemia and toxic mussel poisoning, *Neurotoxicology*, *12*(3), 541-546.

Beal, M. F. (1992), Mechanisms of excitotoxicity in neurologic diseases, *FASEB journal : official publication of the Federation of American Societies for Experimental Biology*, *6*(15), 3338-3344.

Berger, C., W. R. Schabitz, M. Wolf, H. Mueller, C. Sommer, and S. Schwab (2004), Hypothermia and brain-derived neurotrophic factor reduce glutamate synergistically in acute stroke, *Experimental neurology*, *185*(2), 305-312.

Bergman, Y., and R. Mostoslavsky (1998), DNA demethylation: turning genes on, *Biological chemistry*, *379*(4-5), 401-407.

Bernhard, W., K. Barreto, A. Saunders, M. S. Dahabieh, P. Johnson, and I. Sadowski (2011), The Suv39H1 methyltransferase inhibitor chaetocin causes induction of integrated HIV-1 without producing a T cell response, *FEBS letters*, *585*(22), 3549-3554.

Bernstein, B. E., A. Meissner, and E. S. Lander (2007), The mammalian epigenome, *Cell*, *128*(4), 669-681.

Beyer, S., M. M. Kristensen, K. S. Jensen, J. V. Johansen, and P. Staller (2008), The histone demethylases JMJD1A and JMJD2B are transcriptional targets of hypoxia-inducible factor HIF, *The Journal of biological chemistry*, *283*(52), 36542-36552.

Bird, A. (2007), Perceptions of epigenetics, *Nature*, *447*(7143), 396-398.

Black, J. C., C. Van Rechem, and J. R. Whetstine (2012), Histone lysine methylation dynamics: establishment, regulation, and biological impact, *Molecular cell*, *48*(4), 491-507.

Blume, S. W., R. C. Snyder, R. Ray, S. Thomas, C. A. Koller, and D. M. Miller (1991), Mithramycin inhibits SP1 binding and selectively inhibits transcriptional activity of the dihydrofolate reductase gene in vitro and in vivo, *The Journal of clinical investigation*, *88*(5), 1613-1621.

Bock, I., A. Dhayalan, S. Kudithipudi, O. Brandt, P. Rathert, and A. Jeltsch (2011), Detailed specificity analysis of antibodies binding to modified histone tails with peptide arrays, *Epigenetics : official journal of the DNA Methylation Society*, *6*(2), 256-263.

Bruer, U., M. K. Weih, N. K. Isaev, A. Meisel, K. Ruscher, A. Bergk, . . . U. Dirnagl (1997), Induction of tolerance in rat cortical neurons: hypoxic preconditioning, *FEBS letters*, *414*(1), 117-121.

Camelo, S., A. H. Iglesias, D. Hwang, B. Due, H. Ryu, K. Smith, . . . F. Dangond (2005), Transcriptional therapy with the histone deacetylase inhibitor trichostatin A ameliorates experimental autoimmune encephalomyelitis, *Journal of neuroimmunology*, *164*(1-2), 10-21.

Carbone, R., O. A. Botrugno, S. Ronzoni, A. Insinga, L. Di Croce, P. G. Pelicci, and S. Minucci (2006), Recruitment of the histone methyltransferase SUV39H1 and its role in the oncogenic properties of the leukemia-associated PML-retinoic acid receptor fusion protein, *Molecular and cellular biology*, *26*(4), 1288-1296.

Ceballos-Chavez, M., S. Rivero, P. Garcia-Gutierrez, M. Rodriguez-Paredes, M. Garcia-Dominguez, S. Bhattacharya, and J. C. Reyes (2012), Control of neuronal differentiation by sumoylation of BRAF35, a subunit of the LSD1-CoREST histone demethylase complex, *Proceedings of the National Academy of Sciences of the United States of America*, *109*(21), 8085-8090.

Chaib, H., A. Nebbioso, T. Prebet, R. Castellano, S. Garbit, A. Restouin, . . . Y. Collette (2012), Anti-leukemia activity of chaetocin via death receptor-dependent apoptosis and dual modulation of the histone methyl-transferase SUV39H1, *Leukemia*, *26*(4), 662-674.

Chang, Y., X. Zhang, J. R. Horton, A. K. Upadhyay, A. Spannhoff, J. Liu, . . . X. Cheng (2009), Structural basis for G9a-like protein lysine methyltransferase inhibition by BIX-01294, *Nature structural & molecular biology*, *16*(3), 312-317.

Chase, K. A., D. P. Gavin, A. Guidotti, and R. P. Sharma (2013), Histone methylation at H3K9: Evidence for a restrictive epigenome in schizophrenia, *Schizophrenia research*, *149*(1-3), 15-20.

Chatterjee, S., K. Zaman, H. Ryu, A. Conforto, and R. R. Ratan (2001), Sequence-selective DNA binding drugs mithramycin A and chromomycin A3 are potent inhibitors of neuronal apoptosis induced by oxidative stress and DNA damage in cortical neurons, *Annals of neurology*, *49*(3), 345-354.

Chen, A., L. J. Xiong, Y. Tong, and M. Mao (2013), The neuroprotective roles of BDNF in hypoxic ischemic brain injury, *Biomedical reports*, *1*(2), 167-176.

Chen, H., Y. Yan, T. L. Davidson, Y. Shinkai, and M. Costa (2006), Hypoxic stress induces dimethylated histone H3 lysine 9 through histone methyltransferase G9a in mammalian cells, *Cancer research*, *66*(18), 9009-9016.

Chen, X., M. El Gazzar, B. K. Yoza, and C. E. McCall (2009), The NF-kappaB factor RelB and histone H3 lysine methyltransferase G9a directly interact to generate epigenetic silencing in endotoxin tolerance, *The Journal of biological chemistry*, *284*(41), 27857-27865.

Cherblanc, F. L., K. L. Chapman, R. Brown, and M. J. Fuchter (2013a), Chaetocin is a nonspecific inhibitor of histone lysine methyltransferases, *Nature chemical biology*, *9*(3), 136-137.

Cherblanc, F. L., K. L. Chapman, J. Reid, A. J. Borg, S. Sundriyal, L. Alcazar-Fuoli, . . . M. J. Fuchter (2013b), On the histone lysine methyltransferase activity of fungal metabolite chaetocin, *Journal of medicinal chemistry*, *56*(21), 8616-8625.

Cherrier, T., S. Suzanne, L. Redel, M. Calao, C. Marban, B. Samah, . . . O. Rohr (2009), p21(WAF1) gene promoter is epigenetically silenced by CTIP2 and SUV39H1, *Oncogene*, *28*(38), 3380-3389.

Cho, H. S., J. D. Kelly, S. Hayami, G. Toyokawa, M. Takawa, M. Yoshimatsu, . . . R. Hamamoto (2011a), Enhanced expression of EHMT2 is involved in the proliferation of cancer cells through negative regulation of SIAH1, *Neoplasia*, *13*(8), 676-684.

Cho, H. S., T. Suzuki, N. Dohmae, S. Hayami, M. Unoki, M. Yoshimatsu, . . . R. Hamamoto (2011b), Demethylation of RB regulator MYPT1 by histone demethylase LSD1 promotes cell cycle progression in cancer cells, *Cancer research*, *71*(3), 655-660.

Clifford, R. L., A. E. John, C. E. Brightling, and A. J. Knox (2012), Abnormal histone methylation is responsible for increased vascular endothelial growth factor 165a secretion from airway smooth muscle cells in asthma, *J Immunol*, *189*(2), 819-831.

Cloos, P. A., J. Christensen, K. Agger, A. Maiolica, J. Rappsilber, T. Antal, . . . K. Helin (2006), The putative oncogene GASC1 demethylates tri- and dimethylated lysine 9 on histone H3, *Nature*, *442*(7100), 307-311.

Cook, D. J., L. Teves, and M. Tymianski (2012), Treatment of stroke with a PSD-95 inhibitor in the gyrencephalic primate brain, *Nature*, *483*(7388), 213-217.

Copeland, R. A., E. J. Olhava, and M. P. Scott (2010), Targeting epigenetic enzymes for drug discovery, *Current opinion in chemical biology*, *14*(4), 505-510.

Cudkowicz, M. E., P. L. Andres, S. A. Macdonald, R. S. Bedlack, R. Choudry, R. H. Brown, Jr., . . . R. J. Ferrante (2009), Phase 2 study of sodium phenylbutyrate in ALS, *Amyotrophic lateral sclerosis : official*

publication of the World Federation of Neurology Research Group on Motor Neuron Diseases, *10*(2), 99-106.

Cui, H., A. Hayashi, H. S. Sun, M. P. Belmares, C. Cobey, T. Phan, . . . M. Tymianski (2007), PDZ protein interactions underlying NMDA receptor-mediated excitotoxicity and neuroprotection by PSD-95 inhibitors, *The Journal of neuroscience : the official journal of the Society for Neuroscience*, *27*(37), 9901-9915.

Culhane, J. C., D. Wang, P. M. Yen, and P. A. Cole (2010), Comparative analysis of small molecules and histone substrate analogues as LSD1 lysine demethylase inhibitors, *Journal of the American Chemical Society*, *132*(9), 3164-3176.

Czvitkovich, S., S. Sauer, A. H. Peters, E. Deiner, A. Wolf, G. Laible, . . . T. Jenuwein (2001), Over-expression of the SUV39H1 histone methyltransferase induces altered proliferation and differentiation in transgenic mice, *Mechanisms of development*, *107*(1-2), 141-153.

D'Sa, C., and R. S. Duman (2002), Antidepressants and neuroplasticity, *Bipolar disorders*, *4*(3), 183-194.

Danielisova, V., M. Nemethova, M. Gottlieb, and J. Burda (2005), Changes of endogenous antioxidant enzymes during ischemic tolerance acquisition, *Neurochemical research*, *30*(4), 559-565.

Datwyler, A. L., G. Lattig-Tunnemann, W. Yang, W. Paschen, S. L. Lee, U. Dirnagl, . . . C. Harms (2011), SUMO2/3 conjugation is an endogenous neuroprotective mechanism, *Journal of cerebral blood flow and metabolism : official journal of the International Society of Cerebral Blood Flow and Metabolism*, *31*(11), 2152-2159.

Davis, C. A., M. Haberland, M. A. Arnold, L. B. Sutherland, O. G. McDonald, J. A. Richardson, . . . E. N. Olson (2006), PRISM/PRDM6, a transcriptional repressor that promotes the proliferative gene program in smooth muscle cells, *Molecular and cellular biology*, *26*(7), 2626-2636.

de Ruijter, A. J., A. H. van Gennip, H. N. Caron, S. Kemp, and A. B. van Kuilenburg (2003), Histone deacetylases (HDACs): characterization of the classical HDAC family, *The Biochemical journal*, *370*(Pt 3), 737-749.

DeGraba, T. J. (1998), The role of inflammation after acute stroke: utility of pursuing anti-adhesion molecule therapy, *Neurology*, *51*(3 Suppl 3), S62-68.

Dereski, M. O., M. Chopp, R. A. Knight, L. C. Rodolosi, and J. H. Garcia (1993), The heterogeneous temporal evolution of focal ischemic neuronal damage in the rat, *Acta neuropathologica*, *85*(3), 327-333.

Dirnagl, U., C. Iadecola, and M. A. Moskowitz (1999), Pathobiology of ischaemic stroke: an integrated view, *Trends in neurosciences*, *22*(9), 391-397.

Dirnagl, U., and A. Meisel (2008), Endogenous neuroprotection: mitochondria as gateways to cerebral preconditioning?, *Neuropharmacology*, *55*(3), 334-344.

Dirnagl, U., K. Becker, and A. Meisel (2009), Preconditioning and tolerance against cerebral ischaemia: from experimental strategies to clinical use, *Lancet neurology*, *8*(4), 398-412.

Dreier, J. P. (2011), The role of spreading depression, spreading depolarization and spreading ischemia in neurological disease, *Nature medicine*, *17*(4), 439-447.

Ducruet, A. F., B. T. Grobelny, B. E. Zacharia, Z. L. Hickman, M. L. Yeh, and E. S. Connolly (2009), Pharmacotherapy of cerebral ischemia, *Expert opinion on pharmacotherapy*, *10*(12), 1895-1906.

Endres, M., A. Meisel, D. Biniszkiewicz, S. Namura, K. Prass, K. Ruscher, . . . U. Dirnagl (2000), DNA methyltransferase contributes to delayed ischemic brain injury, *The Journal of neuroscience : the official journal of the Society for Neuroscience*, *20*(9), 3175-3181.

Endres, M., G. Fan, A. Meisel, U. Dirnagl, and R. Jaenisch (2001), Effects of cerebral ischemia in mice lacking DNA methyltransferase 1 in post-mitotic neurons, *Neuroreport*, *12*(17), 3763-3766.

Ernst, J., and M. Kellis (2013), Interplay between chromatin state, regulator binding, and regulatory motifs in six human cell types, *Genome research*, *23*(7), 1142-1154.

Esteve, P. O., H. G. Chin, A. Smallwood, G. R. Feehery, O. Gangisetty, A. R. Karpf, . . . S. Pradhan (2006), Direct interaction between DNMT1 and G9a coordinates DNA and histone methylation during replication, *Genes & development*, *20*(22), 3089-3103.

Fan, D. N., F. H. Tsang, A. H. Tam, S. L. Au, C. C. Wong, L. Wei, . . . C. M. Wong (2013), Histone lysine methyltransferase, suppressor of variegation 3-9 homolog 1, promotes hepatocellular carcinoma progression and is negatively regulated by microRNA-125b, *Hepatology*, *57*(2), 637-647.

Faraco, G., T. Pancani, L. Formentini, P. Mascagni, G. Fossati, F. Leoni, . . . A. Chiarugi (2006), Pharmacological inhibition of histone deacetylases by suberoylanilide hydroxamic acid specifically alters gene expression and reduces ischemic injury in the mouse brain, *Molecular pharmacology*, *70*(6), 1876-1884.

Feng, J., and E. J. Nestler (2013), Epigenetic mechanisms of drug addiction, *Current opinion in neurobiology*, *23*(4), 521-528.

Ferrante, R. J., J. K. Kubilus, J. Lee, H. Ryu, A. Beesen, B. Zucker, . . . S. M. Hersch (2003), Histone deacetylase inhibition by sodium butyrate chemotherapy ameliorates the neurodegenerative phenotype in Huntington's disease mice, *The Journal of neuroscience : the official journal of the Society for Neuroscience*, *23*(28), 9418-9427.

Ferrante, R. J., H. Ryu, J. K. Kubilus, S. D'Mello, K. L. Sugars, J. Lee, . . . R. R. Ratan (2004), Chemotherapy for the brain: the antitumor antibiotic mithramycin prolongs survival in a mouse model of Huntington's disease, *The Journal of neuroscience : the official journal of the Society for Neuroscience*, *24*(46), 10335-10342.

Feuerstein, G. Z., and X. Wang (2001), Inflammation and stroke: benefits without harm?, *Archives of neurology*, *58*(4), 672-674.

Fischle, W. (2012), One, two, three: how histone methylation is read, *Epigenomics*, *4*(6), 641-653.

Formisano, L., K. M. Noh, T. Miyawaki, T. Mashiko, M. V. Bennett, and R. S. Zukin (2007), Ischemic insults promote epigenetic reprogramming of mu opioid receptor expression in hippocampal neurons, *Proceedings of the National Academy of Sciences of the United States of America*, *104*(10), 4170-4175.

Forneris, F., C. Binda, M. A. Vanoni, E. Battaglioli, and A. Mattevi (2005), Human histone demethylase LSD1 reads the histone code, *The Journal of biological chemistry*, *280*(50), 41360-41365.

Forneris, F., C. Binda, E. Battaglioli, and A. Mattevi (2008), LSD1: oxidative chemistry for multifaceted functions in chromatin regulation, *Trends in biochemical sciences*, *33*(4), 181-189.

Fritsch, L., P. Robin, J. R. Mathieu, M. Souidi, H. Hinaux, C. Rougeulle, . . . S. Ait-Si-Ali (2010), A subset of the histone H3 lysine 9 methyltransferases Suv39h1, G9a, GLP, and SETDB1 participate in a multimeric complex, *Molecular cell*, *37*(1), 46-56.

Fujita, N., S. Watanabe, T. Ichimura, S. Tsuruzoe, Y. Shinkai, M. Tachibana, . . . M. Nakao (2003), Methyl-CpG binding domain 1 (MBD1) interacts with the Suv39h1-HP1 heterochromatic complex for DNA methylation-based transcriptional repression, *The Journal of biological chemistry*, *278*(26), 24132-24138.

Fuks, F., W. A. Burgers, A. Brehm, L. Hughes-Davies, and T. Kouzarides (2000), DNA methyltransferase Dnmt1 associates with histone deacetylase activity, *Nature genetics*, *24*(1), 88-91.

Fuks, F., P. J. Hurd, R. Deplus, and T. Kouzarides (2003), The DNA methyltransferases associate with HP1 and the SUV39H1 histone methyltransferase, *Nucleic acids research*, *31*(9), 2305-2312.

Gardner, K. E., C. D. Allis, and B. D. Strahl (2011), Operating on chromatin, a colorful language where context matters, *Journal of molecular biology*, *409*(1), 36-46.

Gelderblom, M., F. Leypoldt, K. Steinbach, D. Behrens, C. U. Choe, D. A. Siler, . . . T. Magnus (2009), Temporal and spatial dynamics of cerebral immune cell accumulation in stroke, *Stroke; a journal of cerebral circulation*, *40*(5), 1849-1857.

Gibson, C. L., and S. P. Murphy (2010), Benefits of histone deacetylase inhibitors for acute brain injury: a systematic review of animal studies, *Journal of neurochemistry*, *115*(4), 806-813.

Gifford, C. A., M. J. Ziller, H. Gu, C. Trapnell, J. Donaghey, A. Tsankov, . . . A. Meissner (2013), Transcriptional and epigenetic dynamics during specification of human embryonic stem cells, *Cell*, *153*(5), 1149-1163.

Giulian, D., and K. Vaca (1993), Inflammatory glia mediate delayed neuronal damage after ischemia in the central nervous system, *Stroke; a journal of cerebral circulation*, *24*(12 Suppl), I84-90.

Goldberg, A. D., C. D. Allis, and E. Bernstein (2007), Epigenetics: a landscape takes shape, *Cell*, *128*(4), 635-638.

Graff, J., D. Kim, M. M. Dobbin, and L. H. Tsai (2011), Epigenetic regulation of gene expression in physiological and pathological brain processes, *Physiological reviews*, *91*(2), 603-649.

Gregory, R. I., T. E. Randall, C. A. Johnson, S. Khosla, I. Hatada, L. P. O'Neill, . . . R. Feil (2001), DNA methylation is linked to deacetylation of histone H3, but not H4, on the imprinted genes Snrpn and U2af1-rs1, *Molecular and cellular biology*, *21*(16), 5426-5436.

Greiner, D., T. Bonaldi, R. Eskeland, E. Roemer, and A. Imhof (2005), Identification of a specific inhibitor of the histone methyltransferase SU(VAR)3-9, *Nature chemical biology*, *1*(3), 143-145.

Greiner, D., T. Bonaldi, R. Eskeland, E. Roemer, and A. Imhof (2013), Reply to "Chaetocin is a nonspecific inhibitor of histone lysine methyltransferases", *Nature chemical biology*, *9*(3), 137.

Gyory, I., J. Wu, G. Fejer, E. Seto, and K. L. Wright (2004), PRDI-BF1 recruits the histone H3 methyltransferase G9a in transcriptional silencing, *Nature immunology*, *5*(3), 299-308.

Ha, S. C., A. R. Han, D. W. Kim, E. A. Kim, D. S. Kim, S. Y. Choi, and S. W. Cho (2013), Neuroprotective effects of the antioxidant action of 2-cyclopropylimino-3-methyl-1,3-thiazoline hydrochloride against ischemic neuronal damage in the brain, *BMB reports*, *46*(7), 370-375.

Han, B. H., A. D'Costa, S. A. Back, M. Parsadanian, S. Patel, A. R. Shah, . . . D. M. Holtzman (2000), BDNF blocks caspase-3 activation in neonatal hypoxia-ischemia, *Neurobiology of disease*, *7*(1), 38-53.

Han, B. H., and D. M. Holtzman (2000), BDNF protects the neonatal brain from hypoxic-ischemic injury in vivo via the ERK pathway, *The Journal of neuroscience : the official journal of the Society for Neuroscience*, *20*(15), 5775-5781.

Harms, C., J. Bosel, M. Lautenschlager, U. Harms, J. S. Braun, H. Hortnagl, . . . M. Endres (2004), Neuronal gelsolin prevents apoptosis by enhancing actin depolymerization, *Molecular and cellular neurosciences*, *25*(1), 69-82.

Hasan, M. R., J. H. Kim, Y. J. Kim, K. J. Kwon, C. Y. Shin, H. Y. Kim, . . . J. Lee (2013), Effect of HDAC inhibitors on neuroprotection and neurite outgrowth in primary rat cortical neurons following ischemic insult, *Neurochemical research*, *38*(9), 1921-1934.

Hashimoto, R., N. Takei, K. Shimazu, L. Christ, B. Lu, and D. M. Chuang (2002), Lithium induces brain-derived neurotrophic factor and activates TrkB in rodent cortical neurons: an essential step for neuroprotection against glutamate excitotoxicity, *Neuropharmacology*, *43*(7), 1173-1179.

Hauser, D., H. P. Weber, and H. P. Sigg (1970), [Isolation and configuration of Chaetocin], *Helvetica chimica acta*, *53*(5), 1061-1073.

Hayami, S., J. D. Kelly, H. S. Cho, M. Yoshimatsu, M. Unoki, T. Tsunoda, . . . R. Hamamoto (2011), Overexpression of LSD1 contributes to human carcinogenesis through chromatin regulation in various cancers, *International journal of cancer. Journal international du cancer*, *128*(3), 574-586.

Hebbes, T. R., A. W. Thorne, and C. Crane-Robinson (1988), A direct link between core histone acetylation and transcriptionally active chromatin, *The EMBO journal*, *7*(5), 1395-1402.

Hermann, D. M., and A. Zechariah (2009), Implications of vascular endothelial growth factor for postischemic neurovascular remodeling, *Journal of cerebral blood flow and metabolism : official journal of the International Society of Cerebral Blood Flow and Metabolism*, *29*(10), 1620-1643.

Hickok, J. R., D. Vasudevan, W. E. Antholine, and D. D. Thomas (2013), Nitric oxide modifies global histone methylation by inhibiting Jumonji C domain-containing demethylases, *The Journal of biological chemistry*, *288*(22), 16004-16015.

Hogarth, P., L. Lovrecic, and D. Krainc (2007), Sodium phenylbutyrate in Huntington's disease: a dose-finding study, *Movement disorders : official journal of the Movement Disorder Society*, *22*(13), 1962-1964.

Holmes, A., L. Roseaulin, C. Schurra, H. Waxin, S. Lambert, M. Zaratiegui, . . . B. Arcangioli (2012), Lsd1 and lsd2 control programmed replication fork pauses and imprinting in fission yeast, *Cell reports*, *2*(6), 1513-1520.

Hossmann, K. A. (1994), Viability thresholds and the penumbra of focal ischemia, *Annals of neurology*, *36*(4), 557-565.

Hu, C. J., S. D. Chen, D. I. Yang, T. N. Lin, C. M. Chen, T. H. Huang, and C. Y. Hsu (2006), Promoter region methylation and reduced expression of thrombospondin-1 after oxygen-glucose deprivation in murine cerebral endothelial cells, *Journal of cerebral blood flow and metabolism : official journal of the International Society of Cerebral Blood Flow and Metabolism*, *26*(12), 1519-1526.

Huang, Y., J. J. Doherty, and R. Dingledine (2002), Altered histone acetylation at glutamate receptor 2 and brain-derived neurotrophic factor genes is an early event triggered by status epilepticus, *The Journal of neuroscience : the official journal of the Society for Neuroscience*, *22*(19), 8422-8428.

Humphrey, G. W., Y. Wang, V. R. Russanova, T. Hirai, J. Qin, Y. Nakatani, and B. H. Howard (2001), Stable histone deacetylase complexes distinguished by the presence of SANT domain proteins CoREST/kiaa0071 and Mta-L1, *The Journal of biological chemistry*, *276*(9), 6817-6824.

Ikegami, K., M. Iwatani, M. Suzuki, M. Tachibana, Y. Shinkai, S. Tanaka, . . . K. Shiota (2007), Genome-wide and locus-specific DNA hypomethylation in G9a deficient mouse embryonic stem cells, *Genes to cells : devoted to molecular & cellular mechanisms*, *12*(1), 1-11.

Isham, C. R., J. D. Tibodeau, A. R. Bossou, J. R. Merchan, and K. C. Bible (2012), The anticancer effects of chaetocin are independent of programmed cell death and hypoxia, and are associated with inhibition of endothelial cell proliferation, *British journal of cancer*, *106*(2), 314-323.

Iwasa, E., Y. Hamashima, S. Fujishiro, E. Higuchi, A. Ito, M. Yoshida, and M. Sodeoka (2010), Total synthesis of (+)-chaetocin and its analogues: their histone methyltransferase G9a inhibitory activity, *Journal of the American Chemical Society*, *132*(12), 4078-4079.

Iwase, S., F. Lan, P. Bayliss, L. de la Torre-Ubieta, M. Huarte, H. H. Qi, . . . Y. Shi (2007), The X-linked mental retardation gene SMCX/JARID1C defines a family of histone H3 lysine 4 demethylases, *Cell*, *128*(6), 1077-1088.

Jensen, L. R., M. Amende, U. Gurok, B. Moser, V. Gimmel, A. Tzschach, . . . S. Lenzner (2005), Mutations in the JARID1C gene, which is involved in transcriptional regulation and chromatin remodeling, cause X-linked mental retardation, *American journal of human genetics*, *76*(2), 227-236.

Jenuwein, T., and C. D. Allis (2001), Translating the histone code, *Science*, *293*(5532), 1074-1080.

Kader, A., V. I. Frazzini, R. A. Solomon, and R. R. Trifiletti (1993), Nitric oxide production during focal cerebral ischemia in rats, *Stroke; a journal of cerebral circulation*, *24*(11), 1709-1716.

Kaikkonen, M. U., M. T. Lam, and C. K. Glass (2011), Non-coding RNAs as regulators of gene expression and epigenetics, *Cardiovascular research*, *90*(3), 430-440.

Kim, H. J., M. Rowe, M. Ren, J. S. Hong, P. S. Chen, and D. M. Chuang (2007), Histone deacetylase inhibitors exhibit anti-inflammatory and neuroprotective effects in a rat permanent ischemic model of stroke: multiple mechanisms of action, *The Journal of pharmacology and experimental therapeutics*, *321*(3), 892-901.

Kim, H. J., P. Leeds, and D. M. Chuang (2009), The HDAC inhibitor, sodium butyrate, stimulates neurogenesis in the ischemic brain, *Journal of neurochemistry*, *110*(4), 1226-1240.

Kim, H. J., and D. M. Chuang (2014), HDAC inhibitors mitigate ischemia-induced oligodendrocyte damage: potential roles of oligodendrogenesis, VEGF, and anti-inflammation, *American journal of translational research*, *6*(3), 206-223.

Kleefstra, T., H. G. Brunner, J. Amiel, A. R. Oudakker, W. M. Nillesen, A. Magee, . . . H. van Bokhoven (2006), Loss-of-function mutations in euchromatin histone methyl transferase 1 (EHMT1) cause the 9q34 subtelomeric deletion syndrome, *American journal of human genetics*, *79*(2), 370-377.

Kogure, K., and H. Kato (1993), Altered gene expression in cerebral ischemia, *Stroke; a journal of cerebral circulation*, *24*(12), 2121-2127.

Koh, J. Y., and D. W. Choi (1987), Quantitative determination of glutamate mediated cortical neuronal injury in cell culture by lactate dehydrogenase efflux assay, *Journal of neuroscience methods*, *20*(1), 83-90.

Kondo, Y., L. Shen, S. Ahmed, Y. Boumber, Y. Sekido, B. R. Haddad, and J. P. Issa (2008), Downregulation of histone H3 lysine 9 methyltransferase G9a induces centrosome disruption and chromosome instability in cancer cells, *PloS one*, *3*(4), e2037.

Kostandy, B. B. (2012), The role of glutamate in neuronal ischemic injury: the role of spark in fire, *Neurological sciences : official journal of the Italian Neurological Society and of the Italian Society of Clinical Neurophysiology*, *33*(2), 223-237.

Kouzarides, T. (2007), Chromatin modifications and their function, *Cell*, *128*(4), 693-705.

Krieg, A. J., E. B. Rankin, D. Chan, O. Razorenova, S. Fernandez, and A. J. Giaccia (2010), Regulation of the histone demethylase JMJD1A by hypoxia-inducible factor 1 alpha enhances hypoxic gene expression and tumor growth, *Molecular and cellular biology*, *30*(1), 344-353.

Kubicek, S., R. J. O'Sullivan, E. M. August, E. R. Hickey, Q. Zhang, M. L. Teodoro, . . . T. Jenuwein (2007), Reversal of H3K9me2 by a small-molecule inhibitor for the G9a histone methyltransferase, *Molecular cell*, *25*(3), 473-481.

Kuo, M. H., and C. D. Allis (1998), Roles of histone acetyltransferases and deacetylases in gene regulation, *BioEssays : news and reviews in molecular, cellular and developmental biology*, *20*(8), 615-626.

Lachner, M., D. O'Carroll, S. Rea, K. Mechtler, and T. Jenuwein (2001), Methylation of histone H3 lysine 9 creates a binding site for HP1 proteins, *Nature*, *410*(6824), 116-120.

Landry, J. R., D. L. Mager, and B. T. Wilhelm (2003), Complex controls: the role of alternative promoters in mammalian genomes, *Trends in genetics : TIG*, *19*(11), 640-648.

Langley, B., M. A. D'Annibale, K. Suh, I. Ayoub, A. Tolhurst, B. Bastan, . . . R. R. Ratan (2008), Pulse inhibition of histone deacetylases induces complete resistance to oxidative death in cortical neurons without toxicity and reveals a role for cytoplasmic p21(waf1/cip1) in cell cycle-independent neuroprotection, *The Journal of neuroscience : the official journal of the Society for Neuroscience*, *28*(1), 163-176.

Langley, B., C. Brochier, and M. A. Rivieccio (2009), Targeting histone deacetylases as a multifaceted approach to treat the diverse outcomes of stroke, *Stroke; a journal of cerebral circulation*, *40*(8), 2899-2905.

Lanzillotta, A., G. Pignataro, C. Branca, O. Cuomo, I. Sarnico, M. Benarese, . . . M. Pizzi (2012), Targeted acetylation of NF-kappaB/RelA and histones by epigenetic drugs reduces post-ischemic brain injury in mice with an extended therapeutic window, *Neurobiology of disease*, *49C*, 177-189.

Lautenschlager, M., M. V. Onufriev, N. V. Gulyaeva, C. Harms, D. Freyer, U. Sehmsdorf, . . . H. Hortnagl (2000), Role of nitric oxide in the ethylcholine aziridinium model of delayed apoptotic neurodegeneration in vivo and in vitro, *Neuroscience*, *97*(2), 383-393.

Lee, H. Y., K. Choi, H. Oh, Y. K. Park, and H. Park (2014), HIF-1-dependent induction of Jumonji domain-containing protein (JMJD) 3 under hypoxic conditions, *Molecules and cells*, *37*(1), 43-50.

Lee, J., W. Duan, and M. P. Mattson (2002), Evidence that brain-derived neurotrophic factor is required for basal neurogenesis and mediates, in part, the enhancement of neurogenesis by dietary restriction in the hippocampus of adult mice, *Journal of neurochemistry*, *82*(6), 1367-1375.

Lee, M. G., C. Wynder, N. Cooch, and R. Shiekhattar (2005), An essential role for CoREST in nucleosomal histone 3 lysine 4 demethylation, *Nature*, *437*(7057), 432-435.

Lee, T. I., S. E. Johnstone, and R. A. Young (2006), Chromatin immunoprecipitation and microarray-based analysis of protein location, *Nature protocols*, *1*(2), 729-748.

Lehnertz, B., Y. Ueda, A. A. Derijck, U. Braunschweig, L. Perez-Burgos, S. Kubicek, . . . A. H. Peters (2003), Suv39h-mediated histone H3 lysine 9 methylation directs DNA methylation to major satellite repeats at pericentric heterochromatin, *Current biology : CB*, *13*(14), 1192-1200.

Li, H., and R. Durbin (2009), Fast and accurate short read alignment with Burrows-Wheeler transform, *Bioinformatics*, *25*(14), 1754-1760.

Li, H., B. Handsaker, A. Wysoker, T. Fennell, J. Ruan, N. Homer, . . . R. Durbin (2009), The Sequence Alignment/Map format and SAMtools, *Bioinformatics*, *25*(16), 2078-2079.

Li, M., X. Liu, X. Sun, Z. Wang, W. Guo, F. Hu, . . . Z. Li (2013), Therapeutic Effects of NK-HDAC-1, a Novel Histone Deacetylase Inhibitor, on Collagen-Induced Arthritis Through the Induction of Apoptosis of Fibroblast-Like Synoviocytes, *Inflammation*.

Liesz, A., W. Zhou, E. Mracsko, S. Karcher, H. Bauer, S. Schwarting, . . . R. Veltkamp (2011), Inhibition of lymphocyte trafficking shields the brain against deleterious neuroinflammation after stroke, *Brain : a journal of neurology*, *134*(Pt 3), 704-720.

Linghu, C., H. Zheng, L. Zhang, and J. Zhang (2013), Discovering common combinatorial histone modification patterns in the human genome, *Gene*, *518*(1), 171-178.

Liu, F., N. Pore, M. Kim, K. R. Voong, M. Dowling, A. Maity, and G. D. Kao (2006), Regulation of histone deacetylase 4 expression by the SP family of transcription factors, *Molecular biology of the cell*, *17*(2), 585-597.

Liu, F., X. Chen, A. Allali-Hassani, A. M. Quinn, G. A. Wasney, A. Dong, . . . J. Jin (2009), Discovery of a 2,4-diamino-7-aminoalkoxyquinazoline as a potent and selective inhibitor of histone lysine methyltransferase G9a, *Journal of medicinal chemistry*, *52*(24), 7950-7953.

Liu, F., X. Chen, A. Allali-Hassani, A. M. Quinn, T. J. Wigle, G. A. Wasney, . . . J. Jin (2010), Protein lysine methyltransferase G9a inhibitors: design, synthesis, and structure activity relationships of 2,4-diamino-7-aminoalkoxy-quinazolines, *Journal of medicinal chemistry*, *53*(15), 5844-5857.

Liu, F., D. Barsyte-Lovejoy, F. Li, Y. Xiong, V. Korboukh, X. P. Huang, . . . J. Jin (2013), Discovery of an in vivo chemical probe of the lysine methyltransferases G9a and GLP, *Journal of medicinal chemistry*, *56*(21), 8931-8942.

Liu, Q. R., D. Walther, T. Drgon, O. Polesskaya, T. G. Lesnick, K. J. Strain, . . . G. R. Uhl (2005), Human brain derived neurotrophic factor (BDNF) genes, splicing patterns, and assessments of associations with substance abuse and Parkinson's Disease, *American journal of medical genetics. Part B, Neuropsychiatric genetics : the official publication of the International Society of Psychiatric Genetics*, *134B*(1), 93-103.

Luger, K., A. W. Mader, R. K. Richmond, D. F. Sargent, and T. J. Richmond (1997), Crystal structure of the nucleosome core particle at 2.8 A resolution, *Nature*, *389*(6648), 251-260.

Lv, T., D. Yuan, X. Miao, Y. Lv, P. Zhan, X. Shen, and Y. Song (2012), Over-expression of LSD1 promotes proliferation, migration and invasion in non-small cell lung cancer, *PloS one*, *7*(4), e35065.

Ma, J., J. Qiu, L. Hirt, T. Dalkara, and M. A. Moskowitz (2001), Synergistic protective effect of caspase inhibitors and bFGF against brain injury induced by transient focal ischaemia, *British journal of pharmacology*, *133*(3), 345-350.

Ma, X. D., T. Zhao, and Y. Q. Huang (2013), [Effect of SUV39H1 siRNA silence on apoptosis and proliferation of acute myelogenous leukemia KG-1 cell line], *Zhongguo shi yan xue ye xue za zhi / Zhongguo bing li sheng li xue hui = Journal of experimental hematology / Chinese Association of Pathophysiology*, *21*(1), 82-86.

Marini, A. M., M. Popolo, H. Pan, N. Blondeau, and R. H. Lipsky (2008), Brain adaptation to stressful stimuli: a new perspective on potential therapeutic approaches based on BDNF and NMDA receptors, *CNS & neurological disorders drug targets*, *7*(4), 382-390.

Marinova, Z., M. Ren, J. R. Wendland, Y. Leng, M. H. Liang, S. Yasuda, . . . D. M. Chuang (2009), Valproic acid induces functional heat-shock protein 70 via Class I histone deacetylase inhibition in cortical neurons: a potential role of Sp1 acetylation, *Journal of neurochemistry*, *111*(4), 976-987.

Marinova, Z., Y. Leng, P. Leeds, and D. M. Chuang (2011), Histone deacetylase inhibition alters histone methylation associated with heat shock protein 70 promoter modifications in astrocytes and neurons, *Neuropharmacology*, *60*(7-8), 1109-1115.

Marks, P. A. (2004), The mechanism of the anti-tumor activity of the histone deacetylase inhibitor, suberoylanilide hydroxamic acid (SAHA), *Cell Cycle*, *3*(5), 534-535.

Marks, P. A. (2010), Histone deacetylase inhibitors: a chemical genetics approach to understanding cellular functions, *Biochimica et biophysica acta*, *1799*(10-12), 717-725.

Mehta, S. L., N. Manhas, and R. Raghubir (2007), Molecular targets in cerebral ischemia for developing novel therapeutics, *Brain research reviews*, *54*(1), 34-66.

Melcher, M., M. Schmid, L. Aagaard, P. Selenko, G. Laible, and T. Jenuwein (2000), Structure-function analysis of SUV39H1 reveals a dominant role in heterochromatin organization, chromosome segregation, and mitotic progression, *Molecular and cellular biology*, *20*(10), 3728-3741.

Mergenthaler, P., A. Kahl, A. Kamitz, V. van Laak, K. Stohlmann, S. Thomsen, . . . A. Meisel (2012), Mitochondrial hexokinase II (HKII) and phosphoprotein enriched in astrocytes (PEA15) form a molecular switch governing cellular fate depending on the metabolic state, *Proceedings of the National Academy of Sciences of the United States of America*, *109*(5), 1518-1523.

Mergenthaler, P., and A. Meisel (2012), Do stroke models model stroke?, *Disease models & mechanisms*, *5*(6), 718-725.

Metzger, E., M. Wissmann, N. Yin, J. M. Muller, R. Schneider, A. H. Peters, . . . R. Schule (2005), LSD1 demethylates repressive histone marks to promote androgen-receptor-dependent transcription, *Nature*, *437*(7057), 436-439.

Mikkelsen, T. S., M. Ku, D. B. Jaffe, B. Issac, E. Lieberman, G. Giannoukos, . . . B. E. Bernstein (2007), Genome-wide maps of chromatin state in pluripotent and lineage-committed cells, *Nature*, *448*(7153), 553-560.

Mimura, I., T. Tanaka, Y. Wada, T. Kodama, and M. Nangaku (2011), Pathophysiological response to hypoxia - from the molecular mechanisms of malady to drug discovery: epigenetic regulation of the hypoxic response via hypoxia-inducible factor and histone modifying enzymes, *Journal of pharmacological sciences*, *115*(4), 453-458.

Mimura, I., M. Nangaku, Y. Kanki, S. Tsutsumi, T. Inoue, T. Kohro, . . . Y. Wada (2012), Dynamic change of chromatin conformation in response to hypoxia enhances the expression of GLUT3 (SLC2A3) by cooperative interaction of hypoxia-inducible factor 1 and KDM3A, *Molecular and cellular biology*, *32*(15), 3018-3032.

Minamiyama, M., M. Katsuno, H. Adachi, M. Waza, C. Sang, Y. Kobayashi, . . . G. Sobue (2004), Sodium butyrate ameliorates phenotypic expression in a transgenic mouse model of spinal and bulbar muscular atrophy, *Human molecular genetics*, *13*(11), 1183-1192.

Mir, M. A., S. Majee, S. Das, and D. Dasgupta (2003), Association of chromatin with anticancer antibiotics, mithramycin and chromomycin A3, *Bioorganic & medicinal chemistry*, *11*(13), 2791-2801.

Mozzetta, C., J. Pontis, L. Fritsch, P. Robin, M. Portoso, C. Proux, . . . S. Ait-Si-Ali (2014), The histone H3 lysine 9 methyltransferases G9a and GLP regulate polycomb repressive complex 2-mediated gene silencing, *Molecular cell*, *53*(2), 277-289.

Mungamuri, S. K., E. K. Benson, S. Wang, W. Gu, S. W. Lee, and S. A. Aaronson (2012), p53-mediated heterochromatin reorganization regulates its cell fate decisions, *Nature structural & molecular biology*, *19*(5), 478-484, S471.

Nan, X., H. H. Ng, C. A. Johnson, C. D. Laherty, B. M. Turner, R. N. Eisenman, and A. Bird (1998), Transcriptional repression by the methyl-CpG-binding protein MeCP2 involves a histone deacetylase complex, *Nature*, *393*(6683), 386-389.

Narlikar, G. J., H. Y. Fan, and R. E. Kingston (2002), Cooperation between complexes that regulate chromatin structure and transcription, *Cell*, *108*(4), 475-487.

Nicolas, E., C. Roumillac, and D. Trouche (2003), Balance between acetylation and methylation of histone H3 lysine 9 on the E2F-responsive dihydrofolate reductase promoter, *Molecular and cellular biology*, *23*(5), 1614-1622.

Noh, K. M., J. Y. Hwang, A. Follenzi, R. Athanasiadou, T. Miyawaki, J. M. Greally, . . . R. S. Zukin (2012), Repressor element-1 silencing transcription factor (REST)-dependent epigenetic remodeling is critical to ischemia-induced neuronal death, *Proceedings of the National Academy of Sciences of the United States of America*, *109*(16), E962-971.

Novelli, A., J. A. Reilly, P. G. Lysko, and R. C. Henneberry (1988), Glutamate becomes neurotoxic via the N-methyl-D-aspartate receptor when intracellular energy levels are reduced, *Brain research*, *451*(1-2), 205-212.

Ouyang, Y. B., and R. G. Giffard (2004), Cellular neuroprotective mechanisms in cerebral ischemia: Bcl-2 family proteins and protection of mitochondrial function, *Cell calcium*, *36*(3-4), 303-311.

Ozer, A., and R. K. Bruick (2007), Non-heme dioxygenases: cellular sensors and regulators jelly rolled into one?, *Nature chemical biology*, *3*(3), 144-153.

Papadopoulos, M. C., R. G. Giffard, and B. A. Bell (2000), An introduction to the changes in gene expression that occur after cerebral ischaemia, *British journal of neurosurgery*, *14*(4), 305-312.

Passaro, D., G. Rana, M. Piscopo, E. Viggiano, B. De Luca, and L. Fucci (2010), Epigenetic chromatin modifications in the cortical spreading depression, *Brain research*, *1329*, 1-9.

Peters, A. H., D. O'Carroll, H. Scherthan, K. Mechtler, S. Sauer, C. Schofer, . . . T. Jenuwein (2001), Loss of the Suv39h histone methyltransferases impairs mammalian heterochromatin and genome stability, *Cell*, *107*(3), 323-337.

Peters, A. H., S. Kubicek, K. Mechtler, R. J. O'Sullivan, A. A. Derijck, L. Perez-Burgos, . . . T. Jenuwein (2003), Partitioning and plasticity of repressive histone methylation states in mammalian chromatin, *Molecular cell*, *12*(6), 1577-1589.

Pollard, P. J., C. Loenarz, D. R. Mole, M. A. McDonough, J. M. Gleadle, C. J. Schofield, and P. J. Ratcliffe (2008), Regulation of Jumonji-domain-containing histone demethylases by hypoxia-inducible factor (HIF)-1alpha, *The Biochemical journal*, *416*(3), 387-394.

Prass, K., A. Scharff, K. Ruscher, D. Lowl, C. Muselmann, I. Victorov, . . . A. Meisel (2003), Hypoxia-induced stroke tolerance in the mouse is mediated by erythropoietin, *Stroke; a journal of cerebral circulation*, *34*(8), 1981-1986.

Qi, X., T. Hosoi, Y. Okuma, M. Kaneko, and Y. Nomura (2004), Sodium 4-phenylbutyrate protects against cerebral ischemic injury, *Molecular pharmacology*, *66*(4), 899-908.

Quinlan, A. R., and I. M. Hall (2010), BEDTools: a flexible suite of utilities for comparing genomic features, *Bioinformatics*, *26*(6), 841-842.

Rana, G., A. Donizetti, G. Virelli, M. Piscopo, E. Viggiano, B. De Luca, and L. Fucci (2012), Cortical spreading depression differentially affects lysine methylation of H3 histone at neuroprotective genes and retrotransposon sequences, *Brain research*, *1467*, 113-119.

Rea, S., F. Eisenhaber, D. O'Carroll, B. D. Strahl, Z. W. Sun, M. Schmid, . . . T. Jenuwein (2000), Regulation of chromatin structure by site-specific histone H3 methyltransferases, *Nature*, *406*(6796), 593-599.

Reed-Inderbitzin, E., I. Moreno-Miralles, S. K. Vanden-Eynden, J. Xie, B. Lutterbach, K. L. Durst-Goodwin, . . . S. W. Hiebert (2006), RUNX1 associates with histone deacetylases and SUV39H1 to repress transcription, *Oncogene*, *25*(42), 5777-5786.

Ren, M., Y. Leng, M. Jeong, P. R. Leeds, and D. M. Chuang (2004), Valproic acid reduces brain damage induced by transient focal cerebral ischemia in rats: potential roles of histone deacetylase inhibition and heat shock protein induction, *Journal of neurochemistry*, *89*(6), 1358-1367.

Rice, J. C., S. D. Briggs, B. Ueberheide, C. M. Barber, J. Shabanowitz, D. F. Hunt, . . . C. D. Allis (2003), Histone methyltransferases direct different degrees of methylation to define distinct chromatin domains, *Molecular cell*, *12*(6), 1591-1598.

Robertson, K. D., S. Ait-Si-Ali, T. Yokochi, P. A. Wade, P. L. Jones, and A. P. Wolffe (2000), DNMT1 forms a complex with Rb, E2F1 and HDAC1 and represses transcription from E2F-responsive promoters, *Nature genetics*, *25*(3), 338-342.

Roopra, A., R. Qazi, B. Schoenike, T. J. Daley, and J. F. Morrison (2004), Localized domains of G9a-mediated histone methylation are required for silencing of neuronal genes, *Molecular cell*, *14*(6), 727-738.

Rosenberg, G. A. (1999), Ischemic brain edema, *Progress in cardiovascular diseases*, *42*(3), 209-216.

Rothwell, N. J., and P. J. Strijbos (1995), Cytokines in neurodegeneration and repair, *International journal of developmental neuroscience : the official journal of the International Society for Developmental Neuroscience*, *13*(3-4), 179-185.

Ruscher, K., N. Isaev, G. Trendelenburg, M. Weih, L. Iurato, A. Meisel, and U. Dirnagl (1998), Induction of hypoxia inducible factor 1 by oxygen glucose deprivation is attenuated by hypoxic preconditioning in rat cultured neurons, *Neuroscience letters*, *254*(2), 117-120.

Ryu, H., J. Lee, S. W. Hagerty, B. Y. Soh, S. E. McAlpin, K. A. Cormier, . . . R. J. Ferrante (2006), ESET/SETDB1 gene expression and histone H3 (K9) trimethylation in Huntington's disease, *Proceedings of the National Academy of Sciences of the United States of America*, *103*(50), 19176-19181.

Sananbenesi, F., and A. Fischer (2009), The epigenetic bottleneck of neurodegenerative and psychiatric diseases, *Biological chemistry*, *390*(11), 1145-1153.

Sar, A., D. Ponjevic, M. Nguyen, A. H. Box, and D. J. Demetrick (2009), Identification and characterization of demethylase JMJD1A as a gene upregulated in the human cellular response to hypoxia, *Cell and tissue research*, *337*(2), 223-234.

Schlattmann, P., and U. Dirnagl (2010), Statistics in experimental cerebrovascular research: comparison of more than two groups with a continuous outcome variable, *Journal of cerebral blood flow and metabolism : official journal of the International Society of Cerebral Blood Flow and Metabolism*, *30*(9), 1558-1563.

Schmidt, D. M., and D. G. McCafferty (2007), trans-2-Phenylcyclopropylamine is a mechanism-based inactivator of the histone demethylase LSD1, *Biochemistry*, *46*(14), 4408-4416.

Schones, D. E., and K. Zhao (2008), Genome-wide approaches to studying chromatin modifications, *Nature reviews. Genetics*, *9*(3), 179-191.

Schulte, J. H., S. Lim, A. Schramm, N. Friedrichs, J. Koster, R. Versteeg, . . . J. Kirfel (2009), Lysine-specific demethylase 1 is strongly expressed in poorly differentiated neuroblastoma: implications for therapy, *Cancer research*, *69*(5), 2065-2071.

Schweizer, S., A. Meisel, and S. Marschenz (2013), Epigenetic mechanisms in cerebral ischemia, *Journal of cerebral blood flow and metabolism : official journal of the International Society of Cerebral Blood Flow and Metabolism*.

Semenza, G. L. (1996), Transcriptional regulation by hypoxia-inducible factor 1 molecular mechanisms of oxygen homeostasis, *Trends in cardiovascular medicine*, *6*(5), 151-157.

Shein, N. A., and E. Shohami (2011), Histone deacetylase inhibitors as therapeutic agents for acute central nervous system injuries, *Mol Med*, *17*(5-6), 448-456.

Shi, Y., F. Lan, C. Matson, P. Mulligan, J. R. Whetstine, P. A. Cole, and R. A. Casero (2004), Histone demethylation mediated by the nuclear amine oxidase homolog LSD1, *Cell*, *119*(7), 941-953.

Shi, Y. J., C. Matson, F. Lan, S. Iwase, T. Baba, and Y. Shi (2005), Regulation of LSD1 histone demethylase activity by its associated factors, *Molecular cell*, *19*(6), 857-864.

Shichita, T., Y. Sugiyama, H. Ooboshi, H. Sugimori, R. Nakagawa, I. Takada, . . . A. Yoshimura (2009), Pivotal role of cerebral interleukin-17-producing gammadeltaT cells in the delayed phase of ischemic brain injury, *Nature medicine*, *15*(8), 946-950.

Shimada, N., R. Graf, G. Rosner, A. Wakayama, C. P. George, and W. D. Heiss (1989), Ischemic flow threshold for extracellular glutamate increase in cat cortex, *Journal of cerebral blood flow and metabolism : official journal of the International Society of Cerebral Blood Flow and Metabolism*, *9*(5), 603-606.

Shulha, H. P., I. Cheung, C. Whittle, J. Wang, D. Virgil, C. L. Lin, . . . Z. Weng (2012), Epigenetic signatures of autism: trimethylated H3K4 landscapes in prefrontal neurons, *Archives of general psychiatry*, *69*(3), 314-324.

Sleiman, S. F., B. C. Langley, M. Basso, J. Berlin, L. Xia, J. B. Payappilly, . . . R. R. Ratan (2011), Mithramycin is a gene-selective Sp1 inhibitor that identifies a biological intersection between cancer and neurodegeneration, *The Journal of neuroscience : the official journal of the Society for Neuroscience*, *31*(18), 6858-6870.

Spannhoff, A., A. T. Hauser, R. Heinke, W. Sippl, and M. Jung (2009), The emerging therapeutic potential of histone methyltransferase and demethylase inhibitors, *ChemMedChem*, *4*(10), 1568-1582.

Stenzel-Poore, M. P., S. L. Stevens, J. S. King, and R. P. Simon (2007), Preconditioning reprograms the response to ischemic injury and primes the emergence of unique endogenous neuroprotective phenotypes: a speculative synthesis, *Stroke; a journal of cerebral circulation*, *38*(2 Suppl), 680-685.

Stewart, M. D., J. Li, and J. Wong (2005), Relationship between histone H3 lysine 9 methylation, transcription repression, and heterochromatin protein 1 recruitment, *Molecular and cellular biology*, *25*(7), 2525-2538.

Storkebaum, E., D. Lambrechts, and P. Carmeliet (2004), VEGF: once regarded as a specific angiogenic factor, now implicated in neuroprotection, *BioEssays : news and reviews in molecular, cellular and developmental biology*, *26*(9), 943-954.

Strahl, B. D., and C. D. Allis (2000), The language of covalent histone modifications, *Nature*, *403*(6765), 41-45.

Sun, Y., K. Jin, L. Xie, J. Childs, X. O. Mao, A. Logvinova, and D. A. Greenberg (2003), VEGF-induced neuroprotection, neurogenesis, and angiogenesis after focal cerebral ischemia, *The Journal of clinical investigation*, *111*(12), 1843-1851.

Szydlowska, K., and M. Tymianski (2010), Calcium, ischemia and excitotoxicity, *Cell calcium*, *47*(2), 122-129.

Tachibana, M., K. Sugimoto, M. Nozaki, J. Ueda, T. Ohta, M. Ohki, . . . Y. Shinkai (2002), G9a histone methyltransferase plays a dominant role in euchromatic histone H3 lysine 9 methylation and is essential for early embryogenesis, *Genes & development*, *16*(14), 1779-1791.

Talwar, T., and M. V. Srivastava (2014), Role of vascular endothelial growth factor and other growth factors in post-stroke recovery, *Annals of Indian Academy of Neurology*, *17*(1), 1-6.

Tapley, P., F. Lamballe, and M. Barbacid (1992), K252a is a selective inhibitor of the tyrosine protein kinase activity of the trk family of oncogenes and neurotrophin receptors, *Oncogene*, *7*(2), 371-381.

Tausendschon, M., N. Dehne, and B. Brune (2011), Hypoxia causes epigenetic gene regulation in macrophages by attenuating Jumonji histone demethylase activity, *Cytokine*, *53*(2), 256-262.

Thurman, R. J., E. C. Jauch, P. D. Panagos, M. R. Reynolds, and J. Mocco (2012), Four evolving strategies in the emergent treatment of acute ischemic stroke, *Emergency medicine practice*, *14*(7), 1-26; quiz 26-27.

Tibodeau, J. D., L. M. Benson, C. R. Isham, W. G. Owen, and K. C. Bible (2009), The anticancer agent chaetocin is a competitive substrate and inhibitor of thioredoxin reductase, *Antioxidants & redox signaling*, *11*(5), 1097-1106.

Tran, H. T., H. N. Kim, I. K. Lee, T. N. Nguyen-Pham, J. S. Ahn, Y. K. Kim, . . . H. J. Kim (2013), Improved therapeutic effect against leukemia by a combination of the histone methyltransferase inhibitor chaetocin and the histone deacetylase inhibitor trichostatin A, *Journal of Korean medical science*, *28*(2), 237-246.

Trendelenburg, G., K. Prass, J. Priller, K. Kapinya, A. Polley, C. Muselmann, . . . U. Dirnagl (2002), Serial analysis of gene expression identifies metallothionein-II as major neuroprotective gene in mouse focal cerebral ischemia, *The Journal of neuroscience : the official journal of the Society for Neuroscience*, *22*(14), 5879-5888.

Tropberger, P., and R. Schneider (2010), Going global: novel histone modifications in the globular domain of H3, *Epigenetics : official journal of the DNA Methylation Society*, *5*(2), 112-117.

Tropberger, P., and R. Schneider (2013), Scratching the (lateral) surface of chromatin regulation by histone modifications, *Nature structural & molecular biology*, *20*(6), 657-661.

Tsukada, Y., J. Fang, H. Erdjument-Bromage, M. E. Warren, C. H. Borchers, P. Tempst, and Y. Zhang (2006), Histone demethylation by a family of JmjC domain-containing proteins, *Nature*, *439*(7078), 811-816.

Ucar, D., Q. Hu, and K. Tan (2011), Combinatorial chromatin modification patterns in the human genome revealed by subspace clustering, *Nucleic acids research*, *39*(10), 4063-4075.

Unoki, M. (2011), Current and potential anticancer drugs targeting members of the UHRF1 complex including epigenetic modifiers, *Recent patents on anti-cancer drug discovery*, *6*(1), 116-130.

Van Kanegan, M. J., D. N. He, D. E. Dunn, P. Yang, R. A. Newman, A. E. West, and D. C. Lo (2014), BDNF mediates neuroprotection against oxygen-glucose deprivation by the cardiac glycoside oleandrin, *The Journal of neuroscience : the official journal of the Society for Neuroscience*, *34*(3), 963-968.

Van Lint, C., S. Emiliani, and E. Verdin (1996), The expression of a small fraction of cellular genes is changed in response to histone hyperacetylation, *Gene expression*, *5*(4-5), 245-253.

Vaute, O., E. Nicolas, L. Vandel, and D. Trouche (2002), Functional and physical interaction between the histone methyl transferase Suv39H1 and histone deacetylases, *Nucleic acids research*, *30*(2), 475-481.

Vedadi, M., D. Barsyte-Lovejoy, F. Liu, S. Rival-Gervier, A. Allali-Hassani, V. Labrie, . . . J. Jin (2011), A chemical probe selectively inhibits G9a and GLP methyltransferase activity in cells, *Nature chemical biology*, *7*(8), 566-574.

Wang, H., R. Cao, L. Xia, H. Erdjument-Bromage, C. Borchers, P. Tempst, and Y. Zhang (2001), Purification and functional characterization of a histone H3-lysine 4-specific methyltransferase, *Molecular cell*, *8*(6), 1207-1217.

Wang, Y., E. Kilic, U. Kilic, B. Weber, C. L. Bassetti, H. H. Marti, and D. M. Hermann (2005), VEGF overexpression induces post-ischaemic neuroprotection, but facilitates haemodynamic steal phenomena, *Brain : a journal of neurology*, *128*(Pt 1), 52-63.

Wang, Z., C. Zang, J. A. Rosenfeld, D. E. Schones, A. Barski, S. Cuddapah, . . . K. Zhao (2008), Combinatorial patterns of histone acetylations and methylations in the human genome, *Nature genetics*, *40*(7), 897-903.

Wang, Z., Y. Leng, L. K. Tsai, P. Leeds, and D. M. Chuang (2011), Valproic acid attenuates blood-brain barrier disruption in a rat model of transient focal cerebral ischemia: the roles of HDAC and MMP-9 inhibition, *Journal of cerebral blood flow and metabolism : official journal of the International Society of Cerebral Blood Flow and Metabolism*, *31*(1), 52-57.

Wang, Z., L. K. Tsai, J. Munasinghe, Y. Leng, E. B. Fessler, F. Chibane, . . . D. M. Chuang (2012), Chronic valproate treatment enhances postischemic angiogenesis and promotes functional recovery in a rat model of ischemic stroke, *Stroke; a journal of cerebral circulation*, *43*(9), 2430-2436.

Weisbrot-Lefkowitz, M., K. Reuhl, B. Perry, P. H. Chan, M. Inouye, and O. Mirochnitchenko (1998), Overexpression of human glutathione peroxidase protects transgenic mice against focal cerebral ischemia/reperfusion damage, *Brain research. Molecular brain research*, *53*(1-2), 333-338.

Wellmann, S., M. Bettkober, A. Zelmer, K. Seeger, M. Faigle, H. K. Eltzschig, and C. Buhrer (2008), Hypoxia upregulates the histone demethylase JMJD1A via HIF-1, *Biochemical and biophysical research communications*, *372*(4), 892-897.

West, A. E., P. Pruunsild, and T. Timmusk (2014), Neurotrophins: transcription and translation, *Handbook of experimental pharmacology*, *220*, 67-100.

Wigle, T. J., and R. A. Copeland (2013), Drugging the human methylome: an emerging modality for reversible control of aberrant gene transcription, *Current opinion in chemical biology*, *17*(3), 369-378.

Winkler, J., J. P. Shoup, A. Czap, I. Staff, G. Fortunato, L. D. McCullough, and L. H. Sansing (2013), Long-term Improvement in Outcome After Intracerebral Hemorrhage in Patients Treated with Statins, *Journal of stroke and cerebrovascular diseases : the official journal of National Stroke Association*.

Wolffe, A. P., and D. Pruss (1996), Hanging on to histones. Chromatin, *Current biology : CB*, *6*(3), 234-237.

Wood, P. L., M. A. Khan, J. R. Moskal, K. G. Todd, V. A. Tanay, and G. Baker (2006), Aldehyde load in ischemia-reperfusion brain injury: neuroprotection by neutralization of reactive aldehydes with phenelzine, *Brain research*, *1122*(1), 184-190.

Xia, X., M. E. Lemieux, W. Li, J. S. Carroll, M. Brown, X. S. Liu, and A. L. Kung (2009), Integrative analysis of HIF binding and transactivation reveals its role in maintaining histone methylation homeostasis, *Proceedings of the National Academy of Sciences of the United States of America*, *106*(11), 4260-4265.

Xuan, A., D. Long, J. Li, W. Ji, L. Hong, M. Zhang, and W. Zhang (2012), Neuroprotective effects of valproic acid following transient global ischemia in rats, *Life sciences*, *90*(11-12), 463-468.

Yabuki, Y., and K. Fukunaga (2013), Oral administration of glutathione improves memory deficits following transient brain ischemia by reducing brain oxidative stress, *Neuroscience*, *250*, 394-407.

Yamane, K., C. Toumazou, Y. Tsukada, H. Erdjument-Bromage, P. Tempst, J. Wong, and Y. Zhang (2006), JHDM2A, a JmjC-containing H3K9 demethylase, facilitates transcription activation by androgen receptor, *Cell*, *125*(3), 483-495.

Yang, M., J. C. Culhane, L. M. Szewczuk, P. Jalili, H. L. Ball, M. Machius, . . . H. Yu (2007), Structural basis for the inhibition of the LSD1 histone demethylase by the antidepressant trans-2-phenylcyclopropylamine, *Biochemistry*, *46*(27), 8058-8065.

Yasuda, S., M. H. Liang, Z. Marinova, A. Yahyavi, and D. M. Chuang (2009), The mood stabilizers lithium and valproate selectively activate the promoter IV of brain-derived neurotrophic factor in neurons, *Molecular psychiatry*, *14*(1), 51-59.

Yenari, M. A., J. Liu, Z. Zheng, Z. S. Vexler, J. E. Lee, and R. G. Giffard (2005), Antiapoptotic and anti-inflammatory mechanisms of heat-shock protein protection, *Annals of the New York Academy of Sciences*, *1053*, 74-83.

Yildirim, F., K. Gertz, G. Kronenberg, C. Harms, K. B. Fink, A. Meisel, and M. Endres (2008), Inhibition of histone deacetylation protects wildtype but not gelsolin-deficient mice from ischemic brain injury, *Experimental neurology*, *210*(2), 531-542.

Yokoyama, Y., M. Hieda, Y. Nishioka, A. Matsumoto, S. Higashi, H. Kimura, . . . N. Matsuura (2013), Cancer-associated upregulation of histone H3 lysine 9 trimethylation promotes cell motility in vitro and drives tumor formation in vivo, *Cancer science*, *104*(7), 889-895.

Yu, Y., B. Wang, K. Zhang, Z. Lei, Y. Guo, H. Xiao, . . . D. Chen (2013), High expression of lysine-specific demethylase 1 correlates with poor prognosis of patients with esophageal squamous cell carcinoma, *Biochemical and biophysical research communications*, *437*(2), 192-198.

Zhang, H. S., and D. C. Dean (2001), Rb-mediated chromatin structure regulation and transcriptional repression, *Oncogene*, *20*(24), 3134-3138.

Zheng, F., X. Zhou, C. Moon, and H. Wang (2012), Regulation of brain-derived neurotrophic factor expression in neurons, *International journal of physiology, pathophysiology and pharmacology*, *4*(4), 188-200.

Zibetti, C., A. Adamo, C. Binda, F. Forneris, E. Toffolo, C. Verpelli, . . . E. Battaglioli (2010), Alternative splicing of the histone demethylase LSD1/KDM1 contributes to the modulation of neurite morphogenesis in the mammalian nervous system, *The Journal of neuroscience : the official journal of the Society for Neuroscience*, *30*(7), 2521-2532.

Zimmermann, N., J. Zschocke, T. Perisic, S. Yu, F. Holsboer, and T. Rein (2012), Antidepressants inhibit DNA methyltransferase 1 through reducing G9a levels, *The Biochemical journal*, *448*(1), 93-102.

9. Eidesstattliche Versicherung

„Ich, Sophie Schweizer, versichere an Eides statt durch meine eigenhändige Unterschrift, dass ich die vorgelegte Dissertation mit dem Thema: *Histone Methylation and Neuroprotection in Experimental Cerebral Ischemia* selbstständig und ohne nicht offengelegte Hilfe Dritter verfasst und keine anderen als die angegebenen Quellen und Hilfsmittel genutzt habe.

Alle Stellen, die wörtlich oder dem Sinne nach auf Publikationen oder Vorträgen anderer Autoren beruhen, sind als solche in korrekter Zitierung (siehe „Uniform Requirements for Manuscripts (URM)“ des ICMJE -*www.**icmje**.org*) kenntlich gemacht. Die Abschnitte zu Methodik (insbesondere praktische Arbeiten, Laborbestimmungen, statistische Aufarbeitung) und Resultaten (insbesondere Abbildungen, Graphiken und Tabellen) entsprechen den URM (s.o) und werden von mir verantwortet.

Meine Anteile an etwaigen Publikationen zu dieser Dissertation entsprechen denen, die in der untenstehenden gemeinsamen Erklärung mit dem/der Betreuer/in, angegeben sind. Sämtliche Publikationen, die aus dieser Dissertation hervorgegangen sind und bei denen ich Autor bin, entsprechen den URM (s.o) und werden von mir verantwortet.

Die Bedeutung dieser eidesstattlichen Versicherung und die strafrechtlichen Folgen einer unwahren eidesstattlichen Versicherung (§156,161 des Strafgesetzbuches) sind mir bekannt und bewusst.“

Datum Unterschrift

Anteilserklärung an etwaigen erfolgten Publikationen

Sophie Schweizer hatte folgenden Anteil an den folgenden Publikationen:

Publikation 1:

Schweizer S., Meisel A., Märschenz S., Epigenetic mechanisms in cerebral ischemia, *Journal of Cerebral Blood Flow and Metabolism,* 33(9): 1335-46, 2013.

Beitrag im Einzelnen: Konzeption und Verfassen des Reviews.

Publikation 2:

Schweizer S., Harms C., Lerch H., Flynn J., Hecht J., Yildirim F., Meisel A., Märschenz S., Inhibition of histone methyltransferases SUV39H1 and/ or G9a leads to neuroprotection in an in vitro model of cerebral ischemia. *Journal of Cerebral Blood Flow and Metabolism.* Submitted 03.02.2015.

Beitrag im Einzelnen: Konzeption und Verfassen des Artikels, Experimentelle Planung und Durchführung, Analyse, Auswertung und Interpretation der Daten.

Unterschrift, Datum und Stempel des betreuenden Hochschullehrers/der betreuenden Hochschullehrerin

Unterschrift des Doktoranden/der Doktorandin

10. Lebenslauf

Mein Lebenslauf wird aus datenschutzrechtlichen Gründen in der elektronischen Version meiner Arbeit nicht veröffentlicht.

11. Publikationsliste

Artikel in Zeitschriften

Schweizer S., Meisel A., Märschenz S. (2013), Epigenetic mechanisms in cerebral ischemia, *Journal of Cerebral Blood Flow and Metabolism,* 33(9): 1335-46.

Schweizer S., Harms C., Lerch H., Flynn J., Hecht J., Yildirim F., Meisel A., Märschenz S. (2015). Inhibition of histone methyltransferases SUV39H1 and G9a leads to neuroprotection in an in vitro model of cerebral ischemia. *Journal of Cerebral Blood Flow and Metabolism.* Epub ahead of print.

Poster

Schweizer S., Meisel A., Märschenz S., Histone Methylation in Experimental Cerebral Ischemia and Neuroprotection, *Epigenetics Europe conference*. Munich, Germany, 8-9 September 2011.

Schweizer S., Meisel A., Märschenz S., Histone Methylation in Experimental Cerebral Ischemia and Neuroprotection, *Berlin Brain Days*, Berlin, Germany, 7-9 December 2011.

Schweizer S., Meisel A., Märschenz S., Histone Methylation in Cerebral Ischemia and Neuroprotection, *Max Planck Freiburg Epigenetics Meeting*, Freiburg, Germany, 2-5 December 2012.

12. Acknowledgements

I would like to thank my supervisor Andreas Meisel for giving me the opportunity to work on this exciting topic in his group and for his support and advice regarding this project.

My sincerest thank you to my mentor Stefanie Märschenz for her continuous support and guidance. I benefited so much from her patient encouragements and her trustful manner during these years.

I would further like to pay special tribute to Heike Lerch for her valuable technical teaching and assistance, her constant interest in the advance of the project as well as her hands-on effort to support me whenever possible.

Special thanks go to Christoph Harms for his collaboration and enthusiastic support concerning all matters regarding microRNA and beyond. A lot of my motivation was owed to him.

A big thank you to Jen Flynn for being a gorgeous Master student and friend during her time in the lab and beyond.

I would also like to thank my collaborator Jochen Hecht for his cooperation in the ChIP project.

Thanks to my great colleagues and friends Ines, Hanne, Katarzyna, Marietta, Claudia, Martina, Mareike, Kristin, Juliane, Odilo, Benedikt, Christine, Tian and Prissy who rendered lab-life fun and easy.

Dorette, Renate, Monika, Ingo, Christa, Renate-Louise, Ivonne, Dirk, Janet, and Nadine made great working conditions possible - in the cell culture lab as well as elsewhere in the experimental neurology. Thank you all.

Thank you to Ferah Yildirim whose work I was allowed to continue.

My unconditional thanks go to my father and mother.

Thank you, Philipp.